1982

Effects of a periosteal activation agent on bone repair, bone growth, and bone ingrowth into a porous material in the rabbit

L. Russell Alberts
Iowa State University

Alberts, L. Russell

EFFECTS OF A PERIOSTEAL ACTIVATION AGENT ON BONE REPAIR, BONE GROWTH, AND BONE INGROWTH INTO A POROUS MATERIAL IN THE RABBIT

Iowa State University PH.D. 1982

PLEASE NOTE:

In all cases this material has been filmed in the best possible way from the available copy. Problems encountered with this document have been identified here with a check mark __✓__.

1. Glossy photographs or pages ✓
2. Colored illustrations, paper or print ✓
3. Photographs with dark background _____
4. Illustrations are poor copy _____
5. Pages with black marks, not original copy _____
6. Print shows through as there is text on both sides of page _____
7. Indistinct, broken or small print on several pages _____
8. Print exceeds margin requirements _____
9. Tightly bound copy with print lost in spine _____
10. Computer printout pages with indistinct print _____
11. Page(s) _____ lacking when material received, and not available from school or author.
12. Page(s) _____ seem to be missing in numbering only as text follows.
13. Two pages numbered _____. Text follows.
14. Curling and wrinkled pages _____
15. Other _____

Effects of a periosteal activation agent on bone repair, bone growth, and bone ingrowth into a porous material in the rabbit

by

L. Russell Alberts

A Dissertation Submitted to the

Graduate Faculty in Partial Fulfillment of the

Requirements for the Degree of

DOCTOR OF PHILOSOPHY

Departments: Biomedical Engineering
Engineering Science and Mechanics

Co-Majors: Biomedical Engineering
Engineering Mechanics

Approved:

Signature was redacted for privacy.

In Charge of Major Work

Signature was redacted for privacy.

Professor-in-charge,
Program in Biomedical Engineering

Signature was redacted for privacy.

For the Major Department

Signature was redacted for privacy.

For the Graduate College

Iowa State University
Ames, Iowa

1982

TABLE OF CONTENTS

LIST OF TABLES

LIST OF FIGURES

INTRODUCTION

In the late 1950's and early 1960's Myers and co-workers at the Squibb Institute for Medical Research, extracted a substance from the cancellous bone of growing young mammals. This substance when applied to the periosteal surface of adult rat bones caused a rapid, massive growth of periosteal new bone. Some of the treated bones doubled their diameter in just seven days.

E. R. Squibb & Sons[1] chose not to pursue research on the substance. Some years later, Tornberg and Bassett (1977) obtained some samples of this substance for their experiments. They characterized some of the effects this substance had on the cells of the periosteum, and they hypothesized what the active agent is and how it works.

They showed that the substance activates the resting cells of the cambium layer of the periosteum. In just 72 hours, these cells reproduced themselves to form palisades of active osteoblastic cells. Within seven days, the original bone was covered with a sleeve of cancellous bone that doubled its diameter.

This substance, derived from the cancellous bone of growing mammals, will be referred to as periosteal

---

[1] E. R. Squibb & Sons, Inc., The Squibb Institute for Medical Research, P. O. Box 4000, Princeton, N. J.

activation agent (PAA). The primary objective of this research is to characterize the effects that this periosteal activation agent has on bone repair and bone ingrowth into a porous biocompatible implant. This study will investigate the feasibility of using PAA at the non-human level to encourage bone ingrowth into biocompatible porous implants, to aid healing, and in general, to characterize some of the effects of PAA on bone, medullary, endosteal, and periosteal tissues. It will examine how PAA alters the forms, types, volumes, and time sequence of these tissues. Radioactive tracers, light microscope, photographic, and computer techniques will be utilized to measure the amounts of new bone formation. Research into the chemical composition of PAA and how it biochemically influences cells is beyond the scope of this disquisition.

A specific bone activation substance, if it can be isolated, may lead to many therapeutic applications, including some that may not now be directly foreseen. It may find uses as an agent to stimulate bone ingrowth into porous implant materials. Biocompatible porous materials have been shown to be adequate interfacial materials for making contact between artificial hip replacements and living bone (Lord et al. 1979; Judet et al. 1978; Boutin, 1977). The bone grows into the interstices of the implant, and forms a solid bond between bone and prosthesis that

eliminates the need for methyl methacrylate cement and the deleterious effects that are associated with it (Judet et al. 1978; Holm, 1980). The main disadvantage of such implants is that a method must be implemented to immobilize the bone-implant complex until the bone ingrowth process is sufficiently advanced to adequately bind the bone to the prosthesis under the stresses applied by the patients normal activity. Use of a substance that would accelerate bone ingrowth may greatly increase the success rate of these prostheses.

Something that causes a rapid bone growth at the periosteum may be used to promote the reattachment of tendons and ligaments to bone, or the attachment of artificial ligaments to bone. Large purebred steers often suffer injuries to their stifle joints. Repair of the stifle joint can involve reattachment of the crucial ligament, or attachment of an artificial crucial ligament. In humans suffering from rheumatoid arthritis, the tibial collateral ligaments are often injured. Research is currently underway to develop artificial ligaments for these people. The main research problem would involve the attachment of the artificial ligament to the bone. A periosteal activation substance may lead to a breakthrough in this area of research.

Although a bone activation substance may not be needed

for normal fracture repair, it may be able to promote fracture healing in those cases where it is slow or non-existent. Normal healthy mammalian bone has a great ability to repair itself; in some human cases, gaps of up to six inches have been bridged (Hartshorne, 1841). But in some patients, age, disease, or unknown factors may hinder healing, sometimes creating a permanent false joint or pseudarthrosis. Such a substance might be used to initiate the normal bone healing process in such individuals.

LITERATURE REVIEW

The following sections will discuss bone, bone formation, bone induction, and previous work on activation of the resting periosteum, and will briefly describe morphogens and bioelectricity. A study of some previous work done on bone formation, bone induction, and periosteal activation helps to put this research in perspective and to provide a historical background. Morphogens and bioelectricity may be involved in the mechanism of periosteal activation.

It is important to understand the differences between bone induction and activation of the resting periosteum. Bone induction is the process where cells in a host organism are induced to form new bone by some substance, matrix, or tissue with which they are placed in contact. It is often used to refer to bone formation in tissues that normally do not form bone, such as the inner chamber of the eye or muscle tissue, but it can refer to stimulation of bone growth in normal skeletal tissue. Activation of the resting periosteum differs from this in that bone growth occurs exclusively in the cambium layer of the periosteum. There is no bone growth seen in outlying tissues. Also, the rate of growth is different in activation of the resting periosteum than in classic bone induction. In the classic bone induction studies, bone growth requires about 7 to 11 days to get

started. With activation of the resting periosteum, bone growth is completed in seven days. In some cases, the amount of bone produced by activation of the periosteum can be phenomenal. The diameter of the radius and ulna bones in rats may double in just seven days (Tornberg and Bassett, 1977). Although activation of the resting periosteum may perhaps be viewed as a form of bone induction, its difference from other forms of induction should be recognized.

Bone

Bone is one of several types of mineralized tissue that can occur in the animal body. These mineralized tissues include calcified cartilage, calcified tendon, and dental materials. They are all composed of three major elements: collagen fibers, inorganic materials, and an organic ground substance. In addition, most mineralized tissues contain cells. These tissues differ from each other by their proportion of fibers, minerals, and ground substance; by the types and arrangements of their collagen fibers; and by the types, densities and arrangement of their cells.

In bone, the collagen fibers are 40 nm to 120 nm in diameter, and they account for about one third the dry weight of bone. They are similar, but not identical to collagen elsewhere in the body.

Most of the remaining two thirds of the bone mass is provided by the bone mineral. The bone mineral has been described as a paracrystal similar to hydroxyapatite, $Ca_{10}(PO_4)_6(OH)_2$. The paracrystals occur as either needle shaped or tubular shaped objects about 3 to 5 nm wide and 60 nm long. They are closely associated with the collagen fibers, many of them occurring inside the fibers. The paracrystals are not exactly hydroxyapatite because they contain trace amount of other ions and anions and because their calcium-phosphate ratio is seldom exactly 1.67. They are called paracrystals because X-ray diffraction studies (Wheeler and Lewis, 1977) show that the distances between their atoms vary slightly. A paracrystal is a substance that is midway between an amorphous material and a regular crystalline array.

The third component of bone is often referred to as cement or as ground substance. It is actually not a single entity, but a broad grouping of all the non-collagenous, organic substances that comprise bone. The components include glycosaminoglycans, condroitin sulfates A and B, sialoprotein, CP-S glycoprotein, lipids, peptides, and other glycoproteins and proteins. These substances may assist in the nucleation of bone mineral, and they may aid in the transport of nutrients to the bone cells.

The three main cells associated with bone are

osteocytes, osteoblasts, and osteoclasts. Osteoclasts are large multinucleated cells formed from fused monocytes. They remove bone. They digest the collagen and the ground substance of bone as well as the bone mineral. Osteoblasts are cells that produce bone. They can lay down the fibers, ground substance, and bone mineral. When an osteoblast becomes trapped in its own matrix, it is called an osteocyte. Osteocytes may play a role in maintaining or removing some bone and in mineral homeostasis.

The formation of bone is generally classified into one of two types, intramembranous ossification and endochondral ossification. Intramembranous ossification refers to the mineralization of any membranous tissue. Endochondral ossification is the replacement of cartilage with bone.

In endochondral ossification, the cartilage cells, called chondrocytes, pass through several stages before they are replaced by bone. First, the chondrocytes tend to arrange themselves in long parallel lines called palisades. The chondrocytes in the palisades then begin to mineralize. As the chondrocytes become mineralized, they lose the ability to absorb nutrients. They then hypertrophy and die. The mineralized cell spaces or lacunae of the dead chondrocytes are then invaded by blood vessels and osteoblasts. The osteoblasts deposit a new bone matrix to form a course cancellous bone. When endochondral

ossification is occurring, usually a series of these stages of ossification is present. There is a zone of palisading osteocytes, a zone of osteocyte mineralization and hypertrophy, and a zone of vascular invasion.

Bone can be classified by either its elementary organization or by its higher organization. Classification according to its elementary organization is based on whether or not the fibers occur in coarse or fine bundles and whether or not they occur in a woven, parallel, or lamellar pattern. However, in most histological preparations the fibers can not be seen. For this reason, a simplified system that classifies bone into three types is usually used. The three types are bundle bone, woven bone, and fine-fibered bone.

Bundle bone is bone that contains coarse fiber bundles with osteocytes that follow the pattern of the bundles. It is found in the lower skeleton of vertebrates, at attachments of tendon and ligaments, in some fish scales, and in ossified tendons of birds.

Woven bone is composed of coarse loosely packed fibers, varying in size up to 30 nm in diameter, arranged in an irregular overlapping pattern. It has large, randomly dispersed osteocytes. In hematoxylin and eosin, it stains bluish or purplish due to its basophilic content. It occurs in fish scales, the flat dermal bones of amphibians and

snakes, in the fetal skeleton of mammals, and in the early fracture callus.

Fine-fibered bone includes both parallel and lamellar bone. Much of this classification of bone is lamellated, and polarized light will reveal the lamallae. This type of bone has a clear eosinophilic matrix with small ovoid osteocytes at regular, wide intervals. This is the predominant type of bone found in adult mammals, in some extinct reptiles such as dinosaurs and pterosaurs, and in the long bones of birds.

In mammals, bundle and woven bone are mostly temporary structures found in the growing animal, to be gradually replaced by fine-fibered bone. However, there are some sites in the mammalian skeleton where these types of bone will remain throughout adult life. Woven bone is characteristic of rapid bone growth. It usually possesses a rich vascular supply. Bundle bone generally developes in a more orderly manner from tendon and ligament cells that transform into osteoblasts and osteocytes and develope a mineral matrix. Fine-fibered bone is often formed by the gradual remodelling of bundle and woven bone and by surface apposition. It usually has a single layer of osteoblasts at its surface.

Bone is usually classified into two or three types with respect to its higher organization. Actually these

classification systems are an oversimplification. What is typically classified as compact bone can be identified as over a dozen distinct types of bone. The traditional classifications of bone are coarse cancellous, fine cancellous, and compact bone.

Coarse cancellous bone is the spongy bone found in the medullary canal and formed by deposition of new bone from the endosteal surface. It is comprised of coarse trabeculae of bone arranged in a haphazard, irregular pattern. It may have a lamellar or non-lamellar matrix.

Fine cancellous bone is more dense and compact than coarse cancellous bone, but not as solid as compact bone. It is found in the fetal skeleton, at secondary centers of ossification, in the early fracture callus, and, in general, at any site where bone growth is rapid.

The compact varieties of bone are more dense and compact than the cancellous varieties of bone. They can be formed by: (1) consolidation of fine and coarse cancellous bone, (2) direct apposition on periosteal and endosteal surfaces, and (3) remodelling of existing forms of compact bone with the formation of secondary osteons.

Compacted coarse-cancellous bone is formed when coarse cancellous bone is converted into compact bone. The old trabeculae of the coarse cancellous bone are filled with primary osteons and lamellae that follow the convolutions of

the original trabeculae, leaving a convoluted, whorled arrangement in the new formed cortical area.

Compacted fine-cancellous bone occurs when the fine cancellous bone is compacted.

Inner circumferential lamallae bone is formed by endosteal growth in areas of the diaphysis where there are few cancellous trabeculae. Outer circumferential lamellae are formed by periosteal apposition onto preexisting cortical bone. They are characterized by concentric lamellae that conform to the general contour of the bone.

Many types of compact bone are classified by their type of canal or vascular supply system. In man and other primates, there are many areas of non-vascular bone that are completely lacking a canal system.

Primary vascular bone has primary canals but no osteons. These primary canals are not surrounded by rings of lamellae as the osteons are, and they tend to run in a mostly longitudinal direction. Primary vascular bone is the most common type of bone in most vertebrate groups, and it is the chief type of bone in man during the active growth period following birth.

Primary osteons form an anastomosing network that fill some spaces when cancellous bone is compacted. They are usually smaller then secondary osteons, being just two or three circumferential lamellae rings around two or more

blood vessels. They are formed by the periosteum in the postnatal skeleton and sometimes by the endosteum. They are common in the fast growing animal and often occur in rows or layers.

The secondary osteon is often incorrectly described as forming the basic unit of compact bone. It does not. It occurs only in areas that have been remodelled. In the formation of a secondary osteon, osteoclasts first form a resorption cavity, usually larger than 100 μm in diameter. Osteoblasts then enter the cavity and start laying down concentric layers of bone. After each lamella is formed, a circular layer of osteoblasts become trapped in the margin between each lamella. These osteoblasts become osteocytes that act to maintain the bone matrix and to interact in mineral homeostasis. Extending outward from each osteocyte trapped in its space, or lacuna, are many tiny canals or caniculi that connect each osteocyte to adjacent osteocytes in the same osteon. The caniculi contain cell processes that connect the osteocytes. When the secondary osteon is complete, there is a single capillary in the center surrounded by a "tree ring" formation of lamellae. The outer border of the osteon will be a cement line which marks the limit of the old resorption cavity.

The compact bone in rabbit femurs, as are used in this study, included compacted fine-cancellous, compacted coarse-

cancellous, outer circumferential lamellae, inner circumferential lamellae, and a few areas of primary vascular bone. Primary osteons are common, but secondary osteons are usually only seen at sites of bone repair where necrotic bone near an injury site has been remodelled to secondary haversion bone. The new bone elicited by PAA is fine cancellous bone. This fine cancellous bone is expected to be either resorbed or converted to compacted fine-cancellous bone.

Bone Formation

Fell (1928, 1932a, 1932b) and Bassett (1962) did a series of experiments on the osteogenic capacity of bone cells in vitro. Their experiments will be examined in some detail because they define the basic forces that result in the formation of bone. They outline the different paths that bone precursor tissue can take when it differentiates, and identify the forces that cause these departures. As shown in Figure 1, an explant of bone was placed in a plasma clot on a cover slip. After a few days, an outgrowth of connective tissue elements and some capillaries emerged around the perimeter of the explant. At six days, the original piece of bone was excised from the clot. The remaining clot with its tissue outgrowth contracted, and the growing tissue gradually filled the center. After 14 days,

the clot appeared as shown in Figure 2. An outer shell of bone was formed in the area that was in direct contact with the high oxygen atmosphere. Underneath that was a cartilaginous core. During the process, the clot surface gradually progressed from material that resembled embryonic cartilage to hyaline cartilage to fibrocartilage, and finally to bone.

This experiment was repeated and altered by Bassett (1962). Bassett used explants from bone, skeletal muscle, and tendon. Two types of cells were characterized in the outgrowth around the explant. Originally, amoeboid, spindle-shaped cells were seen embedded in the fibrin network of the clot. These cells gradually changed their outline to become more spherical when the explant was removed and the clot contracted. These spindle-shaped cells accounted for 100% of the cellular population of the outgrowth from tendon cultures. These outgrowths did not differentiate into bone, but rather produced only fibrous tissue. The other cell type was larger, and polygonal or stellate shaped, and contained significant quantities of alkaline phosphatase, which was absent in the spindle-shaped cells. These stellate cells accounted for 90% of the cellular population from the muscle cultures and 75% to 80% in the bone cultures. Chondro-osteoid (Figure 2) was found in 15% of the muscle and bone cultures.

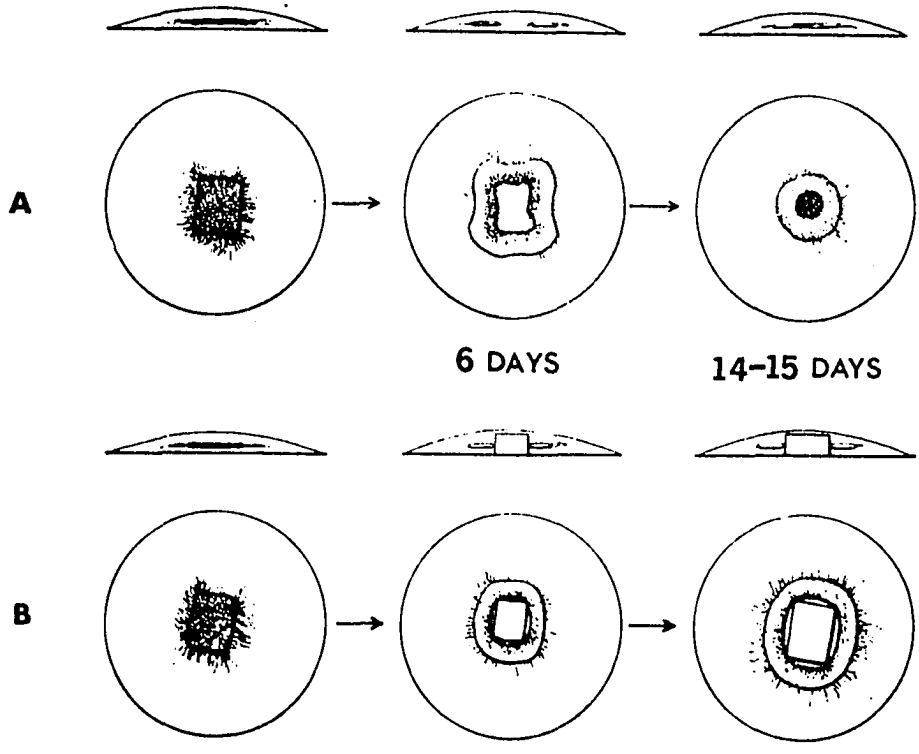

FIGURE 1. Bone explants in plasma clot on glass coverslips; A shows the clot with the explant excised, B shows the clot with the explant replaced by a plastic rod (Fell, 1932a; Fell, 1932b; Bassett, 1962)

Bassett showed that by increasing the oxygen concentration in the atmosphere, he could increase the percentage of cultures that developed an osseous shell. By reducing the oxygen concentration, he could reduce the percentage of cultures developing bone to zero. In low oxygen atmospheres, only cartilage developed from bone and muscle explant cultures.

Another variation in the experiment Bassett performed was to place a square plastic rod in the center of the outgrowth material, just after the explant had been removed, to keep the material from contracting. The square rod was regularly replaced by a larger rod to keep the outgrowth material under constant tension, as shown in Figure 1. The results were as shown in Figure 3. Along the sides of the rod, cartilaginous material formed with an osseous shell. However, at the corners, fibrous tendon-like tissue formed. Bassett's results can be summarized in the top half of Figure 4. When the primitive fibroblasts from the outgrowth are exposed to a high oxygen content and compaction (or perhaps just lack of tension) they form bone. When they are exposed to low oxygen partial pressure and compaction, cartilage is formed. When they are exposed to tension and high oxygen partial pressure, fibrous tissue forms. Bassett speculates that the same thing happens to primitive fibroblasts in the milieu of the living organism. These

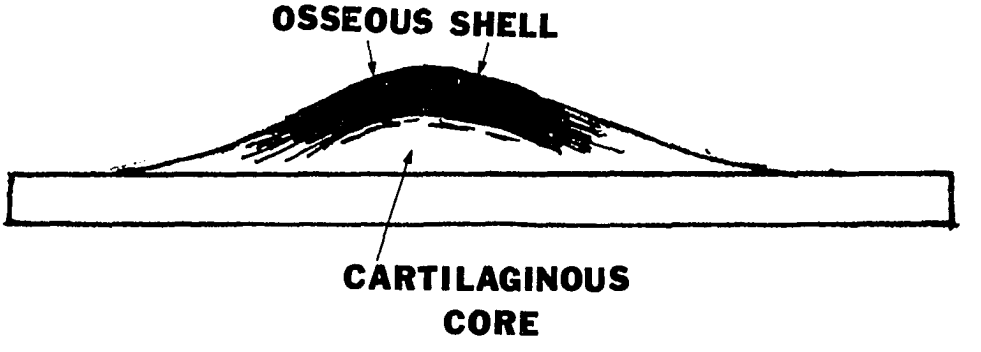

FIGURE 2. Appearance of outgrowth from explant after 14 days (Bassett, 1962)

cells are directed to differentiate into cartilage forming cells (chondroblasts), or bone forming cells (osteoblasts), or fibrous tissue forming cells (collagenoblasts), by tensile and compressive forces and by the partial pressure of oxygen present.

In summary, Bassett (1962) stated that osteogenesis requires three basic elements; (1) proper cells, (2) adequate nutrition, and (3) proper stimulus.

Bassett and Ruedi (1966) and Ruedi and Bassett (1967) performed an in vivo experiment that in many aspects models a single, large pore that fills with bone. Their work provides insights into what observations are expected in the porous implants that are introduced into the femurs of rabbits in our experiments. They cut 0.4 mm by 20 mm defects into the cortex of femora of adult mongrel dogs. The periosteum was removed; the defect was cut through one cortex, and the underlying medullary tissue was removed. The defect was isolated by a millipore filter. Slits were cut through the cortex on either side of the defect, and the millipore filter was threaded through the slits and wrapped over the outer opening, as shown in Figure 5.

Animals were destroyed at various periods postoperative, ranging from one day to one year. The area around the defect was sectioned as shown in Figure 5 and decalcified in a formic acid, sodium formate solution. The

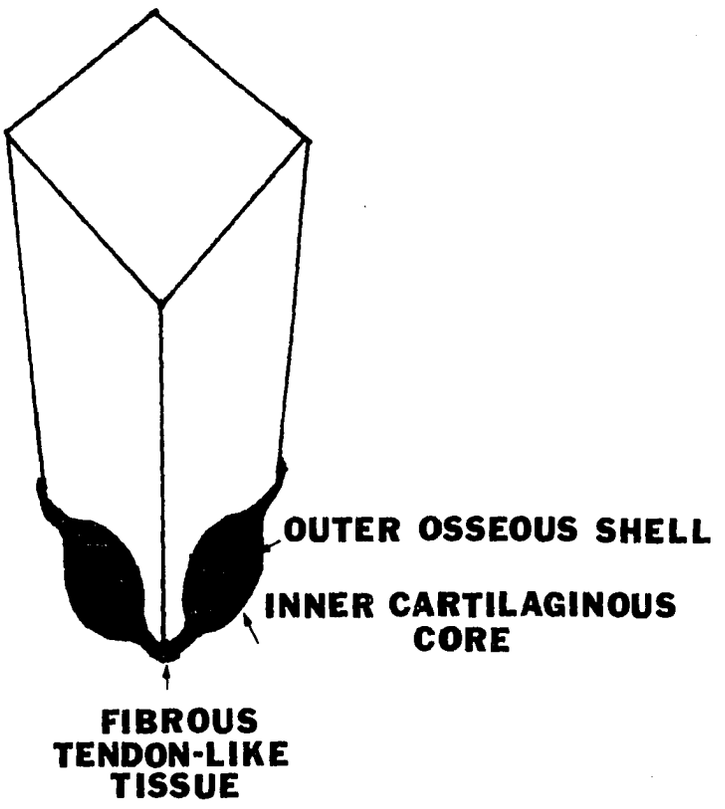

FIGURE 3. Appearance of outgrowth after 14 days when rectangular plastic rod had been inserted (Bassett, 1962)

specimens were stained for histological examination with hematoxylin and eosin, Van Gieson, phosphotungstic acid-hematoxylin, and Luidlow. These stains were selected to distinguish collagen, fibrin, and reticulin.

The histological examinations in the cortical regions A and B surrounding the defect showed the death of osteocytes. The osteocytes were shrunken and pyknotic. Many of the lacunar spaces were empty. Cellular elements of the vascular system, the haversion and Volkmann canals, were generally viable for longer periods, but after five days, no living cells were observed. At eight days postoperative, cortical revascularization began. This started with resorption of the necrotic tissue followed by deposition of new bone. Revascularization generally occurred sooner in the proximal region than in the distal region. The endosteal 1/2 or 1/3 of the cortex usually revascularized faster than the periosteal part. The time required for complete revascularization varied from 180 days to 320 days.

The chamber clot region remained empty in various animals for periods of 1, 3, 5, or 8 days. In other animals, it was filled with a fibrin clot in less than one day. After eight days there were no empty chambers, all were filled with fibrin. The fibrin may have formed from fibrinogen, and the cascade of clotting factors released by the ruptured capillaries of the cortex, or it may have

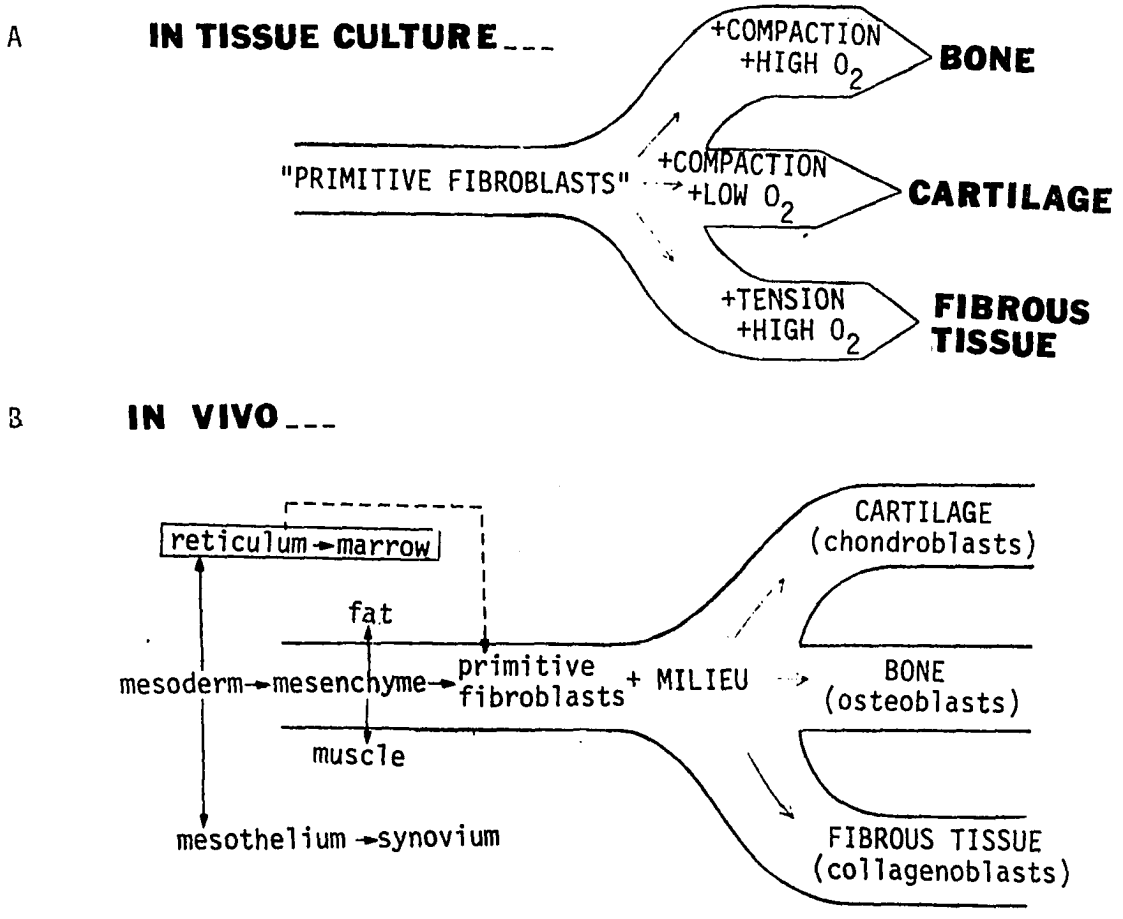

FIGURE 4. Tissue differentiation in A, tissue culture, and in B, in vivo (Bassett, 1962)

formed from fibrinogen and clotting factors that diffused through the millipore filter. The pores of the filter were 0.45 μm in diameter. This size is too small to permit cells to pass through (red blood cells are about 7 to 8 μm long and 1 to 2.4 μm thick), but it is sufficiently large enough to permit macromolecules and fluids to pass through.

The strands of fibrin were originally parallel to the bony surface and the millipore filter. Occasionally, white blood cells were seen in the clot, but neither the granulocytes nor the monocytes appeared to survive more than 24 hours.

The fibrin clot was lysed by a centripetal invasion of connective tissue elements. The cellular population of the clot began usually at the endosteal portion of the chamber, and as a rule, followed the preexisting arching fibrin strands. For up to 30 days, closely packed capillaries invaded on a broad front. The capillaries were surrounded by large basophilic cells. Spindle-shaped cells, morphologically similar to fibroblasts, were seen several millimeters ahead of the advancing capillaries. The spindle-shaped cells penetrated the clot and became surrounded by a network of argentophilic (silver staining) reticulin fibers.

This loose fibrous connective tissue was followed by a dense fibrous connective tissue. The denser fibrous tissue

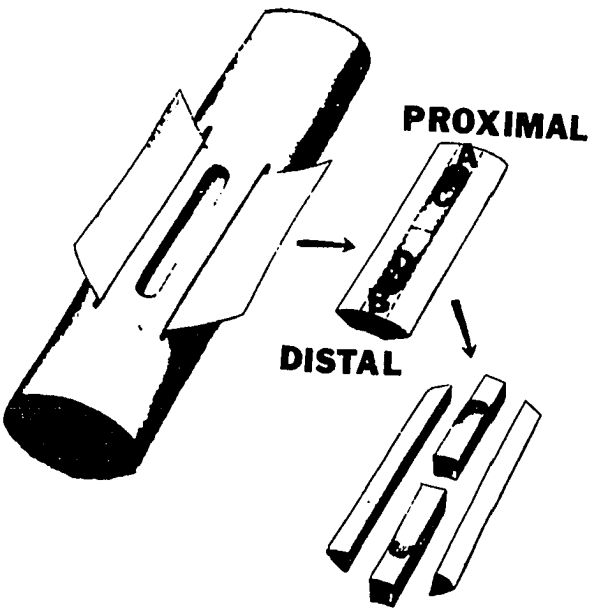

FIGURE 5. Millipore defects in the cortex of rabbit femurs (Reudi and Bassett, 1967)

was less cellular. Its collagen fibers were organized in bundles parallel to the millipore membrane and the long axis of the bone.

The millipore isolated chamber gradually became filled with fibrous connective tissue that was later transformed directly to bone. Thus, the bone formation was a type of intramembranous ossification, where a membrane is replaced by bone, rather than endochondral ossification where cartilage calcifies and is replaced by bone. Sometimes there was bone present before all of the clot was gone. When the bone completely bridged the defect it first formed a periosteal cover, converting the chamber into an arching vault.

In all specimens, the same sequence of events from fibrin to fibrous tissue to bone was followed. However, the rate that these tissues progressed through the chamber varied greatly. In the slowest specimen, complete bridging required 180 days, while in the fastest this was done in only 30 days.

Polygonal cells resembling osteoblasts were seen on the surface of trabeculae of bone in the chamber. Away from the trabeculae, toward the center of the implant, fiber bundles were less thick and the cells more spindle-shaped. The tissue between the trabeculae was poor in fibers and cells, and rich in capillaries and wide sinusoids. Its appearance

was thus very different from the dense fibrous connective tissue.

The first bone formed was woven bone. This woven bone appeared to be transformed directly to lamellar bone without creeping substitution. Creeping substitution is the process of resorption of woven bone followed by replacement with lamellar bone. How this direct transformation from woven bone to lamellar bone was accomplished is a mystery. Ruedi and Bassett (1967) suggest that individual osteocytes may be remodelling the bone in their immediate vicinity.

The specimens in the animals destroyed after one year, all showed complete healing of the defect. However, considerable variations were seen in the earlier specimens in regards to the timing of events and the amount of bone formation. Variations were attributed to five sources.

1. Whether or not the defect was placed in one femur or both femurs of the animal. If it was done in only one leg, the animal would avoid using that leg. The resulting absence of normal compressive and tensile forces being applied to that leg would hinder healing. Faster healing occurred when both legs were operated on and the animal had no choice but to use both hind legs.
2. Variations in anatomy; long legs versus short, bowed legs versus straight, thick bones versus

thin.

3. Variations in the vascular patterns of the bones. This includes both vascular variations between animals and within the same animal.
4. Gross variations in the mechanical properties of bones of different breeds.
5. Variations in age. Healing was generally faster in younger animals.

Overall healing was more active in the proximal side than the distal side. The results seem to confirm that the inner 2/3 of the cortex is supplied by vessels that originate in the medullary canal, and the outer 1/3 by vessels from the periosteum. The arrangement of fibers was generally in line with the tensile stresses. This would indicate that piezoelectric properties of the collagen may be influencing bone formation.

The progression of tissues observed in the millipore isolated cortical defects is illustrated in Figure 6.

What Ruedi and Bassett (1967) observed in the millipore isolated defect is not identical to what is seen in normal fracture repair.

In a typical fracture, the bone first responds with the usual tissue reaction of hemorrhage and organization of the clot by ordinary granulation tissue. Over time, the granulation tissue becomes a dense connective tissue.

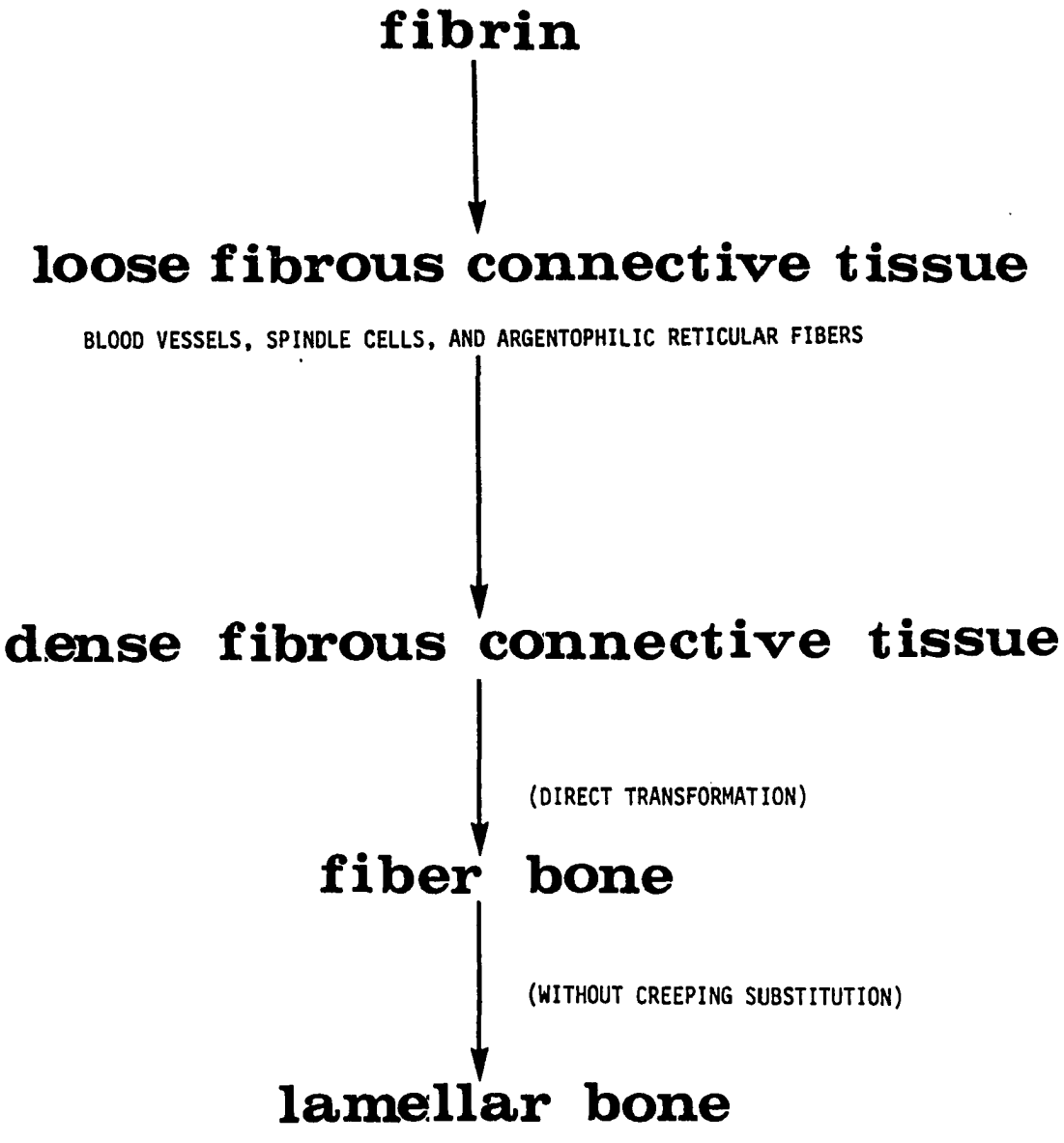

FIGURE 6. Progression of tissues observed in the chambers of millipore isolated defects (Ruedi and Bassett, 1967)

Cartilage and fibrocartilage form within it, creating what is called the fibrocartilaginous callus. The fibrocartilaginous callus fills the gaps between the broken ends. Osteoprogenitor cells, of both the endosteum and periosteum, form new bone some distance from the fracture line. A meshwork of subperiosteum trabeculae begins to form the bony callus, with a similar network emerging from the endosteum. The fibrocartilaginous callus slowly erodes with the fibrocartilage being gradually replaced by new bone, in a manner similar to endochondral ossification. A bony union occurs when trabeculae from opposite sides of the fracture merge. The cancellous trabeculae then undergo compaction and reorganization. Excess bone is resorbed and bone is remodelled so that the gap is bridged with compact bone.

Bone Induction

Numerous bone induction experiments have been done using various host sites and implant substances. Ostrawski and Wlodarski (1971) have separated these experiments into three types. In one type, living tissues are used as inductors. These transplants can be autogenic, to the same animal; allogenic (or homogenic), to another animal of the same species; or zenogenic (or heterogenic) to another animal of a different species. The second type of experiment involves transplants of devitalized or dead

tissue, and the third type involves transplants of tissue extracts or chemical substances injected or applied in some way. The living tissues that have induced bone formation include transitional epithelium, gall bladder epithelium, some stable cell lines, bone tissues, cartilage, and gastric fundus epithelium.

In the Anterior Chamber of the Rat's Eye

Urist and McLean (1952) performed a series of experiments where various tissues were placed in the anterior chamber of the rat's eye. The eye was used because it provided a readily accessible and uniform implant space not in direct contact with the muscular-skeletal system of the host. The implants were inserted through the barrel of a blunt 16-gauge needle. The eyes were removed at intervals between 6 and 36 days postoperative and fixed in a 10% solution of neutral formalin. The eyes were examined roentgenographically, by gross sectioning, and by histological stained sections.

The tissues transplanted into the eye included periosteum, muscle, fascia, tendon, capsular ligament, bone marrow, cancellous and cortical bone, viable and devitalized fibrocartilaginous callus, various types of cartilage, and blood clot from a fracture. Negative results were obtained with implants of muscle, fascia, tendon, urinary bladder epithelium, ureter, and capsular ligament. None of these

implants showed any new bone formation or absorption of donor tissue. No new bone formation was seen with implants of specimens of the organizing hematoma from fractures of the shaft of the tibia. Ear cartilage and semi-lunar cartilage failed to induce new bone formation, although autogenous epiphyseal, allogenous epiphyseal, and autogenous articular cartilage all showed bone formation within 21 postoperative days. Autogenous transplants from cancellous bone, cortical bone, bone marrow, and periosteum were all able to induce new bone growth to various degrees. The transplants of bone marrow and cancellous bone were organogenetic, meaning that they did not just induce the formation of new bone tissue, but the implants were resorbed and replaced by a sphere-shaped ossicle of bone with a primary marrow cavity and active hematopoietic tissue inside. The implants from periosteum, however, were classed as histogenetic since they produced only new bone tissue and not a complete bone organ. It is interesting to note that only the periosteum from young rats and from healing bone induced new bone growth. The periosteum from adult rats produced no new bone. Transplants from autogenous fibrocartilaginous callus induced new bone formation in 23 out of 27 rats in 10 to 36 days. However, implants from autogenous fibrocartilaginous callus that had been devitalized by boiling in normal saline or by freezing with

carbon dioxide seldom showed new bone formation. Even when they did show new bone formation, it took 4 to 5 weeks to initiate a thick capsule of fibrous tissue with limited deposits of new bone.

This was not the first time researchers had characterized bone induction from tissue implants. Barth (1893) had made observations suggesting undifferentiated connective tissue cells are transformed into bone forming cells.

The process of new bone formation characterized in the eye followed the same sequence for all tissues that formed new bone, but not all transplanted tissues caused the process to carry to completion. At the end of the first week, the transplant was attached to the iris and encapsulated in inflammatory and granulation tissue. By the second week, a two layer capsule enveloped the transplants. The outer layer of the capsule was composed of dense connective tissue while the inner layer was composed of mesenchymal cells and vascular tissue. Spindle-shaped cells, granulation tissue, and fibrocartilage cells were observed in the capsule. New bone formation began on the surface of the implant and in the space between the vascular tissue of the host and the cells of the donor. It was difficult to observe if the cells came from the host or the donor, but the ingrowing perivascular connective tissue

cells of the host appeared to be the source. This process took four to five weeks to occur in transplants of cortical bone devoid of periosteum and marrow. Even then, new bone growth was observed in only two of the ten samples. In the four samples where they were certain the cortical bone was devoid of periosteum or marrow, no new bone growth was observed. The samples were encapsulated in fibrous connective tissue, and no absorption of the implant was observed. But the more osteogenic transplants of cancellous bone and fibrocartilaginous callus showed still more absorption of the original donor and new bone growth by the third week. At this point, the appearance was the same as seen in endochondral ossification. By the fourth week, the new bone formed a complete ring around the absorbing transplant. The outer shell changed from spongy to cortical bone while cancellous bone continued to be formed inside. In the transplants of cancellous bone, the donor tissue was completely absorbed by the fifth week and replaced with a single marrow cavity filled with active hematopoietic tissue. The capsule conformed to the shape of the anterior chamber of the eye.

Competence of Various Tissues to Bone Matrix

Urist et al. (1968), did a series of experiments where an organic matrix of teeth and bone was implanted into various organs. They showed that various organs and tissues

in the rat and rabbit display various degrees of osteogenic competence. Using lyophilized allogenic bone that had been decalcified in 0.6 normal HCl at 2 degrees Celsius for 24 hours, they were able to produce new bone formation in over 90% of the implants in bone defects, bone marrow, abdominal muscle, quadriceps femoris, Achilles' tendon, subcutaneous connective tissue, and the kidney calyx. No bone formation was noted in the lymph nodes, ovary capsule, adrenal, uterus, thymus, thyroid, or parathyroid. Intermediate degrees of osteogenic competence were displayed by various other organs, including the brain, eye, lung, pericardium, testes, pancreas, ovary, mesentary, and bladder.

They more completely characterized the sequence of osteogenesis in bone induction than previous researchers had done. Although not all the steps of this sequence are completed in all tissues, the same pattern is always followed. The initial step is the invasive migration of cells from the host to the matrix of the implants. During the first five to ten days, chiefly leukocytes and mesenchymal cells invade the implant. After ten days in muscle tissue and other tissues that will subsequently produce new bone, there occurs proliferation of mesenchymal cell populations with some of the mesenchymal cells fusing into giant cells. This is followed by resorption of the matrix, and then penetration of capillary buds into the

resorption cavities. From 15 to 20 days after the operation there occurs: (1) secretion of new ground substance on the surface of the implanted bone matrix in its resorption cavities, (2) cell hypertrophy, polarization, and palisadization of basophilic mesenchymal cells, (3) pseudopodial extensions of mesenchymal cells into the microcaniculi system of the old matrix, (4) differentiation, and (5) elaboration of calcified matrix.

Urist and his co-workers also experimented with a series of two stage transplants. Their lyophilized bone matrix was first implanted in muscle. Then after new bone formation was induced, it was transferred to a visceral organ such as the spleen, liver, or kidney. These visceral organs, which normally showed no osteogenic competence, produced new bone formation in 80% to 90% of the transplants. Thus, the competent mesenchymal cells from muscle were able to produce new bone even when they were transferred to an environment normally hostile to bone induction.

These experiments tend to indicate that there is a difference in the competence, or state of readiness, of certain mesenchymal cells to differentiate into bone. Although morphologically there is no difference between mesenchymal cells in muscle and in visceral tissue, they are functionally dissimilar. Some time earlier, they had

diverged into different populations.

Induction by Other Tissue Matrixes

Bone which has been demineralized in 0.6 normal HCl induces bone formation in over 90% of the allogenic rat and rabbit muscle into which it is transplanted. Other tissues were similarly treated with 0.6 normal HCl to test their inductive ability in allogenic rat and rabbit muscle. Bone formation was not induced by kidney, liver, muscle tendon, gall bladder epithelium, or stomach epithelium. It was induced to a small extent by urinary bladder, articular xiphoid, nasal septum and ear cartilage. It was induced in 70% of the transplants of costal cartilage, and in 80% of the transplants of placenta.

Certain epithelial tissues such as that of gall bladder and urinary bladder mucosa are known to be inductive agents. Transitional epithelium tissue cultures from guinea pigs will also induce bone formation. In some experiments (Friedman et al. 1968), transitional epithelium has been encased in diffusion chambers with millipore fibers, 150 micrometers thick and 0.45 micrometers in diameter, and implanted in various tissues. The purpose of these diffusion chamber transplants is two-fold. One is to see if the induction substance will diffuse through the chamber and induce bone growth in the surrounding tissue. The second purpose is to see if induction will continue inside the

chamber without direct contact from the cells of the host. Positive results were obtained in both cases. New bone formation occurred both outside and inside the chambers.

Inductive Nature of Bone Matrix

Numerous treatments have been tried on the matrixes of bone and teeth to see what would alter their inductive ability (Urist et al. 1969). Their inductive ability was destroyed by 0.6 normal NaOH, and by the chelating agents ethylenediamine tetraacetic acid, EDTA, and ethylenebis(oxyethylenenitrilo) tetraacetic acid, EGTA. The destruction of inductive ability by decalcification with chromic and osmic acids is believed to be due to oxidation reactions with proteins. Inductive ability was reduced by treatment with acids such as formalin, HCl, trichloracetic acid, and phosphotungstic acid. Inductive ability was also hampered by freezing and thawing three times, irradiation in excess of 1.0 Mrad., ultrasound of 20,000 Hertz, and ultraviolet light of 2600 to 2800 Angstroms. Induction, however was not hampered by 0.9% NaCl at 70 degrees Celsius, irradiation of only 0.2 Mrad., and 70% ether.

The non-inhibitory treatments tend to indicate that the inductive substance is from extracellular protein of bone and not cytoplasmic tissue proteins. This is supported by the diffusion chamber experiments. The treatments that destroy the inductive properties of bone are known to cause

certain chemical and physical changes. These changes then provide clues to the nature of the inductive substance. The inductive properties are not destroyed by the extraction of lipoproteins and lipids, polysaccharides, chondroitin sulfates, and hyaluronate. Many of the treatments that destroy or limit the inductive action of the substrate share the common property of protein denaturization. Bone induction seems to be linked to the three dimensional structure of the crosslinked insoluble bone protein. Treatments that tend to destroy the quaternary structure of protein, reduce the inductive properties of the substrate. Treatments that tend to keep the covalent crosslinked structure intact, such as treatment with 5 molar potassium thiocyanate (KSCN) at 2 degrees Celsius and decalcification in dilute hydrochloric acid, do not hinder bone induction (Urist et al., 1968).

Metaplastic bone formation in the stroma of tumors of various origin is often described by histopathologists (Ostrawski and Wlodarski, 1971). Injection of Dunn osteosarcoma cell cultures in the muscles of CBA and AKR strains of cortisone-immunosuppressed mice almost invariably produce tumors somewhat different in composition from the original Dunn osteosarcoma. When triplicate subcultures of the same cells are freeze-dried to kill the tumor cells and then implanted in a muscle pouch in CBA mice, the dead cells

produce a unique response. Within one to two weeks, the host red blood vessels, macrophages, and other connective tissue cells resorb and replace the dead tumor cells with normal woven bone. By the third week, woven bone is infiltrated with osteoclasts, and by the fourth week it is remodeled into lamellar bone in the form of an ossicle filled with bone marrow (Urist et al. 1979b).

Induction by Chemical Substance

The chemicals that have been used to induce bone formation include ethanol, $AgNO_3$, $CaCl_2$, $CuSO_4$, $NaHPO_4$, chloric acids, quinine, and quinine hydrochloride. Heterotopic bone formation has been reported in man and rabbits after intermuscular quinine injections for malaria. Local irradiation by X-rays was once reported to cause bone formation in the lungs of rabbits (Engelstad, 1934). Some of the substances that produce bone formation tend to indicate that necrosis of muscle tissue liberates a bone inductor. Bridges and Pritchard (1958) investigated this by placing muscle fragments which had been devitalized by alcohol under the renal capsules of rabbits. Bone and cartilage formation was elicited, but such induction is easy to elicit in the rabbit (Ostrawski and Wlodarski, 1971).

Recent Induction Studies

Utilizing principles of induction developed by Urist (1965), Glowacki et al. (1981) were able to use demineralized bone implants for cranio-maxillofacio reconstruction and construction in 34 human patients. The clinical advantages of using demineralized bone in these cases include rapid union with the surrounding bone, the healing of large defects, avoidance of harvesting problems associated with removing patches of bone from the patient's body, and a potentially unlimited supply of banked bone.

A study by Mellonig et al. (1981) compared the inductive potential of autogenous coagulum, and autogenous bone blend, freeze-dried allograft (FDBA), and decalcified freeze-dried bone allograft (DFDBA), all applied in nylon chambers implanted in defects in the calvaria of 35 guinea pigs. In their study, both the strontium-85 uptake data and the histological examination indicated that DFDBA had a greater osteogenic potential then the other four substrates used ($p<.001$).

Their histological examination of the nylon chambers showed a blood clot after the third day, and vascular invasion with immature connective tissue, but no new bone, at day seven. By the fourteenth day, some new bone began to appear with a greater amount seen in DFDBA chambers than in the other chambers. By the 21st day, still more new bone

was seen, particulary in DFDBA chambers. By the 42nd and 55th days, bone was more abundant in the DFDBA chambers. Large areas of osseous coagulum and bone blend were walled off by new bone. The control defects, which contained empty nylon chambers, were filled with connective tissue with new bone occurring only at the wound margin.

Using demineralized bone powder and bone powder not demineralized, Kaban and Glowacki (1981) found demineralized bone powder to be the more potent induction agent in mandibular defects in rats. Their results were based on calcium-45 uptake data, gross examination, and histological examination.

It is interesting to note that in many of these recent bone induction studies, a common theme that emerges is that demineralized bone is a more potent induction agent than mineral bone. That is true regardless of whether or not the bone has been lyophilized or powdered. Urist et al. (1979a) have used demineralized bone to isolate bone morphogenic protein (BMP). The periosteal activation agent used in this study is extracted from bone chips that were demineralized by a sodium chloride solution. Rather then using the mineral in implanted bone to be incorporated into existing bone, the cells of the host must first remove the mineral component of the implanted bone matrix. After the matrix has been demineralized, it is then used as a substrate for

new bone growth.

Theories Concerning Bone Induction

In general, it can be said that the new bone growth produced by tissue implants is due to induction of the host cells, and not just transformation of the grafted tissue. The precursors of the induced chondroblasts and osteoblasts may be of local and/or peripheral origin. Cells resembling small lymphocytes infiltrate the vicinity of the inductor, and perhaps differentiate into osteoblasts. Ostrawski and Wlodarski (1971) suggest that there are two kinds of osteoblast precursors: one type that is genetically determined and forms bone tissue that is not resorbed, and a second kind that forms bone only under the influence of an inductor and can not survive long without an inductor.

Urist et al. (1968) have commented that the inductive agent directs differentiation of competent hypertrophic mesenchymal cells like a television channel selector. Many authors have noted that the direction of the differentiation of induced cells depends upon their environmental conditions. Bone is formed in heavily vascularized regions, but chondrogenesis occurs in avascular sites of implantation. This is similar to the work of Bassett (1962) on bone formation and partial oxygen pressure. However, it should be recalled that osteogenesis occurred in diffusion chambers (Friedman et al. 1968) and that the initial step of

induction is chondrogenesis in a highly vascular muscular environment.

Urist et al. (1968) have stressed that bone induction is closely related to the crosslinked pattern of the inductive matrix. Tissues that lack a highly crosslinked pattern, and highly crosslinked bone matrixes that had their covalent crosslinking destroyed, do not induce new bone formation.

Urist has proposed that a chemical stimulus derived from decalcified bone and dentine elicits bone induction. He has theorized that this substance, that he has called bone induction principle (BIP), or the bone morphogenic protein (BMP), is a moiety of a non-collagenous proteinacous nature, intimately linked to the collageneous matrix. In more recent published reports, Urist and Mikulski (1979) and Urist et al. (1979a) have claimed to have isolated a BMP. This was obtained by digestion of demineralized rabbit cortical bone matrix with bacterial collagenase. Their observations indicate that BMP is a glycoprotein with a disulfide bonded structure. The possibility exists that BMP is a protein aggregate. BMP is not species specific; rabbit BMP induces new bone formation in the rat.

Two major theories were proposed to explain the process of bone induction. They are the molecular assembly conveyer belt theory and the semiconductor theory. The assembly belt

theory proposes that noncovalently bound cell exudates travel along a connection of intercellular polysaccharides and tissue specific proteins. This would explain why some bone formation may be seen at a site some distance from the transplant, but it leaves questions about the transmission of bone induction through a millipore membrane where, as described previously, inductive matrixes have been shown to induce new bone growth without direct contact with the host cells.

The theory that has received the most attention in recent years is the semiconductor theory and its variations. These theories are based on the known effects of electrical current on bone growth. It has been shown that an electric current in the microampere range applied to bone will encourage bone growth at the negative electrode. In recent years Fukada et al. (1975) has shown that a polymer with a permanent electrical charge, called an electret (an electrical version of a magnet), will encourage bone growth when implanted in bone. Clinical applications of directly applied and directly induced electrical currents have been used to encourage fracture healing and healing of pseudarthroses in humans. It has also been shown that a nonuniform electrical field will cause cytodifferentiation of certain cells.

This theory assumes a covalently locked-in-place matrix

that acts as a polycrystalline semiconductor. The net charge on the inductive substrate is positive. The glycoamino acids in mesenchymal cell exudates serve as doping and convey a negative surface charge upon the mesenchymal cells. Thus, a solid state p-n junction is formed when a mesenchymal cell is on the surface of the inductive substrate. The matrix then acts as an emitter, the interface as a capacitor, the cell exudates as the diffusion media, and the hypertrophied mesenchymal cells as the collector. The cell membrane is the collector depletion layer component. The BMP would form and move like a stream of electrons from regions of higher to lower concentrations, from positive to negative and back from negative to positive. The polysaccharide moiety of the bone matrix may constitute an npn junction. The mesenchymal cells, including intracellular new deposits of collagen fibrils, may add a pnp junction to produce a forward bias at one junction and a reverse bias at another. Thus, circuitous or reciprocal inductive interactions of cells may develop (Urist et al. 1968).

An attempt has been made by de Groot (1973) to combine the electrical theory and the chemical theory of bone induction by proposing that the BMP has a positive charge. The electrical theory can be described by the equations:

$$M + e^- \longrightarrow O$$

where M is mesenchymal cells, e- is the electron, and O is osteogenesis. The chemical induction theory of Urist then states that:

$$M + BMP \longrightarrow O$$

By assuming the bone morphogenic protein has a positive charge, de Groot suggests:

$$e^- + BMP^+ \longrightarrow BMP^+(\text{concentrated}),$$

$$BMP^+(\text{conc.}) + M \longrightarrow O$$

The ability of several polymers to induce bone formation after they have been calcified in vivo can be explained by:

$$\text{matrix} \xrightarrow{\text{calcification in vivo}} \text{calcified matrix} + BMP^+(\text{conc.}),$$

$$\text{calcified matrix} + BMP^+(\text{conc.}) \xrightarrow{\text{decalcification}} \text{matrix} + BMP^+(\text{conc.})$$

Then,

$$BMP^+(\text{conc.}) + M \longrightarrow O$$

Although much research has been done on bone induction, there are not now enough basic data to establish any theory of induction. Bone growth by induction remains to this day, over 80 years after the first related experiments, a largely empirical phenomenon.

Activation of the Resting Periosteum

Electrical effects were credited by Tornberg and Bassett (1977) for activation of the resting periosteum. A special extract prepared from the ground metatarsals and metacarpals of calves was shown to cause an "explosive" growth of bone in the periosteum of rats. This osteogenic extract was prepared from ground bone that was first washed in a sodium chloride solution, then decalcified with hydrochloric acid and treated with pepsin. Following pepsin digestion, the extract was separated from the solid residue and then precipitated with alcohol at 4 degrees Celsius. The precipitate was then lyophilized, and then dissolved in physiological saline at a concentration of 60 mg per ml. A volume of 0.1 ml was injected along the periosteal surface of the radius-ulna complex of adult male rats. The contralateral limbs received injections of physiological saline as a control.

The proliferation of new bone was almost immediate. Within one week, the diameter of some of the experimental bones doubled. Histological and electron microscopic examinations showed that this growth was accomplished entirely by the periosteum. Within 24 hours after injection, the cells of the deep, or cambium layer, of the periosteum were transformed into osteoblastic cells. Within another 24 hours, these cells had increased their population

4-fold. By the third day, multiple trabeculae of new bone enveloped the cortex. Leading tips of trabeculae radiated toward the fibrous periosteum. Palisades of osteoblasts were seen between the trabecular projections. By the fourth day, these structures were organized into recognizable cancellous bone. Mineralization continued until the the seventh day. Over the seven day period, the active cells at the tips of the trabeculae projections gradually transformed themselves into more quiescent spindle-shaped cells. During all this active growth, the outer, or fibrous, layer of the periosteum did not participate at any time. It remained intact, and was evidently able to stretch to accommodate the enlarged bone.

Tornberg and Bassett were careful to refer to this phenomenon as "activation" rather than induction. It differed from classic induction in a couple of ways. For one thing, bone growth in previous induction studies took about 7 to 11 days to get started. In this case, it was completed by seven days after a phenomenal doubling of the bone diameter. Also, no evidence of heterotopic bone or cartilage formation was detected in attached muscular areas. Osteogenesis was confined to the cambium layer of the periosteum. Although they had no data to characterize the mechanism of this activation of the resting periosteum, they did strongly suggest that it may be of an electrical nature.

They emphasized the known electrical properties of bone, how an electrical current due to injury exists during healing of bone and how elecrical currents and electrets stimulate osteogenesis. They also pointed out that many long chain biopolymers, such as collagen and protein polysaccharides (proteoglycans) have fixed charge and behave as electrets. They suggest that the active agent may be a proteoglycan which is a strong, negatively charged polyanion that exerts its influence by means of its electret nature.

Possible Mechanisms of Periosteal Activation

It has been proposed that periosteal activation may be established by morphogens or through bioelectricity.

Morphogens

Morphogens are molecules that act as initiators or inhibitors of morphogenic development. They can be effective at extremely low concentrations. Schaller and Gierer (1973) demonstrated that a morphogen will stimulate head formation in hydra at concentrations lower then 10^{-10} molar. Berking (1977) demonstrated that another substance exists that inhibits regeneration in hydra. It is effective at concentrations of less then 10^{-8} molar.

The inhibitor that Berking worked with is a remarkably stable molecule. Its activity was not destroyed by 6 normal HCl at 110° Celsius for 24 hours, by one normal NaOH for one

hour, by Pronase B (500 μg/ml) at 37 degrees Celsius for two hours, nor by trypson (200 μg/ml) at 37 degrees Celsius for 48 hours. Like PAA, it was purified from a precipitate that was formed in an ethanol-water solution at -4 degrees Celsius. Both PAA and Berking's inhibitor appear not to be peptides. Peptides would be destroyed by the proteases.

These facts raise questions about PAA being, or containing, a similar morphogen. If the response elicited by PAA is caused by a single morphogen, then that morphogen may be a very small fraction of the total PAA extract. If such a morphogen is effective at concentrations of 10^{-8} or 10^{-10} molar, then the response elicited by PAA may be duplicated by applications of just micrograms of substance.

Bioelectricity

Lately, interest in bioelectricity has been spurred by the development of the vibrating probe. Lionel Jaffe (Purdue University) and Richard Nuccitelli (University of California at Davis) pioneered the development of this vibrating microelectrode which consists of a probe terminating in a platinum black ball, about 10 to 13 micrometers in diameter. The probe measures the voltage at the two terminal points of its vibration. From this voltage drop and the resistance of the fluid, the current density can be calculated using Ohm's law. This probe can be used to measure the current field that surrounds an individual

cell.

From research conducted by Jaffe and many others, it has been shown in a number of examples that current (defined as the flow of positive to negative) flows into the site where growth originates. Current enters at the developing end of fucoid embryos (Nuccitelli and Jaffe, 1974), of lilly pollen (Weisenseel et al. 1975), of barley root (Weisenseel et al. 1979), and through the regenerating, anucleate stalk segments of Acetabularia mediterranea (Novak and Bentrop, 1972).

When electrical currents have been artificially applied to living systems, growth and regeneration have sometimes been stimulated where they otherwise would not occur. An externally applied voltage has been able to stimulate some degree of limb regeneration in frogs that normally do not regenerate (Smith, 1967). In animals that regenerate naturally, this regeneration seems to be stimulated by currents originating in the skin. When the skin heals and covers the amputated stump, shorting the current source, regeneration will often cease (Borgens et al. 1979). Such regeneration has been shown to occur to a limited extent in humans. Children up to the age of 11 have been shown to regenerate the amputated tips of their fingers if the fingers are splinted and the skin is not allowed to cover the stumps too soon (Douglas, 1972; Illingworth, 1974;

Illingworth and Barker, 1980). In humans, artificially applied electrical currents and fields are used to treat stubborn cases of psuedarthrosis with a high degree of success (Bassett et al. 1977; Becker et al. 1977).

Is the activation response of the periosteum related to electrical phenomena? Tornberg and Bassett (1977) have pointed out that PAA may contain glycoproteins. An electrical field created by charged glycoproteins may then stimulate growth and development of the cells of the resting periosteum. The charged glycoproteins would then be stimulating bone growth in much the same way that it has been show that implanted electrets stimulate bone growth (Fukada et al. 1975).

How then do electric fields stimulate growth and development in certain cells? One possible mode of action may be through electrophoresis of essential nutrients, hormones, or morphogens to the cells of interest, and to the proper receptive areas within these cells. It has been shown that the endogenous current gradient in the oocyte-nurse cell synctium of Hyalophora cecropia (an insect) can influence the flow of charged soluble proteins within the cytoplasm. Negatively charged species will flow from the negatively charged nurse cells into the positively charged oocyte, but not in the reverse direction. Conversely, species with a positive charge will flow from the oocyte

into the nurse cells, but not in the reverse direction. Neutral proteins migrate in both directions across the cytoplasmic continuum that connect the nurse cells and the oocyte (Woodruff and Telfer, 1980). Such electrophoresis may be an important step in the growth and development of many cells.

The PAA that is applied to the periosteum may be establishing an electric field that permits such electrophoresis. Conversely, instead of establishing such a field, PAA may be providing essential morphogenic agents that are transported in such a field. PAA may be doing both, establishing or enhancing an electric field and providing morphogenic agents to transport across the field.

ANIMALS, MATERIALS, AND METHODS

Animals

New Zealand white rabbits were chosen as the primary experimental animal. Preliminary experiments on rats, rabbits, and puppies showed that PAA is generally more effective in the smaller animals. Larger mammals have larger bones and required a correspondingly larger dose of the extract, which was in limited supply. The rabbit is a small animal, but its femora are large enough to permit implant work. Since the rate of bone ingrowth and bone repair may be sensitive to differences in individuals (Weinstein et al. 1976), to minimize genetic differences only the New Zealand white strain of rabbits were used. To avoid any sexual differences, only male rabbits were used. Estrogen may have an effect on bone growth (Smith et al. 1976), and female mammals may show variations in bone growth with the estrus cycle.

To avoid differences that occur in the rate of bone repair with age, an attempt was made to use young rabbits of the same size. The average weight of the rabbits used in the two main series of experiments was 2.17 kg, with a standard deviation of 0.24 kg, and a range of 1.59 kg to 2.64 kg. These were the weights at the time of surgery.

Preliminary experiments were performed on rats,

rabbits, and puppies to assay the potency of the activation agent used.

Porous Material

The required characteristics of a porous implant material include compatibility with the living tissues, a pore structure that is well characterized and exhibits an average pore size large enough to permit bone infiltration, and sufficient mechanical strength to withstand the forces applied to it by the organism. All these characteristics are met by the high density polyethylene material, Biopore®, produced by Glasrock[2]. High density polyethylene has been shown to be biocompatible (Spector et al.1976; Klawitter et al. 1976; Spector et al. 1979). It is available with an average pore size of 127 μm in diameter, which is large enough to permit bone ingrowth (Klawitter et al. 1976). Also, preliminary work with fabrication and implantation of ultra high molecular weight polyethylene was performed (Ferguson, 1976; Alberts, 1978).

The manufacturer produced the material as cylinders 4 mm in diameter. At the time of surgery, they were cut to the appropriate length, about 8 mm, to fit through one

---

[2] Lot number 814112. Made from medical grade high density polyethylene lot number MM0877. Glasrock, 7380 Bohannon Road, Fairburn, GA.

cortex and the medullary canal of a rabbit's femur. The pore size distribution, as found by mercury intrusion porosimetry by the manufacturer, is shown in Table 1. The average pore volume is 46.8%.

TABLE 1. Pore size distribution of Biopore® high density polyethylene implants, as found by mercury intrusion porosimetry.

Pores Less Than	Percent,%
350 μm	92.5
233 μm	86.2
175 μm	65.7
140 μm	38.9
117 μm	10.5
88 μm	9.0
58 μm	7.5
35 μm	6.0
12 μm	3.7

Prior to surgery, the Biopore® cylinders were washed with distilled water in an ultrasonic bath to remove any loose particles. They were washed for at least 15 minutes in an ultrasonic bath, and then with running distilled water for 5 minutes. They were not washed with a surfactant, as it is very difficult to remove such material from the porous material. Prior to implantation, the material was autoclaved at 121° Celsius.

Extraction of PAA

The procedure outlined in U.S. Patent 3,458,397 (Myers et al. 1966) was followed to obtain the activation extract from cancellous immature bovine bone. Twenty kilograms of cancellous bone samples from waste calf ribs were shipped from Dubuque, Iowa[3]. After 9 kg of soft tissue was removed, the bones were ground in a large meat grinder at the Iowa State University Meat Laboratory into particles about 2 mm in diameter. A total of 11.3 kg of ground bone was recovered. A box diagram outline of the extraction procedure is shown in Figure 7.

Salt Extraction

The cancellous bone was agitated in a 15% NaCl (w/w) solution at 0^0 Celsius to 4^0 Celsius for 13 hours. A volume of 1.5 liters of NaCl solution per kilogram of bone was used. The solvent was then removed from the ground residue by extrusion through cheesecloth. A second salt extraction was performed on the ground residue for 21 hours, and a third extraction for 22 hours, for a total of 56 hours. The sodium chloride solution used for each extract was discarded. The remaining residue from the cancellous bone weighed 9.77 kg.

---

[3] Blue Ribbon Foods, Ltd., 698 White Street, Dubuque, Iowa.

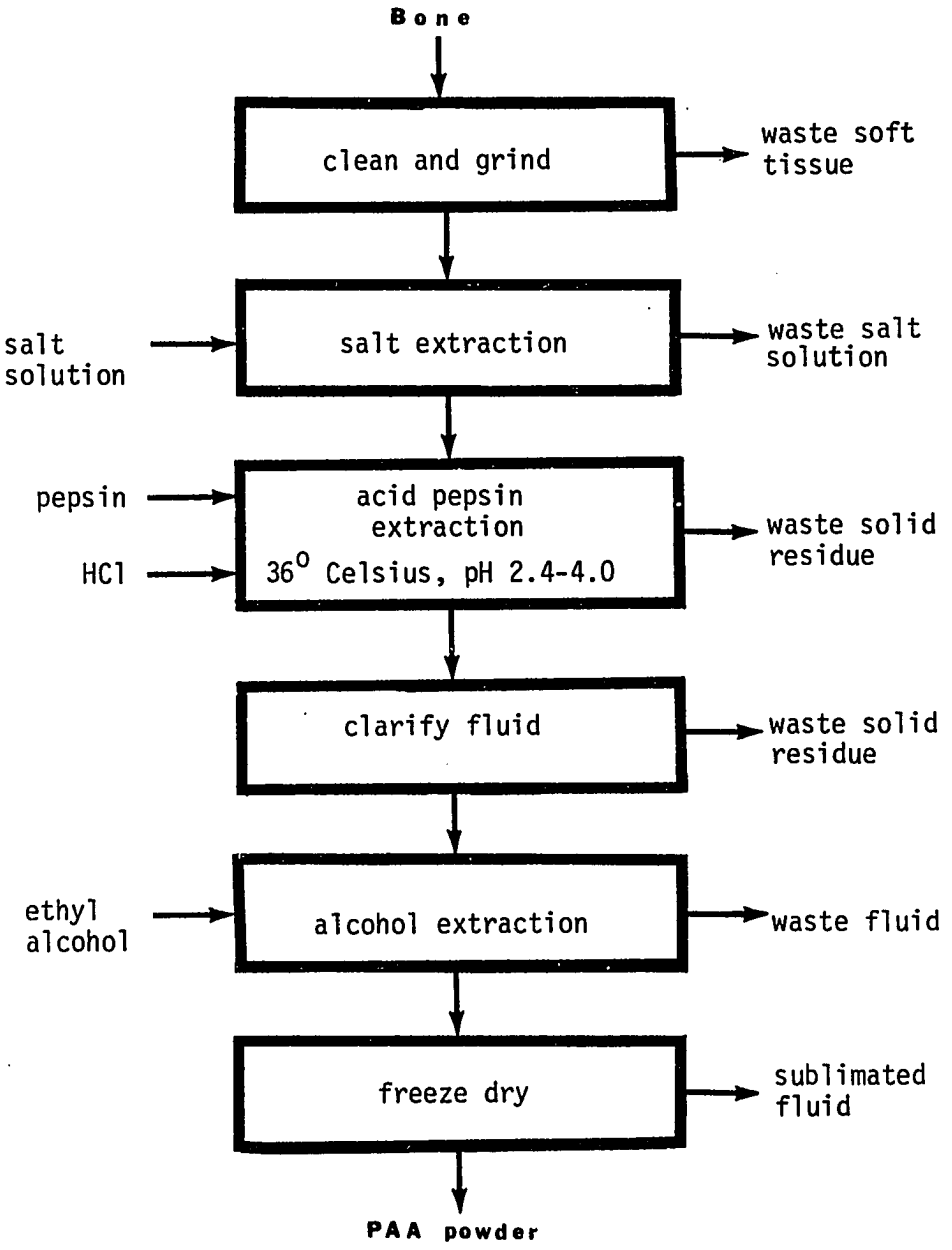

FIGURE 7. Diagram of steps used to extract PAA following U.S. Patent 3,458,397 (Myers et al. 1966)

Acid-Pepsin Extraction

The remaining residue was divided into two batches, and each batch was agitated in distilled water at 36° Celsius for 15 minutes. The pH was maintained at between 2.4 to 4.9 with 6 normal HCl. Pepsin was then dissolved in the solution (10g/kg of bone residue). Agitation was continued with a bent glass stirring rod for 45 hours. The container was loosely covered with parafilm which was lifted occasionally to adjust the pH.

Clarification of Extract

The acid-pepsin extract was separated from the ground residue by extrusion through cheesecloth. About 2.7 kg of solid residue remained from both batches. This solid residue was discarded, and over 27 liters of turbid extract was saved.

The extract was centrifuged in small batches at about 2200 revolutions per minute in a 15 cm diameter centrifuge (1200 x G) for 30 minutes. The solid layer was discarded, and a total of 26.4 liters of turbid extract remained. This extract was then filtered through coarse filter paper. The pH of the clear and slightly yellow filtrate was adjusted to 2.50 with 6 normal HCl.

Alcohol Extraction

The clarified extract was adjusted to pH 2.5 and cooled to 4° Celsius. Ethyl alcohol which was cooled to -20° Celsius was added to produce a 30% (v/v) ethanol solution. The alcohol was added throughout a two minute period while the extract was being stirred. The extract was refrigerated at 4° Celsius overnight. In numerous batches, the extract was then centrifuged at 9,000 revolutions per minute in a 0.8 cm radius centrifuge (13,000 x G) at 3° Celsius for 30 minutes. The precipitate was saved and slurried in about one liter of distilled water, and the pH was adjusted to 6.98.

The slurry was transferred into sterile glass containers and lyophilized. From 11.3 kg of ground cancellous bone, about 65 g of freeze-dried extract was obtained.

Storage

The lyophilized powder was stored at -9° Celsius. When needed, the powder was dissolved or slurried in pyrogen free physiological saline at a concentration of 100 mg per ml.

Potency Assay

The potency of the extract was assayed by injecting varying amounts of the PAA along the periosteal surface of the radius-ulna complex of mature, 200 g, male rats and

along the periosteal surface of the femurs of male rabbits and male puppies. A week later, each animal received a two microCuries intrathoracic injection of strontium-85 HCl. The animals were killed the next day, and the radioactivity of their bones that had received the PAA extract was compared to the activity of the control contralateral bones that had received an injection of pyrogen free physiological saline. Since strontium is absorbed by growing bone, the ratio of the activity of the experimental limb to the activity of the control limb gave a measure of the potency of this batch of extract. The potency of the substance was expressed by the formula:

$$\frac{(\text{experimental femur} - \text{bkg})}{(\text{control femur} - \text{bkg})} \times 100 = \text{Potency Value.}$$

Potency values above 100 indicate enhanced osteogenic activity in the treated bone. This radio-tracer technique is similar to what other groups have used to measure new bone growth relative to a control (Myers et al. 1966; Mellonig et al. 1981; Kaban and Glowacki, 1981). A brief review of radiation statistics with examples is given in Appendix A.

In the potency assay on the rabbits in Table 4, a special technique was performed to optimize the counting geometry. The midshafts of the femurs were ashed and ground into a powder that was placed in test tubes of uniform size.

The base of each test tube was then mechanically lowered into the well detector of a Picker deep well counter that was used for all the radiation measurements in this study. If the rabbit femurs were counted whole, the part of the femur near the top of the well would not be counted as well as a part deep in the well of the detector. The radiation measured from a given source decreases proportionally to the inverse of the square of the distance of the detector from the source. To provided all potency samples with a more uniform and homogenous geometry, samples were powdered and placed in the bottom of test tubes of uniform size. The data from these samples are expressed as ratios of counts per minute per milligram of sample.

For the rest if the study (i.e., the endosteal activation series, the implant series, the empty defect series, and other potency assays), ashing the radioactive bone samples was not performed for three reasons. First, ashing the radioactive samples and grinding them into a powder was hazardous work. Second, the ashing and grinding technique destroyed the sample, making it unavailable for histological examination. Third, adequate geometry for radiation counting could be acquired by sectioning the samples into small segments, and counting each segment individually.

For the data in Table 5 and for the rest of the

radiation data, the counting geometry was improved by dividing the femur into smaller sections so that the pieces were in contact with the detector, but separated. The main disadvantages of this method are that it does not homogenize the samples as well, and it does not provide as uniform a geometry as the ashing method does. A discussion of the counting geometry and the self-absorption problem is given in Appendix B.

Sterility Assay

A culture test performed on the extract in a petri dish showed no bacterial growth after three days.

Surgery

In the empty defect (ED) series and the implant (I) series, aseptic surgery was performed on the rabbits so holes could be drilled in their femurs. The rabbits were anesthetized with intermuscular injections of acepromozine maleate[4] (16 mg/kg of body weight), xylazine hydrochloride[5] (3 mg/kg of body weight), and ketamine hydrochloride[6] (50 mg/kg of body weight). Acepromozine, a tranquilizer, was

---

[4] Bristol Laboratory, Division of Bristol-Myers Co., Syracuse, N.Y.

[5] Rompon, Baynet Division, Cutter Laboratories, Inc., Shawnee, Kansas.

[6] Fort Dodge Laboratories, Inc., Fort Dodge, Iowa.

the first one injected. Five minutes later, the xylazine and ketamine were injected. Xylazine is an analgesic drug, and ketamine is an anesthetic drug.

The surgical area over the femur was shaved and scrubbed. The subcutaneous fat and superficial fascia were excised directly under the skin incision. The fascia lata that connects the biceps femoris muscle and vastus laterolis muscle, were incised along the cranial border of the biceps femorous muscle. Gelpi clamps were used to retract the biceps muscle caudally and to retract the vastus latus muscle to excise the fascial intermuscular septum between these muscles on the lateral side of the bone. When the bone was exposed, incisions were cut in the periosteum so that a flap of periosteum could be folded away from the area to be drilled. Holes, 4 mm in diameter, were then drilled in each femur using a hand operated drill and bit. The defects were drilled through the cortex and through the medullary canal, but not through the opposite cortex. Two defects were drilled in each femur. The first defect was drilled 20 mm distad from the third trochanter, and the second defect was drilled 20 mm distad from the first defect.

To optimize data which could be collected for each rabbit, a maximum of 2 holes were drilled in each femur. A greater number would have resulted in a high incidence of

failure due to fracture.

In the ED series, the holes were left empty, while in the I series the defects were filled with a Biopore® implant. The empty defects were designed to permit the observation of the effects of PAA on a reproducible defect. The geometry of other types of defects that could have been used, such as a fracture or a chip, would have been difficult to repeat exactly. A fracture defect would have caused other complications. The animal would have needed a cast, or braces, or bone plates to aid healing and to avoid unnecessary suffering to the animal. The purpose of using the Biopore® implant was to examine the effects of PAA on bone ingrowth into a porous implant. The implant was first pressed into the defect until its end abutted against the opposing endosteum and the other end protruded out of the defect. The point where the cylindrical implant met the outer edge of the lateral cortex was marked on the implant. The implant was then removed, and the implant was cut at that point. The shortened implant was then pressed back into the defect so that it was flush with the periosteum of the femur and it did not protrude out of the defect. Illustrations of positioning of the implants into the defects are shown in Figure 8 and Figure 9.

The flap of periosteum was then carefully placed back over the defect, or over the implant in the defect, without

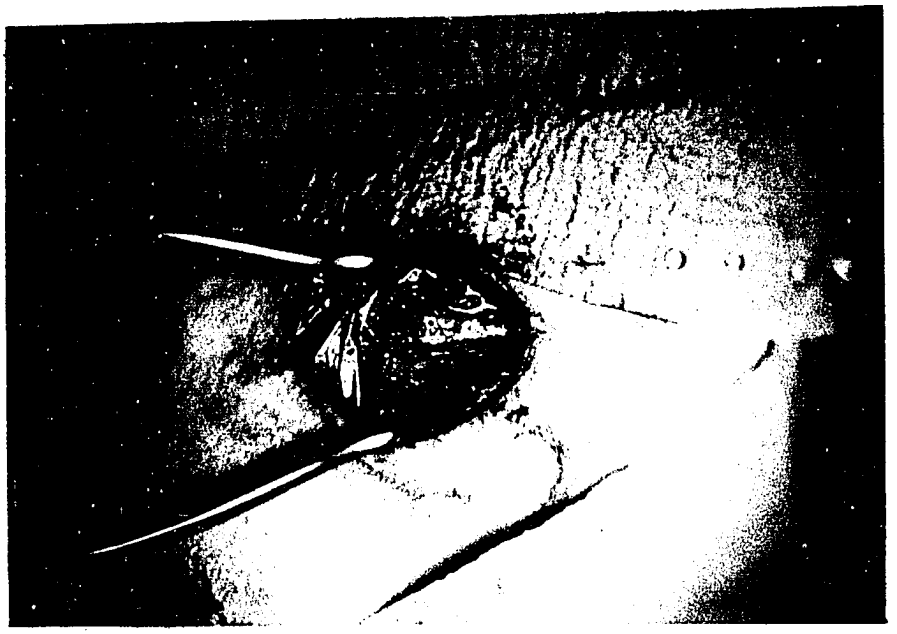

FIGURE 8. Exposure of femur showing the distal defect

FIGURE 9. Femur showing a protruding cylindrical implant

suturing it. The wound was sutured shut in three tiers of sutures. The fascial lata was first sutured to the cranial border of the biceps femoris muscle in one tier,[7] the subcutaneous fat and fascia were sutured in the second and the skin was sutured in the third tier[8].

An identical surgery, with either empty defects or implants, was then performed on the contralateral femur. In each animal, one femur served as the experimental femur while the other served as the control femur.

So as not to interfere with bone growth and repair, no antibiotics were given to the animals after surgery.

Periosteal Application of PAA

Seven days after surgery had been performed on both femurs (long enough to permit healing of the periosteum), pyrogen free physiological saline containing 100 mg of PAA per ml of volume was injected along the periosteal surface of the experimental femur. The contralateral control femur received an identical injection of the same saline, but without any PAA. The PAA was applied so that 400 mg was delivered per kg of body weight. Thus, a rabbit that

---

[7] Silk or polypropylene. Ethicon, Inc., Somerville, N.J.

[8] Vetafil. Processed from imported materials by S. Jackson, Inc., Washington D.C.

weighed 2 kg received an injection of 8 ml of fluid in each femur. This dosage was selected on the basis of results from the potency assay. Both the PAA saline solution and the control saline solution were injected using sterile 18 gauge needles. The needle was pierced through the overlying skin and muscle. The surgical wound was not reopened to apply PAA. The third trochanter was palpated to use as a reference point for the placement of the needle. The first defect was 20 mm distad from the third trochanter and the second defect was 40 mm distad. Half of the solution was injected over the site of the proximal defect and the other half over the site of the distal defect. The solution was extruded from the needle with the bevel of the needle held flat to the periosteal surface of the bone while the needle was pulled from proximal to distal, from about one cm above the defect to about one cm below the defect, passing over the defect. This motion was repeated until half of the solution for that femur had been extruded, and then the rest of the solution was similarly applied over the other defect in the femur.

Experimental Series

Three series of experiments were performed, the empty defect (ED) series, the implant (I) series, and the endosteal activation (EA) series. These series can also be

compared with the rabbits used in the potency assays. In the potency assays, there were a set of rabbits that had PAA applied to the periosteum of one femur without any previous surgery. The contralateral femur was a control. There were also rabbits in the potency assays that did not have any PAA applied to either femur. In the ED series, two holes 4 mm in diameter and 20 mm apart were drilled in the femurs. They were drilled through the lateral cortex and through the medullary canal, but not through the opposite cortex. The holes were left open without an implant being inserted. Seven days after surgery, 400 mg of PAA per kg of body weight were injected along the periosteal surface of one of the femurs and an equal volume of pyrogen free saline was injected along the periosteal surface of the contralateral femur as a control. The rabbits were then sacrificed at periods of 1, 3, 5, 7, 10, and 14 days after the application of PAA. Three rabbits were used for each time period.

The implant (I) series was performed exactly as the ED series, except in the I series, porous implants were placed in the holes drilled in the femurs. As in the ED series, PAA was injected along the periosteal surface of the femurs one week after surgery at a dosage of 400 mg per kg of body weight, and the contralateral femur was used as a control. In the I series, the rabbits were sacrificed at periods of 1, 3, 5, 7, 10, 14, and 56 days. Three rabbits were used

for each time period.

The endosteal activation (EA) series was a study of the effects of PAA on the endosteum. Although Tornberg and Bassett (1977) had stated that PAA only affected the periosteum, it actually had not been applied to the endosteum in that study. Since the endosteum is also an active participant in bone growth and repair, it was decided that it would be worthwhile to specifically investigate its effect on the endosteum.

The endosteal application of PAA was accomplished by inserting a long 18-gauge needle into the medullary canal, through a hole punched in the trochanter fosse (at the proximal end of the femur). PAA was then slowly injected as the point of the needle was moved from the distal to the proximal end of the medullary canal. This was repeated until all of the PAA had been applied.

The first rabbits that received an endosteal application of PAA, received it a week after defect surgery had been performed on them as in the ED series. Holes, 4 mm in diameter, were drilled in their femurs and left open. This preliminary procedure for the EA series was abandoned due to a high mortality of rabbits. Nearly all of the rabbits involved died from an anaphylactic-type response within hours after the intermedullary application of PAA in a dosage of 300 mg to 400 mg per kg of body weight.

However, due to an unusually high activation ratio in the one rabbit that did survive this preliminary procedure, it was decided to continue with a modified EA series. This rabbit had an activation ratio for the entire femur of 2.361, which is higher than any activation ratio in either the I or ED series.

In the modified EA series, survivability of the rabbits was improved by implementing three changes in the procedure. First, the rabbits did not suffer the trauma of a defect surgery as was done in the ED series or the I series. Except for the small hole needed to permit entry of an 18-gauge needle, holes were not drilled in the femurs of the EA series rabbits. Second, to prevent embolism, an amount of medullary material and fluids equal to the volume of fluid to be injected was removed from the medullary canal of each femur immediately prior to the application of PAA. Third, the amount of PAA applied was reduced to 100 mg per kg of body weight. In the endosteal activation series, rabbits were sacrificed at time periods of 1, 3, 5, 7, and 10 days. At least four rabbits were sacrificed at each time period.

Characterization Procedures

Gross Examination

When the rabbits were killed and their bones were removed, observations were recorded of the gross appearance of the bones and overlying soft tissues. Measurements were also made with a micrometer to estimate the surface area and volume of the midshaft region of representative specimens from the femurs of male rabbits, the femurs of male rats, and the radius-ulna complex of male rats used in this study. The surface area was estimated by assuming the cross sectional surface area of the bones to be elipses. For each measurement, an average was made from three specimens.

Strontium-85 Tracer, Segmenting, and Sectioning

Twenty-four hours before an animal was killed, it was given an intrathoracic injection of 0.2 microCuries of strontium-85. Then, after an animal was killed with an overdose of sodium pentobarbital,[9] the PAA treated femurs and control femurs were removed, cleaned of excess tissue, and fixed in neutral buffered formalin. Material was stored in buffered formalin for periods up to 14 days. The control femurs were the contralateral femurs that had experienced the same surgery, but had not received any PAA.

---

[9] Sleepaway, Fort Dodge Laboratories, Inc., 4713 D Street, Fort Dodge, Iowa.

Each femur was cut into three test segments as shown in Figure 10. When cutting these segments, the blade of a Stryker saw was guided by pre-cut grooves in a plexiglass template to give segments of reproducible length. The "mid" segments were always 10 mm long and were located midway between the defects. The "proximal" segment contained the proximal defect, and the "distal" segment contained the distal defect. The proximal and distal segments were always 15 mm long. This type of sectioning allowed most of the midshaft of the femur to be counted for strontium-85 decay.

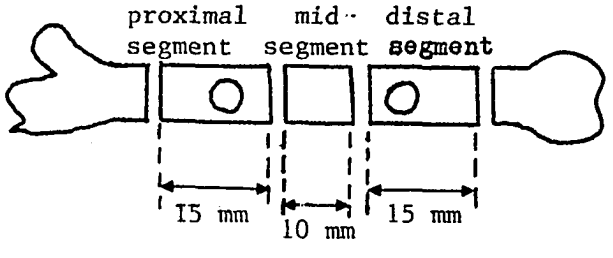

FIGURE 10. Division of femur into three segments.

Each segment was placed in a separate test tube with 2 ml of neutral buffered formalin. Each test tube was then counted in a Picker deep well counter[10] that was adjusted to selectively measure gamma rays of an energy characteristic

---

[10] Picker Nuclear Autowell II, Automatic Sample Changer. Intertech, Inc., 333 State Street, North Haven, Connecticut.

for strontium-85 decay. The counter was adjusted by placing a strontium-85 standard in the counter and adjusting the appropriate potentiometers until the maximum count rate was obtained. Identical test tubes, containing 2 ml of neutral buffered formalin with similar bone segments taken from rabbits not treated with strontium-85, were used to measure the background radiation. From these counts, an activation ratio was calculated for each segment (Myers et al. 1966) such that:

(Count from a segment from the experimental femur - background)/

(Count from identical segment from the control femur - background)

= Activation Ratio

Such a ratio adjusts for slight differences in the amount of strontium individual rabbits may have received, and also adjusts for differences due to radioactive decay in samples that could not be counted at the same time after harvesting. However, when the samples were counted, paired samples from the same rabbit were always counted within minutes of each other. An activation ratio greater then 1.0 indicates enhanced bone growth in the experimental femur, and one equal to or less than 1.0 indicates no enhanced bone growth in the experimental femur.

The uptake of strontium by bone occurs primarily by two

methods. One method is through incorporation into new bone, and the other method is by surface exchange and diffusion with calcium and strontium in the extracellular fluid into old bone. A study by Elves (1974) attempted to measure the fraction of strontium tracer that was in the bone due to new bone formation. He showed that after 24 hours, 78.6% of the strontium taken up could not be washed away by elution with $CaCl_2$. It can be assumed that most of this "non-elutable" strontium had been incorporated into new bone. The problems of the counting geometry and self-absorption by the sample are discussed briefly in Appendix B.

Demineralization and Preparation for Staining

After the segments from the rabbits had been counted, the segments from some of the rabbits were selected for microscopic histological examination and for computerized image analysis to measure the amount of bone ingrowth. The samples from 7 rabbits from the ED series, 13 rabbits from the I series, and 7 rabbits from the EA series were selected on the basis of having exceptionally large or exceptionally small osteogenic values. At least one rabbit was selected from each time period of each of the series. From these rabbits, the proximal and midsegments were demineralized in ethylenediamine tetraacetic acid (EDTA) so that they could be thin-sectioned and stained for histological examination. The distal segments from the ED series and the I series were

stained and demineralized using Lillie's silver impregnation technique for bone (Lillie and Fullmer, 1976) so that the amount of bone ingrowth into the implants could be quantitatively measured using computerized image analysis. Lillie's technique stains only calcium bearing tissues black, which makes it ideal for computerized image analysis.

The demineralizing proximal and midsegments were kept on top of cotton matting inside of test tubes filled with EDTA. The cotton matting kept the samples near the top of the EDTA solution to enhance demineralization. The EDTA solutions were changed every three days. The total demineralization procedure took about two months. Personnel from the Environmental Health and Safety office of Iowa State University verified at the end of the demineralization process that the bone samples did not have radioactivity significantly above background levels.

When completely demineralized, the proximal and midsegments were cut with a razor blade so that a microscope section could be taken from the desired plane. The proximal section was cut through the center of the defect as shown in Figure 11. A 6 μm thin section was then taken from the plane perpendicular to the long axis of the bone, through the center of the implant or defect.

A similar section was taken from the midplane of the midsegment as shown in Figure 12.

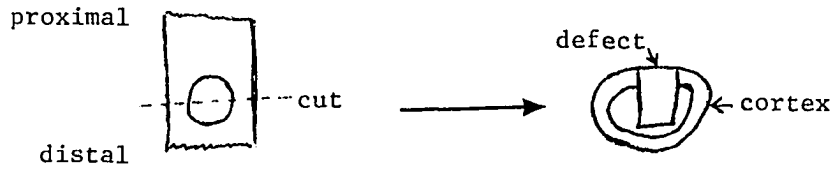

FIGURE 11. Transverse slice and cross section from proximal segments

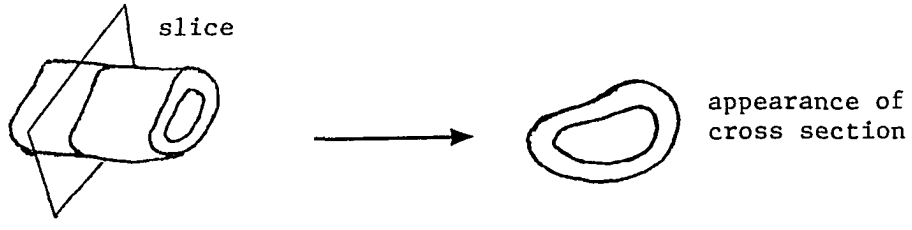

FIGURE 12. Transverse slice and cross section from mid segment

Stains

The primary stains used in this study were hematoxylin and eosin (H and E) and Lillie's silver impregnation technique (Lillie, 1928). The H and E stain was applied to demineralized tissues and the Lillie's silver stain was applied to hard samples.

Hematoxylin and eosin is probably the stain most frequently applied to demineralized bone. The bone matrix absorbs the eosin stain which turns the matrix a pinkish red. New woven bone tends to have more of a purple hue. Basophilic tissues such as cell nuclei absorb the blue hematoxylin stain.

Lillie's silver impregnation technique uses silver nitrate. To enhance penetration of the silver nitrate, the bone samples were cut into sections 2 mm thick with a jewelers saw and treated in a silver nitrate solution at 37° Celsius for two weeks. After the stain had been applied, the samples were demineralized in Ebner's decalcification solution (Lillie, 1928). The complete procedure followed is listed below:

1. 70% alcohol, one day
2. 90% alcohol, one day
3. 100% alcohol, one day
4. 100% benzene, one day to remove fats that may interfere with absorption of the silver nitrate stain
5. 90% alcohol, one day
6. 70% alcohol, one day
7. distilled water, one day
8. 2.5% (w/w) silver nitrate solution in a water bath at 37° C, two weeks with one change of

solution

9. Ebner's decalcification solution (150 ml sodium chloride saturated distilled water, 150 ml distilled water, 4.5 ml concentrated HCl). Each sample was placed in 6 ml of Ebner's decalcification solution, and every day 0.06 ml of 3 normal HCl solution was added to each sample until it was demineralized, typically 90 days for samples this size.
10. Rinse in half saturated sodium chloride solution, four days
11. Rinse in running tap water, one day
12. 70% alcohol

The samples were then embedded in paraffin and thin-sectioned.

Lillie's silver impregnation technique stains all calcium bearing tissues black, while other tissues are left either unstained or stained light brown. It is a treatment that clearly distinguishes bone, but not new bone from old bone.

For the hematoxylin and eosin stain, cross sections cut from the EDTA demineralized samples were stored in 10% neutral buffered formalin for at least 24 hours. They were then taken through increasing solutions of alcohol, 70%, 95%, and absolute, to dehydrate them. Before being embedded

in molten paraffin, they were soaked in xylene to remove the alcohol. Thin sections six micrometers thick were cut from the paraffin blocks with a microtome. The thin sections were mounted on microscope slides and soaked in the following series of solutions:

1. Xylene
2. Absolute alcohol
3. 95% alcohol
4. 70% alcohol
5. Distilled water
6. Hematoxylin
7. Acid alcohol
8. Lithium carbonate
9. Distilled water
10. Eosin
11. 95% alcohol
12. Absolute alcohol
13. Xylene

A series of special stains were applied to corresponding control and experimental femur samples from the 7 day period of the endosteal activation series. One sample was taken from each leg. Once a sample was demineralized and embedded in paraffin, a minimum of five 6 μm thick sections were cut from it, and each section was stained with a different dye. The stains used on this

sample comparison were: Gomori's reticulin to bring out reticular fibers, Masson's trichrome for collagen fibers and fibrin, periodic acid-Schiff for carbohydrates, alcian blue at pH 1.0 for sulfated glycoaminoglycans, and alcian blue at pH 2.5 for glycoaminoglycans, in general. The procedures for each of these special stains are given in the Manual of Histological Staining Methods of the Armed Forces Institute of Pathology, Third Edition (Luna, 1968).

Gomori's reticulin (Gomori, 1937) is a silver stain that is used to distinguish reticular fibers which are stained black, while collagen fibers are stained red or purple.

Masson's trichrome (Masson, 1929) stains collagen fibers either green or deep blue. Cartilage and bone are stained lighter shades of blue, and fibrin is stained red.

Periodic acid-Schiff (PAS) (McManus, 1948) reacts with carbohydrates, turning them red. Fibrin shows as red to pink.

Alcian blue (Lev and Spicer, 1964) is a stain for glycoaminoglycans. At pH 1.0 it is selective for sulfated mucosubstances, while at pH 2.5 it is a general stain for mucosubstances.

These stains will distinguish certain fibers, tissues, and substances that may be involved in new bone formation. For example, an increase in glycoaminoglycans, particularly

sulfated glycoaminoglycans, is associated with the early development of bone in the mammalian fetus. In endochondral ossification, bone is first formed by cartilage cells of chondrocytes. After the chondrocytes begin to mineralize, they hypertrophy and are replaced by a vascularized front of new bone formation. Masson's trichrome stain can illustrate these steps. Reticular fibers found in medullary tissue may or may not be involved in bone formation in this study. Where there are cells that are very active, there may be an enhanced presence of carbohydrates, and this can be illustrated by the PAS stain.

Image Analysis

The purpose of using image analysis was to quantitatively measure the area of new cancellous bone growth seen in the microscope slides from the empty defect and implant series and to measure the area of bone ingrowth in the slides of the implants from the implant series. The area of cancellous new bone was measured from photographic enlargements of the slides using an electronic planimeter, the MOP-III,[11] for the proximal and distal segments, and measured directly from slides using the MOP-III in conjunction with the camera lucida for the midsegments. A camera lucida is a simple light tube that projects an image

---

[11] Carl Zeiss, Inc., 444 5th Avenue, New York, NY.

onto a surface. The measurements of the areas of bone ingrowth were made with the Quantimet® Image Analysis Computer[12] from photographic enlargements of the implant areas stained by Lillie's silver impregnation technique for bone.

The microscope slides from the proximal and distal segments were photographed with Kodak Technical Pan film 2415[13] with a Zeiss "Tessovar" photomicroscope[14]. The slides stained with hematoxylin and eosin were photographed through a Kodak gelatin filter No. 13G (green), at a magnification of 2.5, and with the automatic shutter set at an ASA of 37.5. The slides stained by Lillie's silver impregnation technique (only distal segments) were photographed with no filter, and with an ASA setting of an automatic shutter of 25. A magnification of 2.5 was used if the entire sample was being photographed; a magnification of 4 was used if just the implant was being photographed. The film was developed in a 1:1 solution of D-76 developer[15] for eight minutes, then placed in Kodak stop bath for 30 seconds, and followed by two minutes in Kodak rapid fixer,

---

[12] Imanco, Image Analysis Computers, 40 Robert Pitt Drive, Monsey, N.Y.

[13] Eastman Kodak Company, Rochester, N.Y.

[14] Carl Zeiss, Inc., 444 5th Avenue, New York, N.Y.

[15] Eastman Kodak Company, Rochester, N.Y.

before being rinsed in running water for about 5 minutes.

Prints of the slides were made on 20.3 cm by 25.4 cm (8 inches by 10 inches) Kodak polycontrast R.C. or Kodabrome II R.C. paper. With each roll of film, at least one photograph was made of a ruler to determine the actual magnification of the final print.

An electronic planimeter, MOP-III, was used to measure the area of apparent new cancellous bone seen on both photographs of the H and E stained slides and the slides stained by the Lillie's technique. The photographs were placed on a special table that carried magnetic fields which were sensed by a stylus. The stylus was then used by the operator to outline the perimeter of the tissue being measured. As the stylus moved, it sensed the surges of magnetic fields that moved in the X and Y directions. The magnetic surges were counted by the MOP-III computer and translated into X and Y coordinates. The computer was programed to use these coordinates to calculate the area of the space outlined by the user operated stylus.

With the H and E stained slides, tinctural guides and cement lines were used to outline the apparent parimeters of the new bone formation. On the slides stained with the Lillie's technique, there were no intermediate shades of the stain; the tissue was either stained deep black or hardly stained at all. On these slides, less information was

available to outline the general area of new cancellous bone. Separate measurements were kept of new bone that formed on the periosteum of the samples, and bone that formed on the defect or inside the medullary canal. The area of new bone on the slides from the midsegments could be more conveniently measured by using the camera lucida[16] in conjunction with the MOP-III. This technique eliminated the need to photograph the slides. A light emitting diode was affixed to the end of the stylus used to mark the outline of areas on the MOP-III table. The camera lucida projected the image of this light on to the image of the slide as viewed by the operator through the microscope. By moving the stylus around on the MOP-III table, the operator, with some practice, could make the image of the light appear to travel along the border of the tissue of interest seen in the slide. When the projected light image had completely encircled this tissue, the MOP-III gave an area measurement that was calibrated to the actual area of the tissue seen in the microscope.

The Quantimet® Image Analysis computer was used to measure the area of bone ingrowth in the implants from the silver nitrate stained distal segments. Lillie's silver impregnation technique for bone was selected for this

---

[16] Carl Zeiss, Inc., 445 5th Avenue, New York, N.Y.

because it stains deep black only calcium bearing tissues. Photographic enlargements were made of the implant in these segments, and the area of the implant was cut out of each photograph. The photographs of just the implant areas were provided to Barry Ritman[17]. Using the Quantimet® image analysis computer, Mr. Ritman measured the total area of the deep black phase on each photograph and the percentage of the photograph covered by the deep black phase.

A Quantimet® image analysis computer works by dividing a viewing surface into as many as 605,000 picture points. A densitometer determines the light intensity at every picture point, and assigns to each a six bit binary code between 1 and 63, equivalent to the true log of the optical absorption at that point. A range setting system can then extend the optical density range up to 3.00 optical density units. The operator then selects an optical threshold that separates the darkly stained calcified material from the more lightly stained non-calcified material, so that nearly all of the calcified area lies on one side of the threshold and the uncalcified area on the other side of the threshold. The computer can then be commanded to give the number of picture points that fall in the dark area and the number that fall in the light area. The Quantimet® system includes

---

[17] Barry Ritman, College of Dentistry, The University of Iowa, Iowa City, Iowa.

a television screen that illustrates the areas of different light intensity on the slide. This television image gives the operator feedback on what the computer is classifying as "bone". The threshold can be adjusted until the best fit is reached.

RESULTS

Potency Assays and Preliminary Experiments

Since different extacts of PAA display different potencies, a new potency assay must be done for each extract. Potency values from rats, using PAA from a trial batch, and PAA from the extraction used in this study are shown in Tables 2 and 3, respectively. Similar potency experiments were performed on the femora of puppies and of rabbits to examine its effects on different species. These results are shown in Tables 4, 5, and 6.

In Table 2, the potency values obtained from each individual rat generally increased with increasing dosage of PAA until a plateau was reached at about 120 mg/kg of body weight. In Table 3, the potency values obtained for a dosage of 125 mg/kg of body weight were similarly greater than those obtained with a dosage of 75 mg/kg of body weight. However, the potency values from the batch of extract used in Table 3, were less then those obtained from slightly smaller dosages in Table 2. This would indicate that the batch used in Table 3 (which was also used in the ED, I, and EA series) may have been somewhat less potent than the batch obtained from the trial batch used in Table 2.

Tables 4 and 5 contain the results of potency assays

TABLE 2. Potency values obtained from 200 g male rats using a trial batch of PAA

Rat number	mg Injected	mg Injected per kg Body Weight	Potency Value
1	0	0	95
2	0	0	106
3	6	30	147
4	6	30	121
5	12	60	190
6	12	60	231
7	24	120	319
8	24	120	393
9	48	240	367
10	48	240	306

done on rabbits. The results are from a trial batch of PAA and from the batch of PAA used in this study, respectively. Potency values tended to peak at dosages of 300 mg/kg to 600 mg/kg, and declined at dosages of 1000 mg/kg and 1500 mg/kg. The potencies of these particular extracts are considerably less than that used by Tornberg and Bassett (1977). They were able to get about the same results using 1/40th the concentration we used. The potency of PAA is known to vary from batch to batch, perhaps due to different concentrations in the bones of different individual animals (R. C. Millonig, The Squibb Institute for Medical Research,

TABLE 3. Potency values obtained from 200 g male rats using the extract of PAA used in the ED, I, and EA series

Rat number	mg Injected	mg Injected per kg Body Weight	Potency Value
1	0	0	98
2	15	75	136
3	15	75	148
4	25	125	213
5	25	125	301

Princeton, N. J. 08540, personal communication), and perhaps due to differences in laboratory techniques and equipment.

In addition to the strontium-85 data, a gross examination was made of the rabbit femurs listed in Table 5. The femurs were rated 0, +, ++, or +++, depending upon the amount of periosteal new bone growth seen in the experimental femur compared to the control. A mark of 0 means that the experimental femur did not show any more periosteal new bone than the contralateral control, + means that the active experimental femur has one or two small nodules of periosteal new bone, ++ means that it had one or two large masses of periosteal new bone, and +++ means that it had massive amounts of periosteal new bone.

To test the effect of PAA on another species, a potency

TABLF 4. Potency values obtained from male rabbits using a trial batch of PAA

Rabbit number	Dosage (mg per kg of body weight)	Potency value from ashed bone, adjusted for the dry weight of the ashed residue	Potency value prior to ashing
1	0	79.2	103.4
2	0	90.8	87.9
3	100	104.7	109.3
4	100	162.3	123.0
5	150	85.7	99.1
6	150	120.3	116.6
7	200	130.6	116.3
8	250	117.4	100.2
9	250	145.7	130.6
10	300	145.2	112.2
11	300	125.2	126.2
12	500	119.6	134.8
13	500	131.0	136.9
14	1000	109.7	106.3
15	1000	94.7	109.5
16	1500	115.6	117.7
17	1500	89.3	120.9

assay was performed on two puppies. The puppies were both males and weighed 3 to 4 kg. The results from these two puppies (Table 6) were similar to the data from the rabbits in that similar dosages of PAA applied resulted in similar potency values. For the higher dosage used here, a high

TABLE 5. Potency values and gross examination grades from male rabbits using the extract of PAA used in the ED, I, and EA series

Rabbit number	Dosage (mg/kg body weight)	Potency value	Gross examination grade
1	0	108.5	0
2	0	102.8	0
3	200	110.9	+
4	200	111.6	+
5	200	118.3	+
6	400	198.6	+++
7	400	116.0	+++
8	400	(died the 6th day)	+++
9	600	170.1	++
10	600	106.4	++
11	600	235.0	++

TABLE 6. Potency values from femora of two puppies

Amount injected (mg/kg body weight)	Potency value
99.5	118
354.0	176

potency value was obtained.

Based on the results of these potency assays, it was decided that for the main experiment, PAA would be applied at a concentration of 400 mg per kg of body weight (mg/kg). A dosage of 400 mg/kg showed the most new bone growth in the gross examination (Table 5) and was in the range of the higher potency values in Tables 4 and 5. Overall, these preliminary experiments showed that although PAA accelerated the uptake of strontium-85 in the rabbit, it did not do it as spectacularly as it did in the much smaller rat. The difference was also noticeable grossly. In the rat, the diameter of the radius-ulna complex would nearly double, while in the rabbit the effect was noticed as localized nodules of periosteal new bone. A much higher dosage of PAA in terms of mg per kg of body weight had to be given to the rabbit or the puppy to produce a noticeable effect. This may be due to a difference in the surface to volume ratio of the tested bones of these animals. A periosteal activation agent would be expected to have a more noticeable effect on bones that have more periosteum in comparison to their total size. An examination of a sampling of rabbit bones and rat bones from these experiments produce surface to volume ratios shown in Table 7.

TABLE 7. Ratios of surface area to volume estimated for various bones

Bone	Area (mm^2)	Volume (mm^3)	Area/volume[1] (mm^{-1})
Femur, 2 kg male rabbit	1013	1979	0.51
Femur, 0.2 kg male rat	240.3	212	1.13
Radius-ulna 0.2 kg male rat	177.4	63.2	2.81

[1]See page 72 for procedure.

Gross Examination

Rabbits from the Potency Assay as a Control Group

The rabbits from the potency assay can serve as a control to the I and ED series, since the former are rabbits that recieved a periosteal application of PAA in one femur without a previous defect or implant surgery.

The rabbits in the potency assay were all killed seven days after the application of PAA. Observations of these rabbits showed similarities with the I and ED series at day 7. Exudate formation and some fibroplasia was often seen in the muscles adjacent to the femur that had received the PAA (the experimental femurs). Such exudate formation was not

observed adjacent to the femurs that received the application of saline (the control femurs).

Small areas of periosteal new bone growth were observed in the experimental femurs, but not in the control femurs. At an application of 200 mg of PAA per kg of body weight, there was usually just a few scattered nodules of new bone on the midshaft of the experimental femur. The new bone was usually concentrated in irregularly shaped nodules about 2 to 4 mm long, 1 to 2 mm wide, and protruding about 1 mm above the smooth surface of the midshaft of the bone on the side of the femur that had received the application of PAA. The periosteal new bone seemed to be most extensive in femurs that received an application of about 400 mg PAA per kg body weight. At an application of 400 mg/kg, the nodules of periosteal new bone merged into a large mass that covered about a fourth of the surface area of the diaphysis. At a concentration of 600 mg/kg, the periosteal new bone was more extensive than at 200 mg/kg, but was less extensive than at 400 mg/kg. At 600 mg/kg, the experimental femurs generally had one or two large nodules of periosteal new bone about 3 to 6 mm wide, by 3 to 6 mm long, and protruding about 1 mm above the smooth surface of the femur.

Empty Defect and Implant Series

At one day after application of PAA, the muscles and loose areolar tissue surrounding the femur were loosely separated and filled with blood or a bloody fluid. This phenomenon was usually more extensive in the experimental femur. In one animal, a large clot was observed under the skin sutures.

At day three after application of PAA, exudate formation and some fibroplasia was seen in the muscle adjacent to the bone and in the subcutaneous tissue in the experimental leg. Some blood or watery fluid was still occasionally seen in the muscle adjacent to the bone in both femurs.

At days 5, 7, 10, and 14 after application of PAA, a yellow-gray to white-gray or a pink-brown exudate was almost always seen in the leg with the experimental femur. In one rabbit, exudate was seen in the control femur directly under the skin suture. This was probably a reaction to the suture or a bacterial infection through the skin. Besides that example, there were no other rabbits that showed a exudate formation in the control leg. The exudate that almost always formed in the experimental leg could be found directly under the skin, in the underlying muscle, or in a mass in the muscles adjacent to the femur. Often it was scattered in all three areas. There were only a few animals at these time periods that did not show exudate formation in the

experimental leg. No exudate was observed at day 56.

Periosteal new bone growth could be grossly observed in both the control and experimental femurs at all time periods from day one to day 14 in both the ED series and the I series. At the early time periods of days 1, 3, and 5, the femurs often showed extensive amounts of cartilaginous callus around the defect area. Sometimes these calluses completely covered the defects.

At longer time periods of 7, 10, and 14 days there tended to be less of the soft cartilaginous calluses. These femurs, both control and experimental, tended to have ridges or lumps of periosteal new bone around the areas of the defects. By day 10 and day 14, the defects in the ED series were becoming filled with new bone. At days 10 and 14 in the I series, the new bone often partially covered the implant. Often the new bone growth made it impossible to locate the defects or the implants in the 10, 14, and 56 day samples. In many of these samples, the location of the defect was found from X-ray photographs of the samples. At day 56, the lumps and ridges of new bone were no longer prominent.

Endosteal Activation Series

In the endosteal activation series, the formation of exudate was confined to the muscles and soft tissues in the area of the trochanter of the activated femur. No callus

formation was observed on the outside of any of the bones.

Summary of the Contralateral Control Series

With the exception of one rabbit, exudate formation was not observed in any of the control legs. In the one control leg where exudate was observed, it appeared to be associated with the skin sutures and not with the femur or the muscles adjacent to the femur.

Nodules of periosteal new bone were not observed in any of the control femurs from the potency assay in any of the animal species examined.

Periosteal calluses and nodules of periosteal new bone were, however, observed in the controls from the ED and I series. At the early time periods of 1, 3, and 5 days in the ED and I series, cartilage calluses were often seen around the defect areas. Sometimes the defects and implants were completely covered by these calluses. At the longer time periods of 7, 10, and 14, days, ridges or lumps of periosteal new bone were often seen around the defects and implants. At days 10, 14, and 56, new bone often partially covered the implants. At day 10 and 14, the empty defects were becoming filled with bone. By day 56, the lumps and ridges of new bone were no longer prominent.

Strontium-85 Tracer

Control Group I: Potency Assay on Rabbits at Zero PAA

In the potency assay, there were four rabbits that received a zero application of PAA. In other words, a saline solution was applied to the periosteum of both femurs in each of these rabbits. These rabbits were all treated with an intrathoracic injection of strontium-85, 24 hours before they were killed. They were all killed seven days after application of PAA.

Activation ratios can be calculated from the radioactivity of these femurs by either taking the ratio of the left femur over the right femur, or the ratio of the right femur over the left femur after subtracting background in both cases. The results of left/right ratios are listed in Table 8. The averages are all from femurs that were not ashed.

The average of both types of ratios came very close to 1.000. The activation ratio calculated from the left femur in the numerator is 1.007, with a standard deviation of 0.089, and a standard deviation of the means of 0.044.

TABLE 8. Activation ratios at seven days after an application of 0 mg of PAA per kg of body weight (unashed bones)

Rabbit	Left/right
1	1.034
2	0.879
3	1.085
4	1.028
Average	1.007
Standard deviation	0.085

Standard deviation of the means = 0.044

These means are exactly what is expected. In the absence of any specific stimulation to just one femur, but not the other, both femurs are expected to be near mirror images of each other. Their average activation ratios should be very near 1.000.

The standard deviation of about 0.085 indicates that within individual rabbits, there can be some difference between their contralateral femurs. The averages of near 1.000 indicates that these differences may be averaged out of a large group of rabbits.

Control Group II: Potency Assays on Rabbits at Dosages of 400 mg PAA per kg of Body Weight

Another control group that can be identified in the potency assay is the rabbits that received an application of 400 mg of PAA per kg of body weight. We should restrict the comparison to rabbits that received the same extract of PAA used in the ED, I, and EA series. There were two such rabbits that such activation ratios were calculated for, and these are shown in Table 9. The average activation ratio for these two rabbits is 1.573 with a standard deviation of 0.584.

The rabbits in the potency assays were all killed seven days after the application of PAA. It would then be reasonable to compare them to the seven day rabbits in the ED and I series which also received 400 mg PAA/kg. The activation ratios of all rabbits from day 7 in the ED and I series are repeated in Table 9.

Table 9 shows that the day 7 rabbits from the I and ED series had nearly identical average activation ratios (1.12 for the I series and 1.126 for the ED series). These values were similar to the average activation ratio of the potency assay where 200 mg PAA per kg body weight was injected (1.136). The average values for I and ED series are considerably less then the average of the 400 mg/kg values from the potency assay.

TABLE 9. Activation ratios of rabbits killed 7 days after an application of 400 mg PAA per kg body weight compared with the activation ratios from the potency assays

Rabbit number	Series	Dosage (mg/kg)	Activation ratio	Average ±95% C.I.[1]
1	ED	400	1.035	
2	ED	400	1.155	1.120
3	ED	400	1.186	±0.134
4	I	400	1.186	
5	I	400	1.123	1.12
6	I	400	0.816	±0.52
9	pot.assay	200	1.109	
10	pot.assay	200	1.116	1.136
11	pot.assay	200	1.183	±0.024
12	pot.assay	400	1.986	1.573
13	pot.assay	400	1.160	
14	pot.assay	600	1.701	
15	pot.assay	600	1.064	1.705
16	pot.assay	600	2.350	±1.08

[1]C.I. = confidence interval.

Empty Defect Series

Table 10 shows the activation ratios from the empty defect series where the PAA was applied to femoral defects without porous implants. The results are expressed as a simple ratio of the activity of the experimental femoral segment divided by the activity of the corresponding control segment after subtracting the background radiation from both counts. Appendix A gives an analysis of the radiation

statistics involved, and an example of how the activation ratio was calculated. The table also gives the results for the femoral midshaft where the activities of all three segments taken from the femur were added; the ratio is the sum of the activated segments divided by the sum of the control segments.

Figure 13 displays the data from the total of the segments of the empty defect series. Figure 14 presents the data from the proximal segments, Figure 15 from the midsegments, and Figure 16 from the distal segments of the ED series. The total bone averages for each time period are displayed in Figure 17.

The data from Figure 17 show that the rate of enhanced bone accretion is fairly constant at all time periods except for the peaks at day 5 and day 14. The peak at day 14 is particularly interesting because previous literature (Tornberg and Bassett, 1977) had described the activation effect as being completed at 7 days. The peak at day 5 is more consistent with the observations of Tornberg and Bassett (1977). They stated that mineralization occurred as early as 60 hours after application of PAA, and continued until 7 days after application.

The graphs for the individual segments, Figures 14, 15, and 16, all show considerably more scatter of data than the graph for the combined segments data, Figure 13. This is

TABLE 10. Activation ratios from the empty defect series

Day	Sample number	Proximal segment	Mid-segment	Distal segment	Total segments	Average, X of total femur, ± 95% C.I.[1]
1	I	1.170	0.895	1.329	1.151	
	IV	1.048	0.894	1.145	1.048	X=1.113
	VI	1.094	1.027	1.265	1.141	±0.094
3	I	1.370	1.234	0.991	1.196	
	II	1.223	0.984	0.820	1.014	X=1.116
	III	1.220	1.142	1.151	1.181	±0.150
5	II	1.148	0.992	1.638	1.247	
	III	1.318	1.708	1.847	1.577	X=1.41
	IV	1.727	1.115	1.192	1.392	±0.28
7	I	2.157	0.793	0.543	1.035	
	IV	1.064	1.064	1.344	1.155	X=1.126
	V	1.121	1.375	1.141	1.186	±0.134
10	II	0.794	0.872	1.556	1.103	
	III	1.452	0.967	0.830	1.063	X=1.090
	IV	1.363	1.324	0.757	1.105	±0.040
14	I	2.003	2.348	1.492	1.862	
	II	1.432	1.692	2.282	1.813	X=1.58
	IV	0.800	1.146	1.415	1.058	±0.76
Average of all total segments = 1.240±0.105						
[1]C.I. = confidence interval.						

expected, since in any given region of bone there can be growth, resorption, or little change going on as part of the normal remodelling process. As a whole, a bone may appear to keep the same silhouette as it grows from a small bone in the infant to a large bone in the adult; various segments of

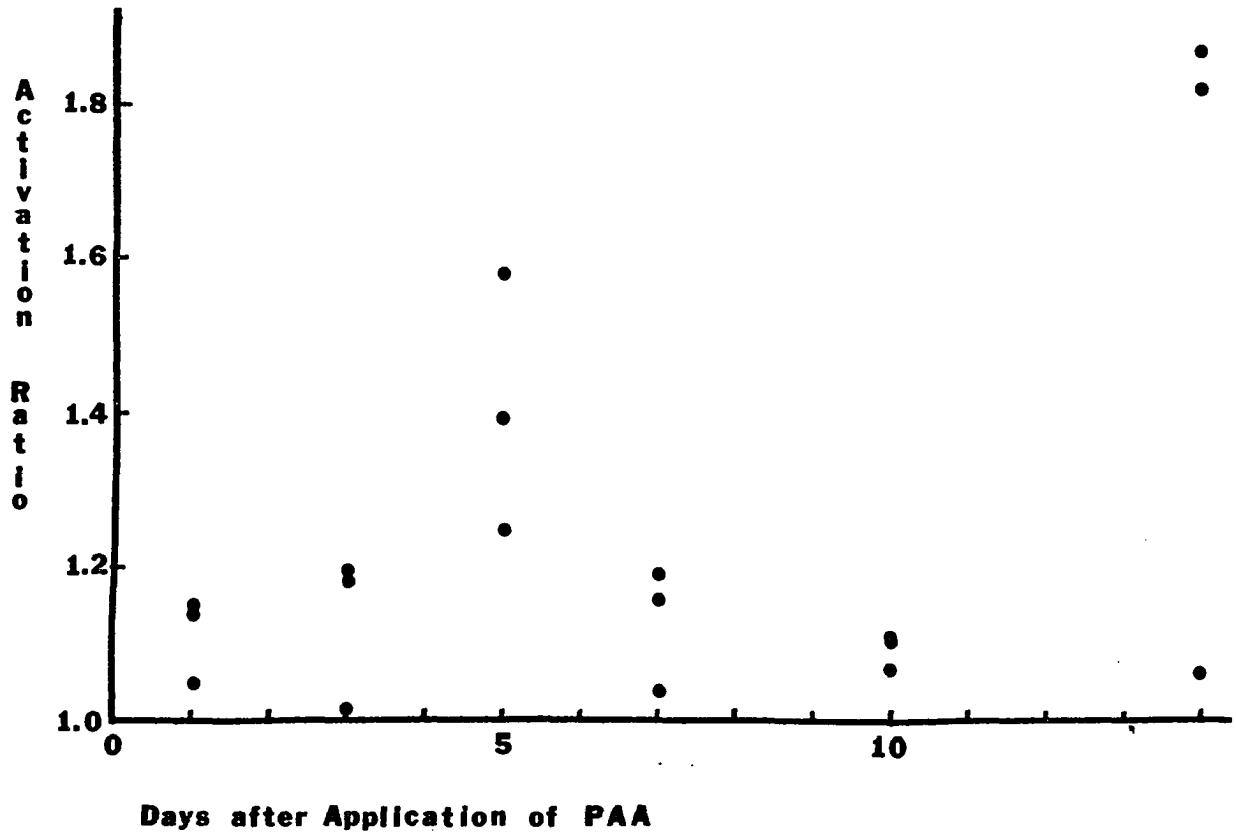

FIGURE 13. Activation ratios from the total midshaft (sum of distal, mid, and proximal segments) of femurs from the ED series

the bone must go through a complicated pattern of growth and resorption cycles to maintain that profile. At any given time, one part of a bone may be undergoing resorption, whether it be for growth, remodelling, repair, or the stresses applied or transmitted at that area, while the identical segment in the contralateral bone may be undergoing some other process. In any large number of rabbits that were not treated with PAA, we would expect roughly half to have activation ratios slightly above 1.0 and half to have activation ratios slightly below 1.0.

In the data for the smaller segments, we see both values above 2.0 as in days 7 and 14 for the proximal segments, day 14 for the midsegments, and day 14 for the distal segments, as well as some values less than 1.0. The activation values that are less than 1.0, occur mainly in the midsegments where there are 7 such values; in the proximal segments there are 2, and in the distal segments there are 4. This may be due to our technique of applying PAA, which tended to concentrate it at the sites of the defects in the proximal and distal segments.

Implant Series

Table 11 shows the activation ratios for the implant series where PAA was applied to femoral defects with porous implants in them. Figure 18 displays the activation ratios for the combined segments. Figures 19, 20, and 21 display

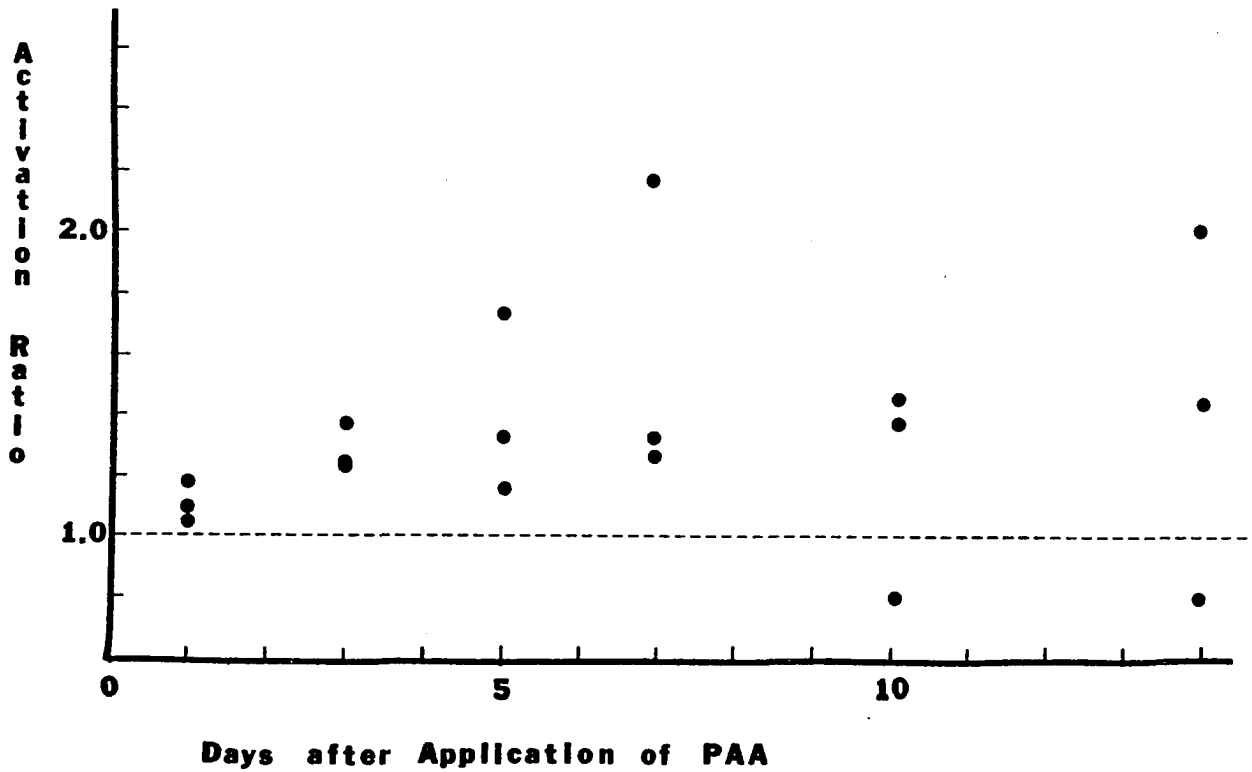

FIGURE 14. Activation ratios from the proximal segments from the ED series

the activation ratios for the proximal, mid, and distal segments, respectively. Figure 22 displays the mean activation ratios for each time period in the implant series.

Perhaps the most noticeable characteristic about the activation ratios from the implant series is their extreme variability. The combined midshaft values in the ED series were all greater than 1.0, but in the implant series, six of the 18 rabbits slaughtered at time periods from 1 to 14 days give ratios less than 1.0, which means there was more new bone growth in the control than in the active implant. The only time period where all three rabbits gave ratios greater than 1.0 was at day 1.

The activation ratios for the proximal, mid, and distal segments, Figures 19, 20, and 21, respectively, also reflect the greater variability of the implant series. For the proximal segments there are 7 activation ratios less than 1.0, for the midsegments there are 6, and for the distal segments there are 5. For the 21 rabbits studied, one-third of the bone segments from the implant series gave activation ratios less than 1.0.

In the implant series, as in the empty defect series, there were two rabbits at the 14 day interval that produced very high activation ratios. This indicates again, that PAA may be activating bone growth up to two weeks after its

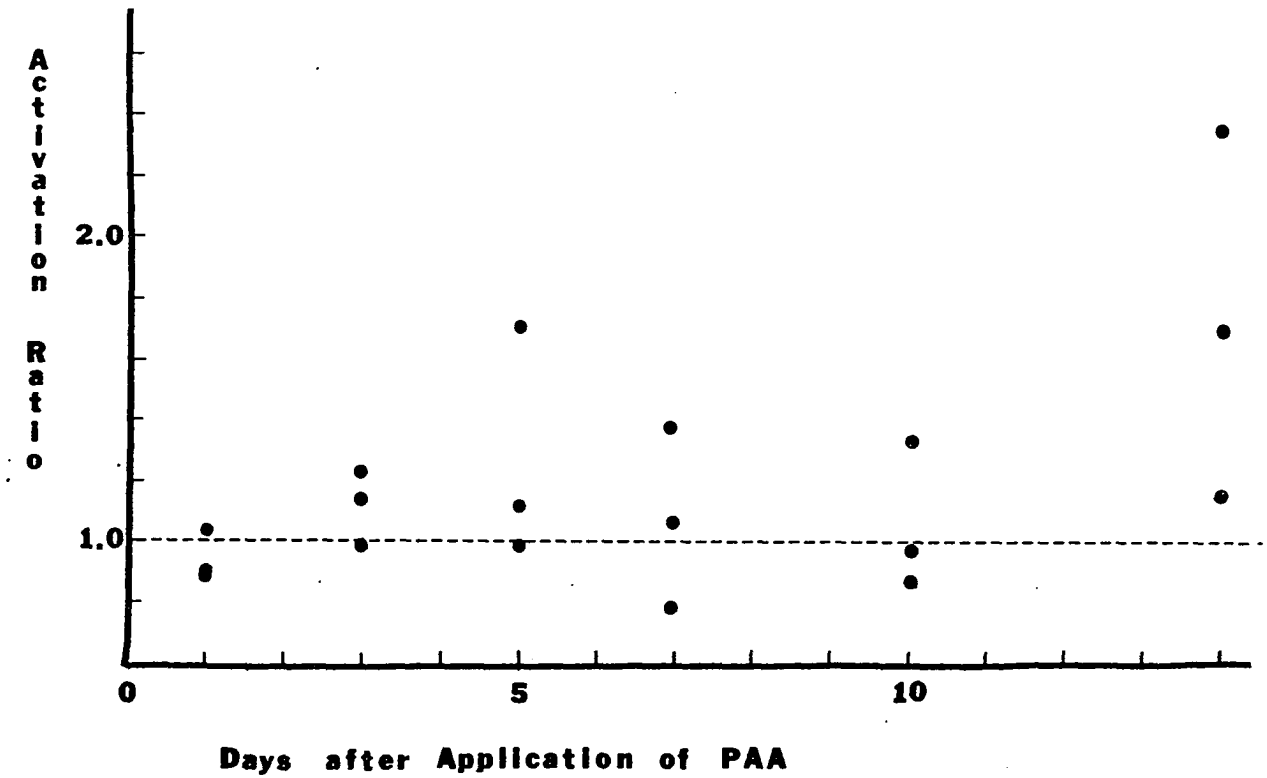

FIGURE 15. Activation ratios from the mid segments from the ED series

application. However, there is a large standard deviation for the 14-day group in the implant series. The mean value at 14 days is not statistically significant at the 95% confidence level. Only at the one day period in the implant series do we find an activation ratio mean that exceeds 1.0 by more than the 95% confidence interval.

Endosteal Activation Series

For the endosteal activation series, the rabbits received an endosteal injection of PAA through the trochanter fosse, without the trauma of defect surgery. The first rabbit injected in this series was one out of three in a test to see if the rabbits could survive such an application of PAA. Out of the three initial rabbits that received the endosteal application, rabbit I in the day 7 group was the largest (3.18 kg), and was the only one to survive. Due to the extremely high activation ratio that was obtained from this rabbit, it was decided to continue with a modified EA series. That rabbit had received an injection of about 300 mg of PAA per kg of body weight. No medullary fluid or tissue was aspirated prior to the application of PAA.

Another series of three rabbits (rabbits II, III, and IV in the day 7 group) were then given a lower dosage of PAA (100 mg per kg of body weight) after an equal volume of medullary fluid and tissue had been aspirated. The

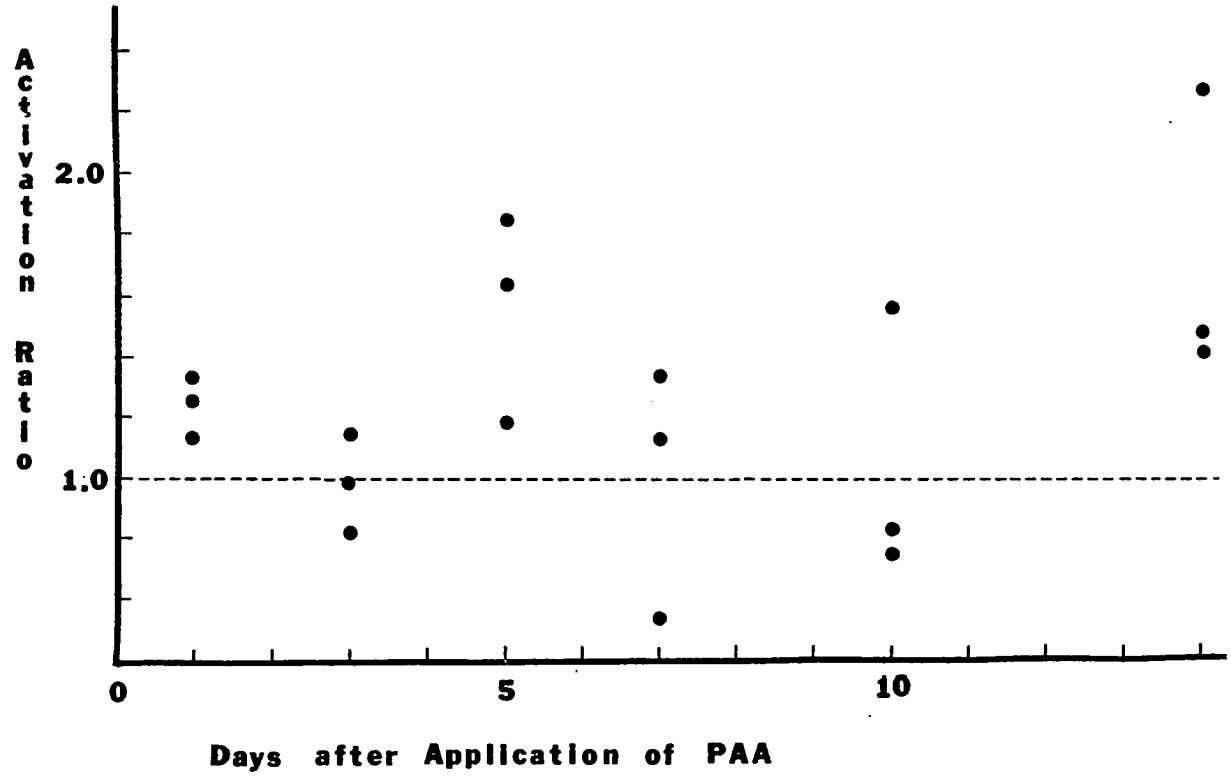

FIGURE 16. Activation ratios from the distal segments from the ED series

aspiration of medullary tissue was done to prevent possible embolism from the large volume of fluid injected. Since all three of these rabbits survived, the remaining rabbits in the EA series all received a similar application of PAA after an equal volume of medullary tissue and fluid had been aspirated.

For the EA series (Table 12), there is a very wide scatter of data that include both very high values, up to 2.67, and very low values, down to 0.518, for activation ratios. In general, the total activation ratios of less than 1.0 occurred mostly at the 1 and 3 day periods. Out of 22 rabbits completed in the EA series, 7 gave activation ratios for the total femoral shaft of less than 1.0, one gave a ratio of 1.000, and 14 produced total activation ratios greater than 1.0. Of the seven rabbits that gave total activation ratios less than 1.0, five of them were from the one and three day groups.

Perhaps there is a tendency for PAA to actually hinder endosteal bone growth during the first three days after application. However, due to the large standard deviation in the data, no statement can be made about this with a high degree of statistical confidence. The activation ratios measured in series EA, both the high ones and the low ones, may be totally random.

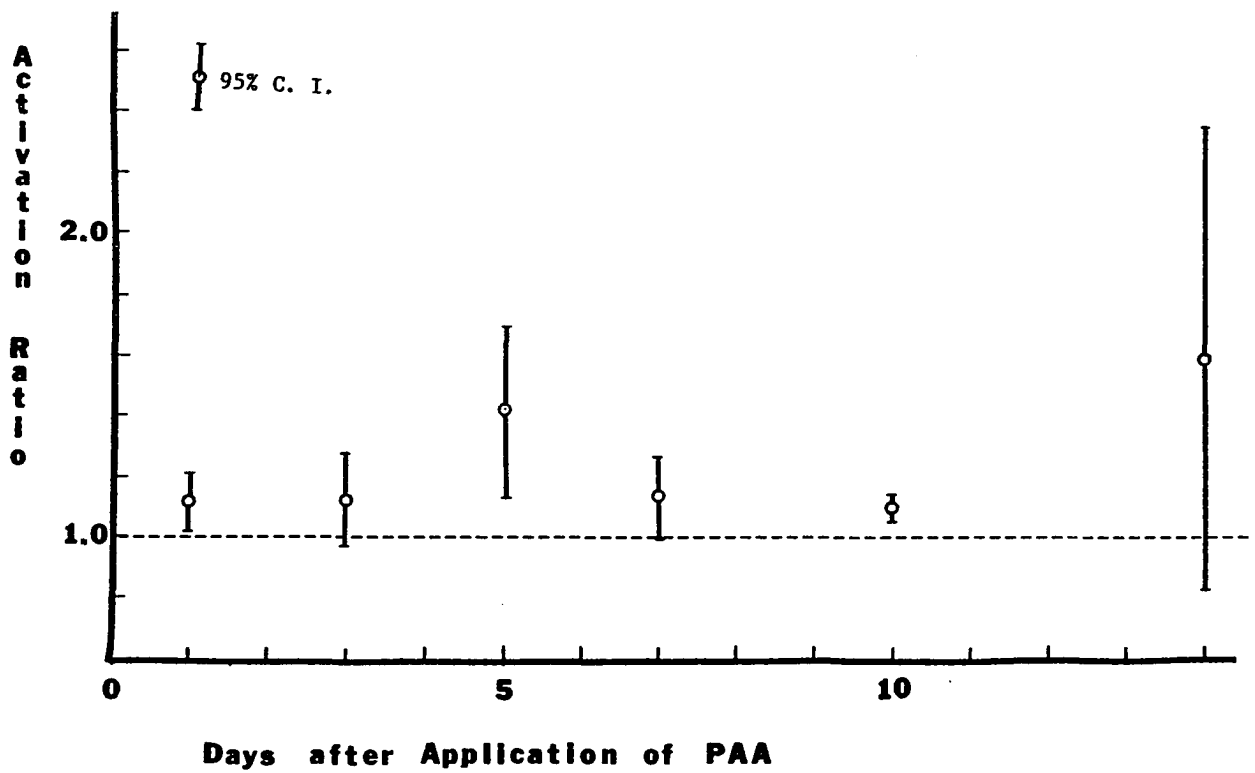

FIGURE 17. Average activation ratios from the total midshaft of femurs of the ED series

TABLE 11. Activation ratios from the implant series

Day	Sample number	Proximal segment	Mid-segment	Distal segment	Total segments	Average, X of total segments, ±95% C.I.[1]
1	I	1.312	1.288	1.388	1.331	
	II	0.939	1.481	1.261	1.127	X=1.30
	III	1.634	1.614	1.081	1.439	±0.27
3	I	0.973	1.176	1.290	1.112	
	II	1.314	1.096	1.095	1.183	X=1.03
	III	0.755	0.718	0.921	0.799	±0.34
5	I	0.835	0.777	0.837	0.821	
	III	1.157	1.514	0.829	1.083	X=0.92
	IV	1.012	0.959	0.645	0.868	±0.24
7	I	1.491	1.740	1.153	1.433	
	II	0.745	1.096	1.859	1.123	X=1.12
	III	0.654	0.812	1.160	0.810	±0.52
10	I	1.545	1.132	0.555	0.912	
	II	1.449	1.102	1.279	1.332	X=1.13
	VI	1.257	1.237	1.018	1.157	±0.35
14	I	1.302	1.374	1.367	1.340	
	II	1.037	0.881	0.647	0.820	X=1.30
	III	1.418	2.372	1.684	1.734	±0.78
56	I	1.064	1.433	1.070	1.128	
	II	0.967	0.686	0.680	0.814	X=1.01
	III	0.709	1.2284	1.434	1.091	±0.29

Average of day 1 through day 14 total segments = 1.135±0.109

[1]C.I. = confidence interval.

Image Analysis

Image analysis was done on a selection of samples from the E[1] and I series. It was decided to perform a general

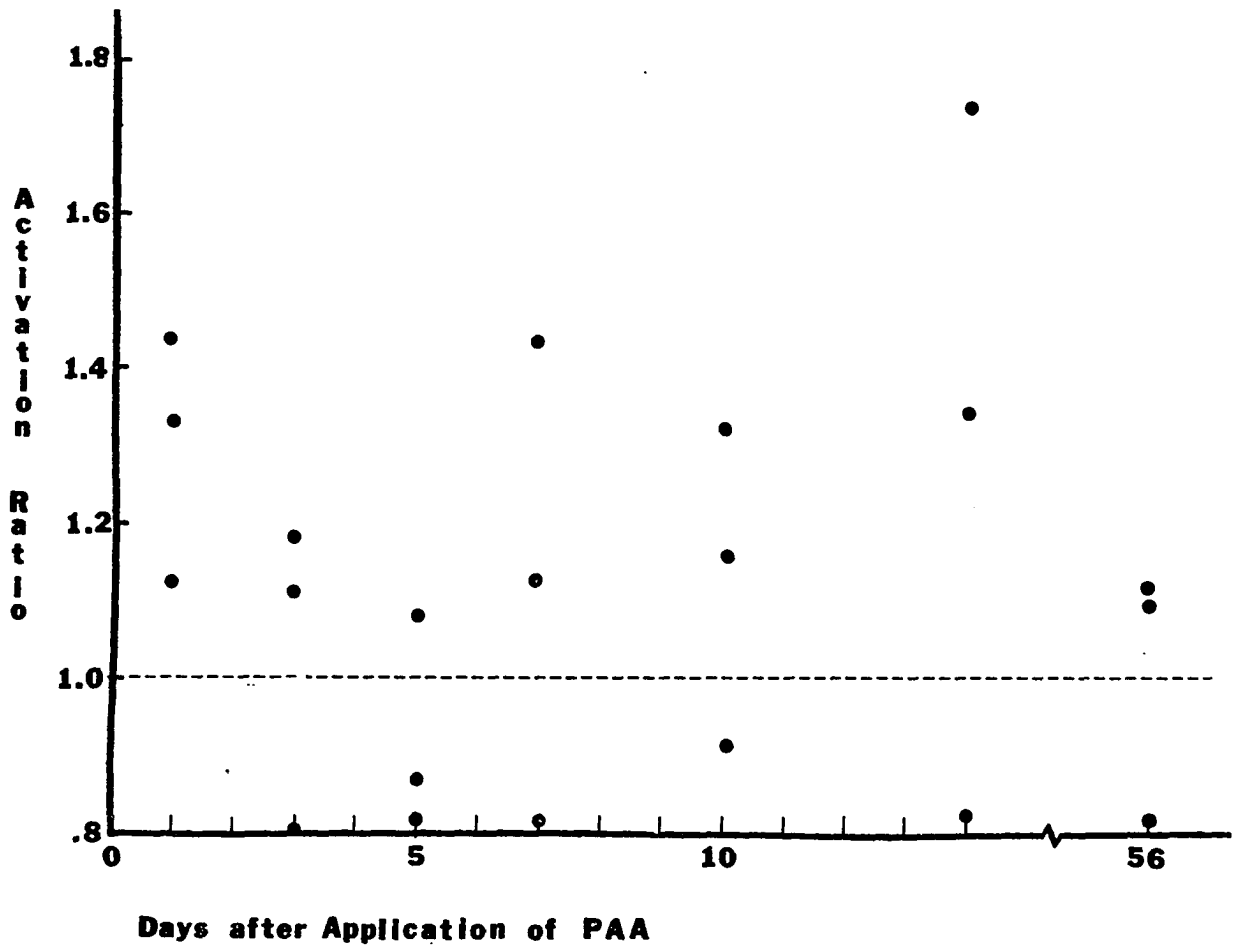

FIGURE 18. Activation ratios from the total midshaft of femurs from the I series

survey for these series by microscopic examination and image analysis of only one or two samples from each time period in each of the two series. The choice of which rabbit samples would be examined was made on the basis of the activation ratios of their total femur segments. In the ED series, where all of the total activation values were above 1.0, it was decided to usually take the rabbit from each group that had the highest activation ratios. The rabbits chosen were the ones numbered 1-I, 3-III, 5-III, 7-I, 7-V, 10-IV, and 14-I. In the seven day group, it was decided to take an additional rabbit, 7-I, that showed a wide variation in the activation ratios from individual segments. In the I series, there was at least one rabbit that had a total activation ratio of less then 1.0 for each time group, with the exception of the day 1 group. In the I series, image analysis and microscopic examination was done on samples from the rabbit at day 1 that had the highest total activation ratio, rabbit 1-III, and on the rabbits that had the highest and the lowest activation ratios in each of the other time periods, rabbits 3-II, 3-III, 5-I, 5-III, 7-I, 7-III, 10-I, 10-II, 14-II, 14-III, 56-I, and 56-II.

The image analysis methods were another way of measuring the amount of new bone growth. The strontium-85 tracer method could detect the amount of new bone in a given volume of bone segment. The two image analysis methods both

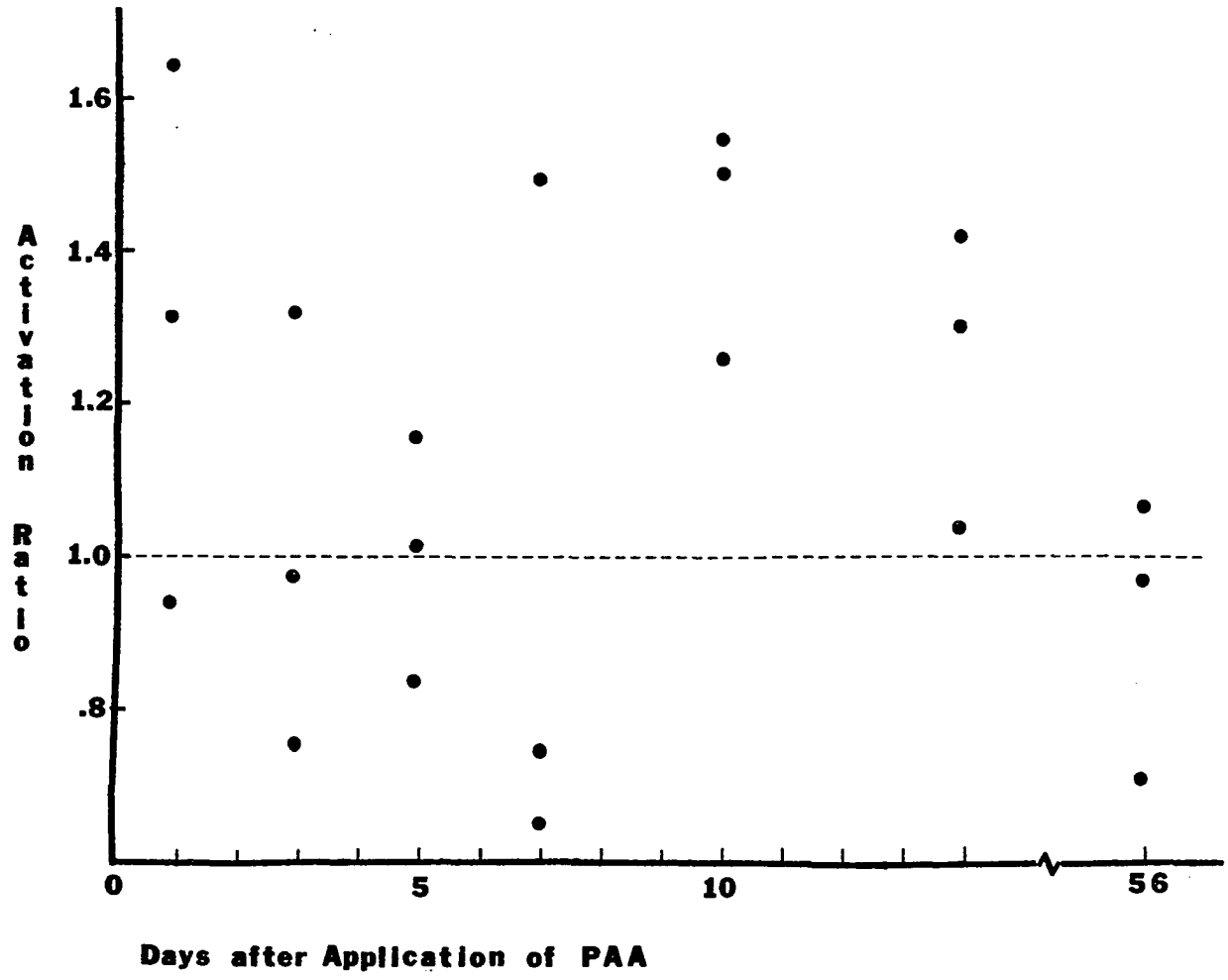

FIGURE 19. Activation ratios from the proximal segments from the I series

attempted to measure the amount of new bone seen in microscope slides made of cross sections of bone segments. In a way, the strontium-85 tracer method measures new bone growth in three dimensions, and the image analysis methods identify new bone growth in two-dimensional plane sections.

Tables 13 through 20 display the image analysis data obtained from the MOP-III. The amount of new cancellous bone seen in each slide is measured in mm^2. The ratio of the new bone in the activated femur to the new bone in the control is calculated for each pair of corresponding segments. For slides from the proximal and distal segments, the new bone is divided into various categories. In the empty defect series, the amount of new bone formed on the periosteum of the bone, the amount of new bone formed inside the medullary canal and, the amount of new bone formed in the defect were counted separately. In the implant series, the new cancellous bone was divided into (1) periosteal new bone, (2) new cancellous bone in the medullary canal, but not within the implant, and (3) new bone within the implant. For the distal segment of the implant series, the new bone within the implant was measured using the Quantimet® image analysis computer. The correlation coefficient, r, was calculated for each segment of each series for the activation ratios found with the strontium tracer method versus the ratios of the image analysis techniques. Where

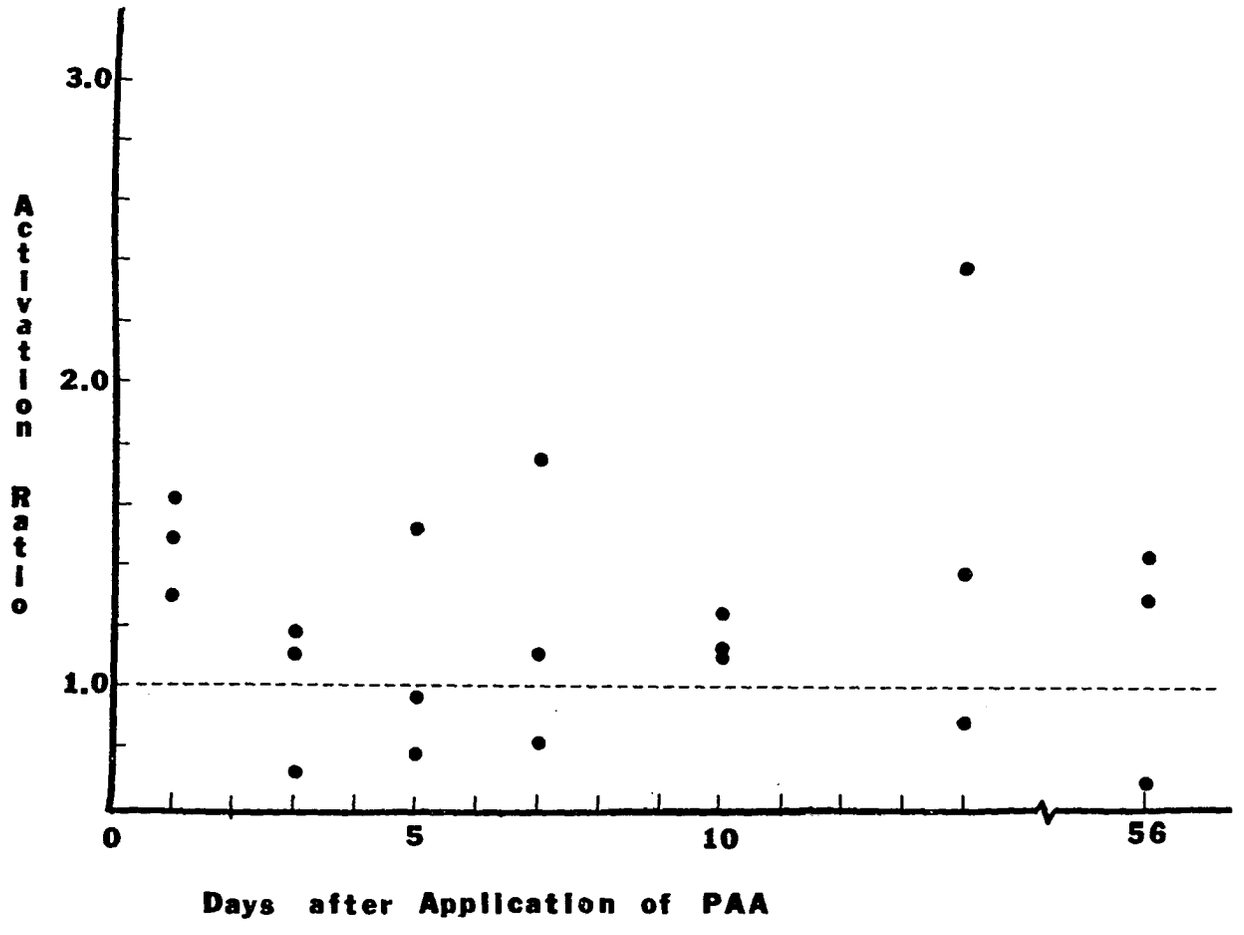

FIGURE 20. Activation ratios from the mid segments from the I series

the new bone formed was divided into different categories, the correlation coefficient was calculated for each category. Ratios were omitted from the correlation data if either the denominator or numerator were zero or close to zero. How the correlation coefficient was calculated is shown in Appendix C.

The new bone ratios calculated from the hematoxylin and eosin stained slides from the implant series correlated very highly with the activation ratios found from the strontium tracer measurements ($r = 0.825$ for the proximal segments of the implant series, 99% confidence interval = 0.30 to 0.98, Table 17; $r = 0.852$ for the midsegments of the implant series, 95% confidence interval = 0.25 to 0.94, Table 19). The correlation was less for the H and E stained slides from the empty defect series ($r = 0.470$ for the proximal segments of the ED series, 95% confidence interval = -.40 to 0.85, Table 18; $r = 0.660$ for the midsegments of the ED series, 95% confidence interval = -.17 to 0.92, Table 19), and very poor for slides stained by Lillie's silver impregnation technique ($r = 0.065$ for the distal segments of the empty defect series, Table 16; and $r = 0.345$ for the distal segments of the implant series, Table 21).

The poor correlation between the strontium tracer data and the Lillie's silver stained slides may be due to the lack of information the stain provides to distinguish new

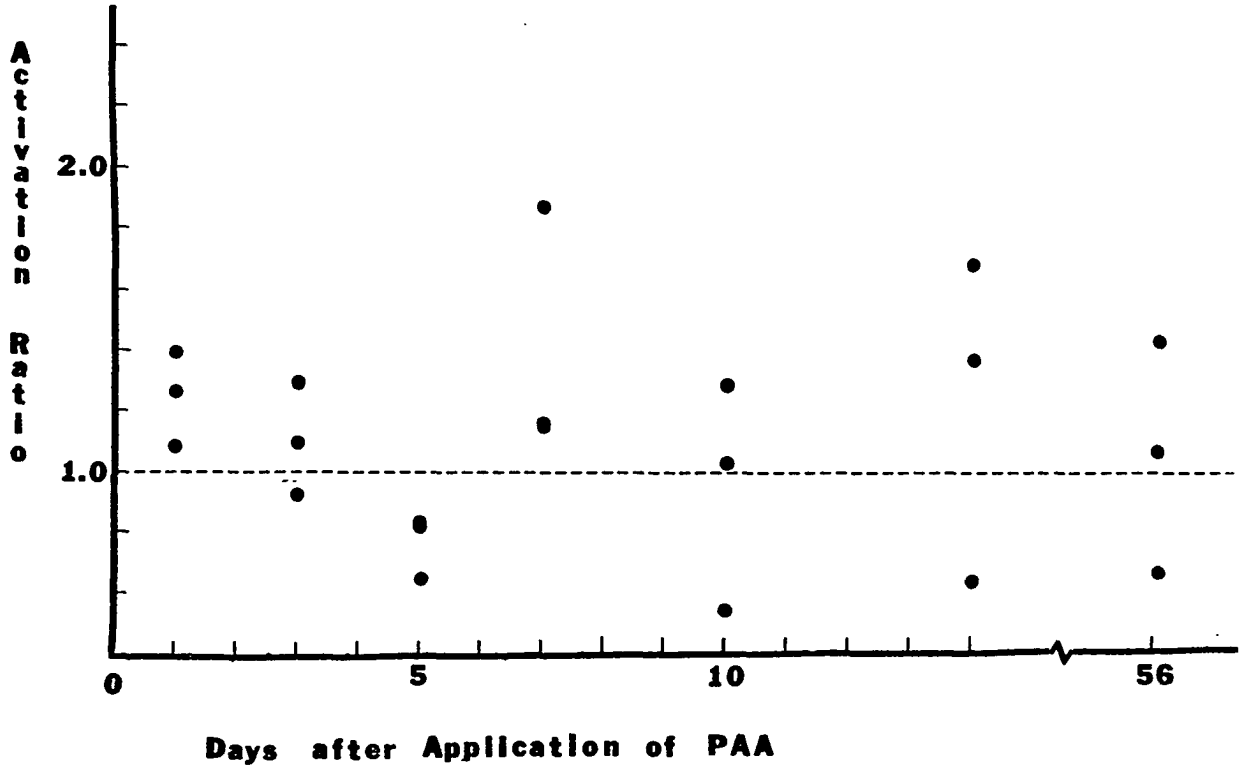

FIGURE 21. Activation ratios from the distal segments from the I series

bone. With Lillie's silver impregnation method for bone, there are no gradations in intensity due to different types of bone. Also, it does not show cement lines that can establish the border between new bone and old bone. The Lillie's method stains black all the calcium bearing tissue that is penetrated by the stain.

Although the correlation was not as good for the H and E stained slides of the empty defect series as it was for the implant series, it should be noted that with the exception of the one day sample from the empty defect series, that whenever the strontium tracer data found the activated femur to be more radioactive than the control, the MOP measurements also found more new bone on the slide from the activated segment than the slide from the control segment. In this study, we have used the correlation coefficient, r, which is a measurement of linear correlation.

In the proximal segments from the empty defect series, Table 13, most of the new cancellous bone was seen "inside", in the medullary canal or in the defect area, with the exception of samples from rabbits 7-I and 14-I where large calluses of new bone were seen "outside" or on the periosteal surface. The outside new bone in these segments correlate modestly with the strontium data ($r = 0.40$, 95% C.I. = $-.50$ to $+.85$), while the new bone formed on the

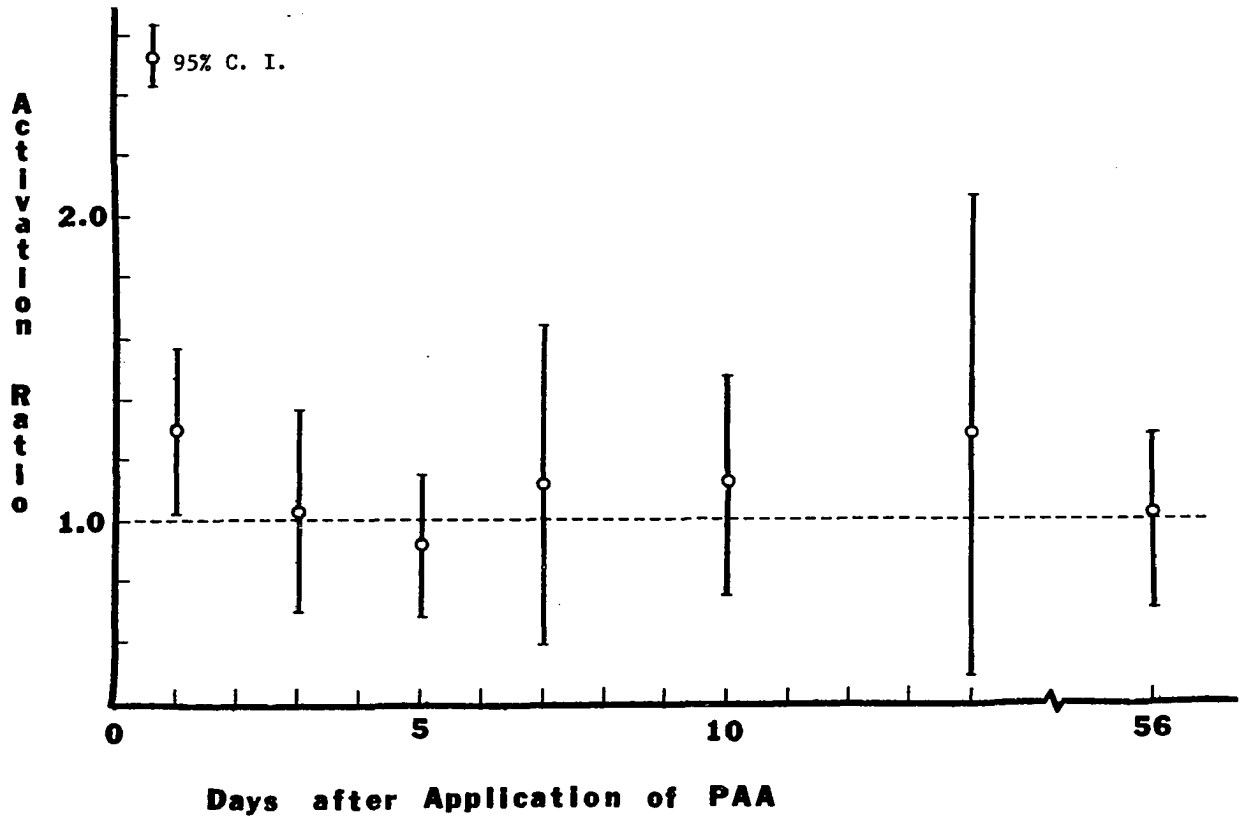

FIGURE 22. Average activation ratios from the total midshaft of femurs from the I series

TABLE 12. Activation ratios from the endosteal activation series

Day	Sample number	Proximal segment	Mid-segment	Distal segment	Total segments	Average, X of total segments, ±95% C.I.[1]
1	I	1.193	0.924	0.793	1.017	
	II	0.989	0.660	0.454	0.733	X=0.88
	III	0.954	0.948	0.875	0.763	±0.18
	IV	1.043	1.036	0.936	1.010	
3	I	0.919	0.922	0.346	0.730	
	II	1.039	0.781	0.870	0.919	X=0.914
	III	1.798	1.639	1.176	1.489	±0.49
	IV	0.548	0.510	0.481	0.518	
5	II	1.564	1.130	2.435	1.716	
	IV	1.472	1.325	1.378	1.367	X=1.30
	V	1.066	1.043	0.896	1.000	±0.36
	VI	1.036	1.213	1.198	1.132	
7	I[2]	2.47	2.46	2.18	2.361	
	II	1.58	1.67	5.06	2.67	X=1.515
	III	0.858	1.257	1.043	1.020	±0.65
	IV	0.841	0.821	0.740	0.803	
	V	0.852	1.155	1.709	1.198	
	VI	1.038	0.740	1.241	1.038	
10	I	2.024	1.214	1.324	1.616	
	II	0.614	0.444	0.610	0.590	X=1.294
	III	1.468	1.916	1.646	1.573	±0.56
	IV	0.953	2.072	1.791	1.398	

Average of all total segments = 1.212±0.198

[1]C.I. = confidence interval.

[2]This rabbit had a slightly different treatment, see text on page 69-70.

inside showed essentially no correlation with the strontium data (r = -.14). How the correlation statistics were

TABLE 13. Areas of new cancellous bone measured with MOP-III electronic planimeter in the empty defect series, proximal segments (H and E stains)

Rabbit femur (r=right l=left) ratio (active/control)	New bone external to defect (mm^2)	New bone inside defect (mm^2)	Total new bone (mm^2)	^{85}Sr Activation ratio
1-I				
active=r	2.076	3.973	6.049	
control=l	1.202	5.031	6.233	
ratio (a/c)	1.727	0.790	0.971	1.17
3-III				
active=l	5.604	6.910	12.514	
control=r	2.613	8.489	11.102	
ratio (a/c)	2.145	0.814	1.127	1.22
5-III				
active=l	4.671	8.203	12.874	
control=r	1.787	6.636	8.423	
ratio (a/c)	2.614	1.236	1.528	1.727
7-V				
active=r	2.965	11.488	14.453	
control=l	1.735	7.068	8.803	
ratio (a/c)	1.709	1.625	1.642	1.121
7-I				
active=r	9.708	4.356	14.064	
control=l	6.260	3.333	9.593	
ratio (a/c)	1.551	1.307	1.466	2.157
10-IV				
active=r	5.497	9.805	15.302	
control=l	3.045	4.576	7.621	
ratio (a/c)	1.805	2.142	2.008	1.363
14-I				
active=r	10.893	1.062	11.540	
control=l	3.363	1.300	4.663	
ratio (a/c)	3.239	0.817	2.546	2.003

TABLE 14. Correlations of the MOP-III measurements with the strontium-85 activation ratios for the proximal segments of the empty defect series

	New bone external to defect	New bone inside defect	Total new bone
r =	0.4022	-0.136	0.470
r^2 =	0.162	0.018	0.221

calculated is explained in Appendix C. It should be remembered that the strontium-85 data measures the total activity of the bulk sample. This activity is due mostly to strontium-85 being incorporated into new bone, but some of it is also due to strontium-85 interchanging with calcium in old bone. The MOP-III data measures what appears to be new bone in a two-dimensional slide. Therefore, perfect correlation is not expected between the two methods, but some correlation is expected. Since the strontium-85 data shows enhanced radioactivity due to new bone, we expect to see some of this new bone on the two-dimensional slides.

In the midsegments, nearly all the new cancellous bone observed was on the periosteal surface of the bone. The midsegments were 10 mm segments midway between the two defects. The midsegments from the ED series, Table 15, had a correlation with the strontium tracer data of 0.660, 95%

TABLE 15. Areas of new cancellous bone measured with the MOP-III electronic planimeter in the empty defect series, midsegments (H and E stain)

Rabbit femur (l=left r=right) ratio (active/control)	Area of new cancellous bone (mm^2)	^{85}Sr activation ratio
1-I		
active=r	0.86	
control=l	1.80	
ratio (a/c)	0.478	0.895
3-III		
active=l	3.44	
control=r	2.68	
ratio (a/c)	1.287	1.142
5-III		
active=l	6.08	
control=r	2.33	
ratio (a/c)	2.61	1.708
7-I		
active=r	4.17	
control=l	6.36	
ratio (a/c)	0.656	0.793
7-V		
active=r	8.18	
control=l	5.25	
ratio (a/c)	1.558	1.375
10-IV		
active=r	8.39	
control=l	3.29	
ratio (a/c)	2.55	1.324

TABLE 15 (Continued)

Rabbit femur (l=left r=right) ratio (active/control)	Area of new cancellous bone (mm^2)	^{85}Sr activation ratio
14-I		
active=r	17.89	
control=l	9.26	
ratio (a/c)	1.932	2.348

r = correlation of total areas of new bone with the strontium-85 activation ratios
$r = 0.66$ 95% confidence interval = (-0.17,+0.92)
$r^2 = 0.44$

C.I. = -.15 to +.90. The two samples from the midsegment of the ED series that had an activation ratio less than 1.0 with the strontium tracer, also had a ratio of less than 1.0 with the image analysis data.

The image analysis data from the distal segments of the ED series, Table 16, showed virtually no correlation with the strontium tracer data. This was probably due to limitations caused by the silver stain used on the distal segments. These slides had less information to distinguish new bone from old bone.

The data from the proximal segments of the I series, Table 17, showed a high correlation with the strontium data ($r = 0.825$, 99% C.I. = +.30 to +.99). As in the slides of

TABLE 16. Areas of new cancellous bone measured with the MOP-III electronic planimeter in the empty defect series, distal segments (Lillie's silver impregnation technique).

Rabbit femur (r=right l=left)	New bone external to defect (mm^2)	New bone inside defect (mm^2)	Total new bone (mm^2)	^{85}Sr Activation ratio (active/control)
1-I				
active=r	0.754	7.629	8.383	
control=l	0.982	2.400	3.382	
ratio (a/c)	0.768	3.179	2.479	1.329
3-III				
active=l	1.293	7.291	8.584	
control=r	3.300	7.696	10.996	
ratio (a/c)	0.392	0.947	0.781	1.151
5-III				
active=l	4.453	3.518	7.971	
control=r	2.389	5.713	8.102	
ratio (a/c)	1.864	0.616	0.984	1.847
7-I				
active=r	2.407	2.572	4.979	
control=l	4.800	2.485	7.285	
ratio (a/c)	0.500	1.035	0.683	0.543
7-V				
active=r	5.804	6.778	12.582	
control=l	(damaged)[1]	9.441	------	
ratio (a/c)	----	0.718	------	1.186
10-IV				
active=r	2.315	2.051	6.237	
control=l	0.579	3.922	2.630	
ratio (a/c)	3.998	0.523	2.371	0.757

[1]This sample was destroyed in the thin sectioning process with the microtome.

TABLE 16 (Continued)

Rabbit femur (r=right l=left)	New bone external to defect (mm^2)	New bone inside defect (mm^2)	Total new bone (mm^2)	^{85}Sr Activation ratio (active/control)
14-I				
active=r	2.713	5.535	8.248	
control=l	2.530	1.598	4.128	
ratio (a/c)	1.072	3.464	1.948	1.492

r = correlation of total new bone with ^{85}Sr activation ratios

$r = 0.065$

$r^2 = 0.004$

the proximal defects of the ED series, this high degree of correlation was due almost entirely to the periosteal new bone on the samples ($r = 0.898$, 99% C.I. = +.45 to +.98). No correlations were found for both the new bone tissue inside the medullary canal ($r = 0.22$) and inside the implant ($r = 0.13$). Unlike the proximal segments from the ED series, Table 13, most of the new bone observed in most of the proximal segments of the I series, Table 17, was periosteal new bone. The midsegments of the I series, Table 19, showed a high correlation with the strontium tracer data ($r = 0.852$ for up to day 7, 95% C.I. = +.25 to +.99). The fact that the strontium-85 data correlates highly to the

TABLE 17. Areas of new cancellous bone measured with the MOP-III electronic planimeter in the implant series, proximal segments (H and E stains)

Rabbit femur (r=right l=left) ratio (active/control)	New bone external to implant (mm^2)	New bone inside implant (mm^2)	New bone inside medullary canal (mm^2)	Total new bone (mm^2)	^{85}Sr Activation ratio
1-III					
active=r	2.906	0.071	3.814	6.791	
control=l	0.122	0.0	0.006	0.128	
ratio (a/c)	23.82	_____	635.7	53.05	1.639
3-II					
active=r	2.006	0.262	1.834	4.102	
control=l	1.868	0.118	1.522	3.508	
ratio (a/c)	1.074	2.220	1.205	1.169	1.314
3-III					
active=l	1.415	0.613	2.180	4.208	
control=r	4.055	0.283	1.246	5.584	
ratio (a/c)	0.349	2.166	1.750	0.754	0.755
5-I					
active=r	2.964	0.297	1.979	5.240	
control=l	4.052	0.410	1.103	5.564	
ratio (a/c)	0.732	0.725	1.794	0.942	0.835
5-III					
active=l	1.927	0.804	1.628	4.359	
control=r	2.148	0.330	1.594	4.072	
ratio (a/c)	0.897	2.436	1.021	1.070	1.157
7-I					
active=r	7.928	0.128	1.131	9.187	
control=l	4.079	0.876	1.184	6.139	
ratio (a/c)	1.944	0.146	0.955	1.446	1.491
7-III					
active=l	1.441	0.262	0.564	2.267	
control=r	9.818	0.722	1.286	11.826	
ratio (a/c)	0.147	0.363	0.439	0.192	0.654

TABLE 17 (Continued)

Rabbit femur (r=right l=left) ratio (active/control)	New bone external to implant (mm^2)	New bone inside implant (mm^2)	New bone inside medullary canal (mm^2)	Total new bone (mm^2)	^{85}Sr Activation ratio
10-I					
active=r	6.952	0.884	0.720	8.556	
control=l	4.155	0.516	0.227	4.898	
ratio (a/c)	1.673	1.713	3.712	1.747	1.545
10-II					
active=r	2.115	1.503	1.149	4.767	
control=l	1.316	0.811	1.048	3.175	
ratio (a/c)	1.607	1.853	1.096	1.501	1.449
14-II					
active=r	1.901	0.508	0.085	2.494	
control=l	2.273	0.646	0.436	3.359	
ratio (a/c)	0.836	0.786	0.195	0.742	1.037
14-III					
active=l	7.127	0.307	0.050	7.483	
control=r	2.965	0.407	0.294	3.666	
ratio (a/c)	2.404	0.754	0.168	2.041	1.418
56-I					
active=r	0.0	1.532	1.116	2.748	
control=l	0.0	1.560	0.0	1.560	
ratio (a/c)	---	0.082	-----	1.697	1.064
56-II					
active=r	0.0	1.529	0.0	1.529	
control=l	0.0	1.184	0.0	1.184	
ratio (a/c)	---	1.291	---	1.774	0.967

area of periosteal new bone seen in the cross sections would indicate that the cross sections examined are fairly

TABLE 18. Correlations of the MOP-III measurements with the strontium-85 activation ratios for the proximal segments of the implant series

	External to implant	Inside implant	Inside medullary canal	Total new bone
r =	0.898	0.131	0.222	0.825
95% C.I. =	(0.60,0.95)	(-.5,+.5)	(-.55,+.55)	(0.48,0.94)
99% C.I. =	(0.45,0.98)			(0.30.0.98)
r^2 =	0.806	0.017	0.049	0.681

representative of the amount of new bone growth seen.

Image analysis data from the distal segments of the implant series, Tables 20 and 21, showed low correlation with the strontium tracer data (r = 0.345, 95% C.I. = -.31 to +.72). The Quantimet® data which measured the amount of bone ingrowth into the implants from the distal segments, showed no significant correlation (r = -.13).

The Quantimet® data from the implants stained by Lillie's silver impregnation technique are shown in Table 22. The strontium-85 data give a good measure of the total amount of new bone formed in a certain bulk volume of sample. The Quantimet® system can measure the area of bone in a given cross section with a high degree of accuracy. In general, the strontium tracer is the better method to analyze the bulk samples, while the Quantimet system is the

TABLE 19. Areas of new cancellous bone measured with the MOP-III electronic planimeter in the implant series, midsegments (H and E stain)

Rabbit femur (l=left r=right) ratio (active/control)	Area of new cancellous bone (mm^2)	^{85}Sr activation ratio (counts active - bkg)/ (counts control - bkg)
1-III		
active=l	1.52	
control=r	0.33	
ratio (a/c)	4.61	1.614
3-II		
active=r	2.27	
control=l	3.37	
ratio (a/c)	0.674	1.096
3-III		
active=l	2.22	
control=r	4.34	
ratio (a/c)	0.512	0.718
5-I		
active=r	6.17	
control=l	8.15	
ratio (a/c)	0.757	0.777
5-III		
active=l	4.66	
control=r	2.97	
ratio (a/c)	1.57	1.514
7-I		
active=r	11.23	
control=l	3.09	
ratio (a/c)	3.63	1.740
7-III		
active=r	6.18	
control=l	9.08	
ratio (a/c)	0.681	0.812

TABLE 19 (Continued)

Rabbit femur (l=left r=right)	Area of new cancellous bone (mm^2)	^{85}Sr activation ratio (counts active - bkg)/(counts control - bkg)
ratio (active/control)		
10-I		
active=r	12.84	
control=l	7.70	
ratio (a/c)	1.668	1.132
10-II		
active=r	1.66	
control=l	0.0	
ratio (a/c)	---	1.102
14-II		
active=r	2.02	
control=l	0.0	
ratio (a/c)	---	0.881
14=III		
active=l	12.14	
control=r	1.10	
ratio (a/c)	11.04	1.371
56-I		
active=r	0.0	
control=l	0.0	
ratio (a/c)	---	
56-II		
active=r	0.0	
control=l	0.0	
ratio (a/c)	---	

$r = 0.852$
99% C.I.= (0.05,0.99) $n = 8$
$r^2 = 0.726$

better method to measure the area of ingrowth in a given cross section. Table 22 shows both the actual area of bone measured by the Quantimet® system, and the percentage of the implant filled by this bone. These data show essentially no correlation with either the strontium tracer data or with the samples that were treated with PAA.

Although the Quantimet® data failed to show a consistent correlation with the strontium tracer data and with the experimental femurs, the data did show a relationship with time. The average percent of the implant filled with bone increased from about 1.5% at day one to about 13.5% at day 56. This increase with time occurred for both the control and experimental femurs.

Special Stains

Transverse sections from the initial surviving rabbit of day seven from the endosteal activation series were examined with five different special stains. In this rabbit, the activated femur showed both endosteal and periosteal new bone growth, while the control femur showed no cancellous new bone growth either along the periosteum or the endosteum. Samples from this rabbit were chosen to illustrate the differences between a femur that had been activated and a contrateral femur that was not activated. This is the lone rabbit that survived an endosteal

TABLE 20. Areas of new cancellous bone measured with the MOP-III electronic planimeter and Quantimet® image analysis computer in the implant series, distal segments (Lillie's silver impregnation technique).

Rabbit femur (r=right l=left) ratio (active/control)	New bone external to implant (mm^2)	New bone inside medullary canal (mm^2)	New bone inside implant (Quantimet® data, mm^2)	Total new bone (mm^2)	^{85}Sr Activation ratio
1-III					
active=l	0.638	0.0	0.182	0.820	
control=r	0.134	2.008	0.204	0.338	
ratio (a/c)	4.762	0.0	0.890	2.424	1.083
3-II					
active=r	0.826	1.311	0.147	2.284	
control=l	0.428	0.971	0.374	1.773	
ratio (a/c)	1.930	1.350	0.393	1.229	1.095
3-III					
active=l	0.729	1.291	0.336	2.356	
control=r	1.465	0.614	0.388	2.467	
ratio (a/c)	0.498	2.103	0.866	0.955	0.921
5-I					
active=r	2.495	1.359	0.474	4.328	
control=r	3.613	0.418	0.084	4.115	
ratio (a/c)	0.691	3.251	5.643	1.052	0.837
5-III					
active=l	1.350	0.689	0.318	2.357	
control=r	3.181	0.297	0.377	3.855	
ratio (a/c)	0.424	2.320	0.844	0.611	0.839
7-I					
active=r	2.574	3.045	0.937	6.556	
control=l	1.773	0.615	1.009	3.400	
ratio (a/c)	1.452	4.951	0.929	1.930	1.153

TABLE 20 (Continued)

Rabbit femur (r=right l=left) ratio (active/control)	New bone external to implant (mm^2)	New bone inside medullary canal (mm^2)	New bone inside implant (Quantimet® data, mm^2)	Total new bone (mm^2)	^{85}Sr Activation ratio
7-III					
active=l	4.286	0.665	0.585	5.536	
control=r	3.238	1.323	0.400	4.961	
ratio (a/c)	1.324	0.503	1.463	1.116	1.160
10-I					
active=r	1.699	0.623	0.740	3.062	
control=l	13.054	1.084	0.763	14.901	
ratio (a/c)	0.130	0.574	0.970	0.205	0.555
10-II					
active=r	0.706	0.943	1.260	2.909	
control=l	0.392	0.278	0.532	1.202	
ratio (a/c)	1.801	3.392	2.368	2.420	1.279
14-II					
active=r	1.437	0.455	0.839	2.731	
control=l	1.371	0.651	0.634	2.655	
ratio (a/c)	1.049	0.699	1.323	1.029	0.646
14-III					
active=l	2.245	0.192	0.712	3.149	
control=r	3.135	0.620	0.839	4.594	
ratio (a/c)	0.716	0.310	0.849	0.685	1.684
56-I					
active=r	0.0	0.0	1.005	1.005	
control=l	0.0	0.833	1.907	2.740	
ratio (a/c)	---	0.0	0.527	0.367	1.070
56-II					
active=r	0.0	0.400	1.150	1.550	
control=l	0.394	0.0	1.832	2.226	
ratio (a/c)	0.0	-----	0.628	0.696	0.872

TABLE 21. Correlations of the MOP-III measurements with the strontium-85 activation ratios for the distal segments of the implant series

	New bone external to implant	New bone inside medullary canal	New bone inside implant (Quantimet®) data)	Total new bone
r =	0.435	0.071	-0.125	0.345
95% C.I.=	(-.27,+.82)			(-.25,+.75)
r^2 =	0.189	0.005	0.016	0.119
n =	10	10	13	13
(excludes 1-III, 56-I, and 56-II)				

application of 300 mg PAA per kg of body weight without first having any medullary tissue aspirated. The description of the following observations is all from this one rabbit. Stained cross sections from the femurs of this rabbit are shown in Figures 23, 24, 25, and 26.

Periodic Acid-Schiff (PAS) Stain

This blue stain, Figure 23, was a deeper blue in both the endosteal and periosteal areas of new bone growth. The areas of old bone and the bone from the control femur were less deeply stained. The cement lines were particularly distinct, indicating, perhaps, the incorporation of carbohydrates into the cement lines. Areas around spaces in the bone that did not seem to have bone forming activity were less intensely stained than the more active areas,

TABLE 22. Quantimet® image analysis data for ingrowth of bone into porous implants

Days-rabbit # femur (l=left r=right)	Area of bone (mm^2)	Percent of implant filled with bone	^{85}Sr Activation ratio
1-III			1.083
active=l	0.181	1.190	
control=r	0.203	1.662	
3-II			1.095
active=r	0.167	1.020	
control=l	0.312	3,324	
3-III			0.921
active=l	0.334	2.391	
control=r	0.386	3.143	
5-I			0.837
active=r	0.471	3.105	
control=l	0.083	1.665	
5-III			0.839
active=l	0.316	2.490	
control=r	0.375	4.109	
7-I			1.153
active=r	0.931	5.88	
control=l	1.003	8.831	
7-III			1.160
active=l	0.582	3.668	
control=r	0.397	3.182	
10-I			0.555
active=r	0.735	4.813	
control=l	0.758	4.863	
10-II			1.279
active=r	1.253	14.822	
control=l	0.529	5.871	

TABLE 22 (Continued)

Days-rabbit # femur (l=left r=right)	Area of bone (mm^2)	Percent of implant filled with bone	^{85}Sr Activation ratio
14-II			0.647
active=r	0.834	8.840	
control=l	0.630	5.597	
14-III			1.684
active=l	0.708	6.165	
control=r	0.834	8.840	
56-I			1.070
active=r	0.999	11.760	
control=l	1.896	16.424	
56-II			0.680
active=r	1.143	12.136	
control=l	1.821	15.277	

indicating that the bone forming areas were utilizing or acquiring more carbohydrates.

Gomori's Reticulin Stain

In this pink stain, the endosteal new bone was stained no darker than the older cortical bone. In some areas, the periosteal new bone was a little more darkly stained. Osteoblastic cells were stained brown. The lamella of the bone was well illustrated by this stain. Reticulin fibers were seen only in the medullary tissue.

FIGURE 23. Section from the experimental femur of the rabbit that survived an endosteal application of PAA of 300 mg/kg (PAS)

Alcian Blue at pH 1.0

This stained the bone a very faint blue, Figure 23. The faintness of the stain is probably indicative of the low concentration of sulfated glycoaminoglycans that occurs in mature bone. But, there were areas of interest that were more deeply stained. The periosteal cement line was made very distinct by this stain. Both the periosteal and endosteal new bone were stained slightly more than the mature cortical bone. Some of the spaces or cavities in the bone were filled with a featureless substance that was deeply stained. The surrounding soft tissue, muscle, and the medullary tissue were left completely unstained.

FIGURE 24. Section from the experimental femur of the rabbit that survived an endostal injection of PAA of 300 mg/kg (Alcian blue, pH 1.0)

Alcian Blue at pH 2.5

This stain is selective for glycoaminoglycans in general. The pattern of staining with this stain was virtually identical to that of Alcian blue at pH.1.0. The only difference was that the stain at pH 2.5 was overall a fainter blue than the stain at pH 1.0. Glycoaminoglycans, GAG, (formerly referred to as mucopolysaccharides) are a basic component of the ground substance of connective tissues. They fill the spaces between the cells and the fibers in connective tissue. Nutrients that feed the connective tissue cells are soluble in the GAGs. Their presence in the bone, and their enhanced presence in new

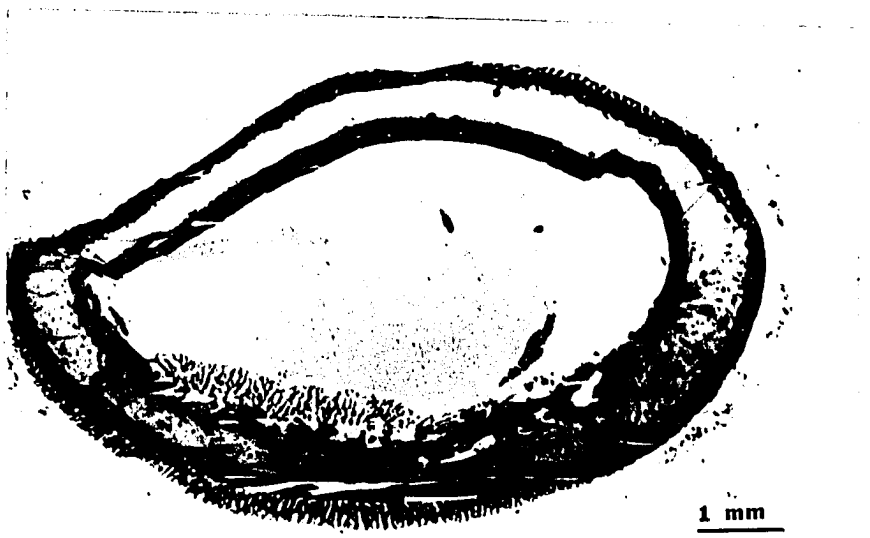

FIGURE 25. Section from the experimental femur of the rabbit that suvived an endosteal injection of PAA of 300 mg/kg (Lillie's silver)

bone and cement lines shown by these slides, is a normal phenomenon.

Masson's Trichrome Stain

With this stain, bone was stained in alternating red and blue stripes. The mature cortical bone was stained predominately red with thin blue stripes. At a magnification of 100, the new periosteal and new endosteal bone appear to be solid blue, but at a magnification of 400, small stripes and spots of red were seen in the blue area. No distinct cement line was discerned. The cells of the medullary tissue were very dark, nearly black. The periosteum was dark brown and blue. The muscle bundles were

FIGURE 26. Section from the control femur of the rabbit that survived an endoseal injection of PAA of 300 mg/kg (Lillie's silver)

red, and the fibrous soft tissue was purple or blue.

Summary of Special Stains

Very little new information was found with these stains that could not be obtained with the H and E stain. Therefore, it was decided not to stain any other samples with these special stains.

Microscopic Examination

The periosteum of the rabbit, as in the rat, is composed of two layers, an outer fibrous layer and an inner cambium layer. The fibrous layer is composed of thick, flattened, spindle-shaped cells imbedded in stromal fibers

that run in a circumferential direction. In the resting periosteum, this layer is about two to four cells deep. The cambium layer is composed of plump basophilic round cells. The matrix of the cambium layer does not have the regular circumferential packing of the fibrous layer. The cells of the fibrous layer tend to be closely packed, while the cells of the cambium layer are loosely packed. With hematoxylin and eosin stain, the cambium layer is more basophilic or blue, while the fibrous layer stains more eosinophilic or red-pink.

Over an area of active periosteal new bone formation, the cambium layer of the periosteum thickened from just one or two cellular layers to perhaps a dozen. Mitotic figures, or dividing cells, were seen on the plump cells of the cambium layer. A layer of polygonal-shaped cells lined the spicules of new bone being formed. These spicules tended to radiate outward perpendicular to the surface of the old cortex. The fibrous layer of the periosteum thickened and dispersed as the periosteum approached a callus. At the callus, the fibrous layer of the periosteum blended into the irregular fibrous connective tissue covering the callus. Near the callus, the cambium layer gradually merged into cartilage cells or into a loose fibrous connective tissue that merged into areas of cartilage and new cancellous bone. This anatomical description of a callus formation was

typically observed in both control and experimental femurs. It is, basically, normal bone callus formation and bone repair.

Empty Defect Series, Proximal Segments

The microscopic slides from the proximal segments were all taken from transverse sections made through the approximate center of the defect or the implant. They were all stained with hematoxylin and eosin.

Day 1, one day after administration of PAA and 8 days after surgery Callus formation was present on the outside of the cortex in both the experimental femurs and the controls. The calluses were composed of cancellous bone, cartilage, and fibrous connective tissue. The new cancellous bone extended radially out of the matrix of the cortex. On top of the cancellous bone, and merging with it, there often were one or more masses of ossifying cartilage. The cartilage callus was covered by a layer of loose to moderately dense fibrous connective tissue. At day one, the cancellous new bone growth had just begun the process of bridging the defect.

In addition to periosteal new bone growth, both the control and experimental samples presented cancellous new bone growth originating from the endosteum. Spicules of endosteal new bone were covered with osteoblastic cells. The spicules of endosteal new bone merged with the

cancellous new bone growth originating from the defect. The new bone growth from the defect merged with the cancellous new bone from the periosteum, forming a continuous matrix of cancellous bone covering much of the outside of the femur and wrapping around the cut edges of the defect and into the medullary canal. Adjacent to the defect, a small area of necrotic acellular cortical bone was undergoing resorption. This was bone that was injured by the creation of the defect.

Day 3 As early as 3 days after the application of PAA (10 days after surgery), the growth of new cancellous bone completely bridged the gap in the cortex in one of the control samples.

Day 5 At the day 5 period, both the control and experimental samples displayed complete bridging of the defect wih cancellous bone at the level of the cortex.

Histologically, the same features were noted in both the control and activated samples. Both control and experimental samples presented calluses composed of cancellous bone, cartilage, and fibrous connective tissue. In a day 5 control, cartilage callus covered the defect area over a bridge of cancellous bone. Both control and experimental samples showed resorption of necrotic bone, and both presented endosteal and periosteal new bone growth.

Day 7 At seven days, the spicules of new periosteal cancellous bone were broadening. In some places, the spaces between the spicules were completely filled with new bone, transforming the cancellous bone into compacted cancellous bone. At 10 days, very few cells of cartilage were seen. The cartilage cells that were left were largely mineralized. At 7 days, one control sample showed the cortical defect to be only half bridged by cancellous bone projecting from both sides of the cut defect. In all the other samples at 7 and 10 days, this gap was completely or almost completely bridged by cancellous bone. In some samples, the two fronts of cancellous bone growing out from the sides of the cortical defect are separated by only a narrow space of highly vascularized loose areolar connective tissue.

Day 10 Even at 10 days, acellular necrotic bone tissue remained along the old cut edges of the defect, but more extensive replacement of this necrotic tissue was seen than at earlier time periods. At 10 days, the first definite examples of Haversian systems or secondary osteons were seen in new bone that replaced necrotic bone. In many textbooks, the Haversian system or secondary osteon is unfortunately described as if it was the typical or only type of bone. In rats and rabbits, Haversian systems are found only at sites of bone repair. The typical bone in the cortex of the rabbit's femur is composed of primary osteons.

The primary osteons in the rabbit are composed of several layers of lamellae around a central blood vessel. The contours of the outer layers blend into the contours of the interstitial bone that lies between the osteons. The secondary osteon results when a resorption cavity is formed in the bone. The resorption cavity is then filled by concentric lamellae of new bone until a single capillary remains in the center. A secondary osteon has a distinct cement line that outlines the border of the former resorption cavity. In the rabbit, osteons with a cement line were observed only in areas where necrotic bone tissue had been replaced by new bone.

Day 14 Even at fourteen days, the gap in the control sample was not completely bridged by cancellous bone. In both control and experimental samples, most of the periosteal new bone was compacted cancellous bone. In the experimental sample, a large callus composed of cancellous bone and fibrous connective tissue still remained. No cartilage was seen in either the control or experimental samples. The periosteum still showed areas of activation where new bone formation was still occurring. The endosteal surfaces of the femurs did not display any spicules of new bone growth.

Summary The active production of periosteal new bone as seen in Figures 27, 29, and 30 occurred at all time

periods examined from day 1 to day 14, and it occurred in both control and experimental femurs. The periosteal activation agent appeared to enhance the natural bone growth phenomenon that occurs in response to an injury.

Endosteal new bone was present the day after application of PAA (8 days after surgery), but it tended to disappear by day 14 (21 days after surgery). Cartilage callus was present in most samples from day one through day seven. It was nearly all gone by day 10. Necrotic bone near the edge of the defect was present at all time periods, but showed signs of being partly replaced by day 10. Bridging of the defect occurred as early as day 3, but in some samples the defect remained partially open even at day 14 as can be seen in Figure 27. Areas of cancellous periosteal new bone were converted into compacted cancellous bone as early as day 7. Compacted cancellous bone was common in samples at days 10 and 14.

Empty Defect Series, Midsegments

The H and E stained slides from the midsegments were transverse sections taken through a point near the center of the midsegments. Although the midsegments did not contain any defects or implants, they did display callus formation, activation of the periosteum, and some endosteal new bone growth.

Periosteal callus formation was seen in both the activated and control samples at all the time periods. At day 1 (8 days after surgery), the periosteal calluses were composed of large masses of cartilage that covered small areas of cancellous new bone. The cartilage masses were covered by loose areolar connective tissue. At day 3 the calluses in the activated sample displayed large areas of cartilage, while the control sample showed very little cartilage. The periosteal calluses were composed of cancellous bone. At day 7, the periosteal callus from one rabbit was mostly compacted cancellous bone in both the control and experimental samples. The samples examined from the other rabbit from day 7 displayed large periosteal masses of both cartilage and cancellous bone. In the activated sample from this day 7 rabbit, there was a layer of cancellous new bone covering a mass of cartilage. The cartilage was actually sandwiched between two layers of cancellous bone. In the day 10 and day 14 samples, very little cartilage was seen. What cartilage was seen was usually in the final stages of mineralization and necrosis of chondrocytes. At these longer time periods, the periosteal calluses were composed of bone that was largely cancellous at the thick part of the callus and compacted at the thinner parts. It seemed that conversion of the cancellous bone into compacted cancellous bone originated

near the old cortex, and perhaps never reached the outermost points of the callus. In the long-term 56 day samples, the callus lumps were gone, evidently having been resorbed.

A few spicules of endosteal new bone surrounded by osteoblastic cells were seen in both the activated and the control day 1 samples, the activated day 3 sample, the activated day 5 sample, and the control day 10 samples. Curiously, an extensive amount of active endosteal new bone was observed in the experimental day 14 sample.

Implant Series, Proximal Segments

In the proximal segments of the implant series, the events in the progression of the calluses formed around the outside of the cortex were essentially the same as in the proximal segments of the ED series. In the implant series, the implants tended to project slightly above the periosteal level of the cortex by appproximately 0.5 mm.

Day 1, one day after application of PAA but eight days after surgery The activated sample showed considerably more new bone growth than the control. Large areas of both endosteal and periosteal new bone were present in the activated sample. Spicules of endosteal new bone occurred whenever the contours of the implant brought it near the endosteum. The interstices of both implants were filled with a loose areolar connective tissue that contained stellate cells, long flat spindle-shaped cells, and round

cells. In the control sample, the implant was capped by two layers of tissue. The first layer above the implant was an irregular fibrous connective tissue, and the second layer was a loose areolar connective tissue. There was no bone ingrowth into the interstices of the control implant, and there was very little ingrowth into the experimental implant.

Day 3 Some osteoid ingrowth in the interstices of the implants were present in the experimental and the control samples as can be seen in Figures 29 and 30. The limited ingrowth occurred where the implant interfaced with the cortex of the femur and where the base of the implant contacted or came near the endosteum. Large amounts of cartilage callus were present around the outside of the cortex.

The interstices of the implant were filled with a loose areolar connective tissue that contained round cells, red blood cells, flat spindle-shaped cells, and some stellate cells.

Day 5 These samples showed much more osteoid and bone inside the interstices of the implant than the 3 day samples. The ingrowth was confined to the region of the implant in contact with the cortex and where the implant came within about 0.5 mm to the endosteum. The sample from one rabbit in this time period presented a small medullary

FIGURE 27. Section from a control femur from the empty defect series at day 14 (H and E).

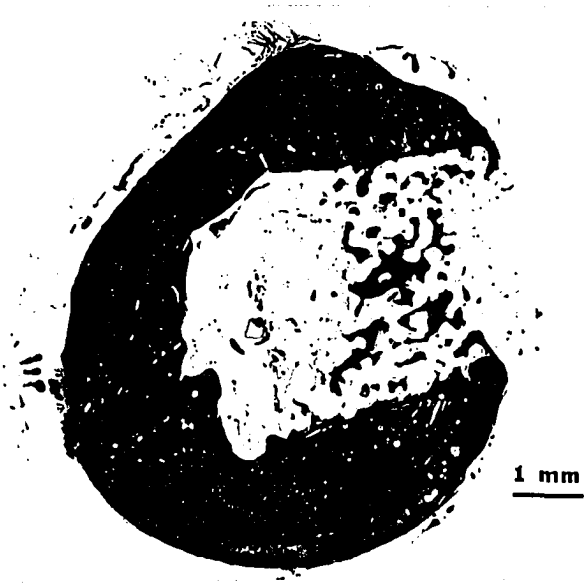

FIGURE 28. Section from the experimental femur from the implant series at day 56 (H and E).

FIGURE 29. Section from an experimental femur from the implant series at day 3 (H and E).

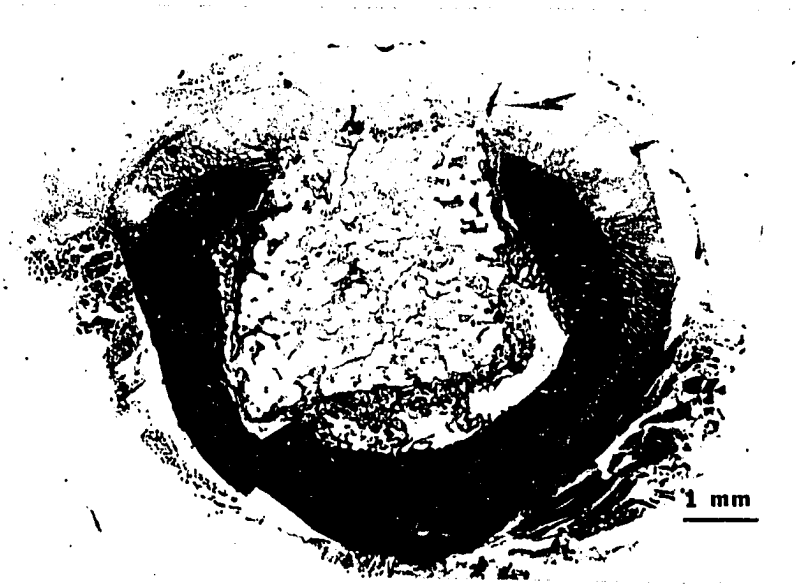

FIGURE 30. Section from the contralateral control femur from the rabbit in Figure 29 (H and E).

canal that was nearly filled by the implant in both the control and experimental femurs. In this animal, bone ingrowth was present all along the sides of the implant.

The implants were covered with a loose connective tissue, and the interstices of the implant were filled with the same type of tissue. Spindle-shaped cells, round cells, and some stellate cells, as are common to a loose areolar connective tissue, were seen in the interstices. The round cells are probably lymphocytes and the spindle-shaped cells are probably fiberblasts which form bundles of collagen fibers. The stellate cells are probably mesenchymal cells that extrude ground substance and a delicate network of collagenous fibers.

Some of the periosteal new bone formed in the calluses around the cortex displayed areas of compacted cancellous bone.

Day 7 The implants showed extensive ingrowth of new bone. The bone ingrowth was most extensive where the implant contacted the cortex. In some samples, the ingrowth of new bone coming in from opposite sides of the implant met and formed a bridge of bone spicules crossing the implant at the level of the cortex.

The interstices of the implant that were not filled with bone were filled with a loose areolar connective tissue similar to what was seen at earlier time periods. However,

at the cortical level of the implant and near areas of bone ingrowth, the fibers of the interstitial tissue were denser and resembled unmineralized osteoid to varying degrees.

The samples all displayed extensive calluses around the outside of the cortex. In one control sample, there was extensive callus formation composed of cancellous bone, cartilage, and loose connective tissue. Some of the periosteal and endosteal new bone was compacted cancellous bone. Some compacted periosteal new bone was seen in all of the seven day samples. In two control samples, some periosteal new bone was seen growing over the top corner of the implant. In one sample, this bony overgrowth occurred even though the implant appeared to have originally extended slightly above the level of the original cortex.

Day 10 The samples tended to display a continuation of the processes occurring at the early time periods. In two samples (one control and one experimental), the front of bone ingrowth bridged the implant at the cortical level. In the other two samples (one control and one experimental), the bone ingrowth from opposite sides of the implant did not quite meet. Spicules of endosteal new bone were often seen lining the sides of the implant. The loose areolar connective tissue that filled the interstices of the implant was more dense near the areas of bone ingrowth. A little more of this denser connective tissue seemed to be present

in the day 7 samples. There also seemed to be more compacted cancellous bone in the periosteal calluses on the outside surface of the femur.

Replacement of necrotic bone was observed in the cortex adjacent to the defect. The pattern of resorption of necrotic bone, and subsequent replacement with new bone containing secondary osteons, occurred in about the same time period as in the endosteal defect series.

Day 14 Even a wait of 21 days after surgery did not insure that bone ingrowth would completely infiltrate across the implant. In the samples from one day 14 rabbit, there was not complete bridging of the implant in either the control or the experimental sample. Only a modest amount of ingrowth was observed in either sample. The samples from the other rabbit displayed complete bridging in both the experimental and the control samples. In the later samples, the bridging occurred at the endosteal level, across the lower part of the cortex. Bone ingrowth did not extend to the top center of the implant. Some ingrowth was observed where the base of the implant contacted the endosteum, and this was observed in both control and experimental implants. In one experimental sample, ingrowth was observed along one entire side of the implant.

The soft tissue infiltrating the implant was a loose to moderately dense connective tissue that contained primarily

flattened spindle-shaped cells and a few stellate cells.

The external calluses were comprised mostly of compacted cancellous bone in all of the day 14 samples. One control sample displayed a particularly large callus. In one experimental sample, the compacted periosteal new bone covered one corner of the implant.

Resorption of necrotic bone was observed in the cortex adjacent to the implant in both control and experimental samples.

Day 56 The long-term implants displayed the greatest amount of bone ingrowth, Figure 28. In the earlier time periods, the ingrowth tended to be narrow spicules that did not completely fill the interstices they entered. In the long-term samples, the spicules of ingrowth were broad, spanning the complete diameter of the openings they entered. As in the short term samples, the ingrowth occurred mostly at the cortical level of the implant. The ingrowth seemed to serve as replacement of the cortex that had been removed. The ingrowth was most intense at the endosteal level of the implant, it never extended to the central axis at the top of the implant. Beneath the level of the cortex, there was scattered bone ingrowth in the implant. In the medullary canal, but outside of the implant, there were no spicules of endosteal new bone in any of the day 56 implants.

The soft tissue that infiltrated the implant was a

loose areolar connective tissue. It contained mostly red blood cells and darkly stained round cells and only a few flattened spindle-shaped cells. It closely resembled regular hematopoietic tissue.

The periosteal new bone was completely compacted in all the samples. The periosteum had returned to its normal resting state. The fibrous layer of the periosteum was only a few cells deep, and the cambium layer was just one or two cells deep. In some places, the cambium layer seemed to have been reduced to one layer of widely separated cells. In one control sample and in one activated sample, the new periosteal bone formed a solid cap over about half of the top of the implant. In one control sample, the periosteal new bone completely covered the top of the implant.

Even at 63 days after surgery, some necrotic bone remained near the implant in all of the samples examined. Some of the necrotic bone was being resorbed; much of it had already been replaced with a bone matrix rich in secondary osteons.

Summary Bone growth into the implants was present as early as 8 days after surgery and one day after the application of PAA. The ingrowth originated where the implant came in contact with the cortex, and also where the edges of the implant contacted bone tissue or came within about 0.5 mm to the endosteum. By day 7 (14 days after

surgery), there were samples where the bone ingrowth from the cortex had penetrated to the center of the implant, forming a bony bridge through the implant at the level of the cortex. The rate that bone ingrowth occurred at was highly variable. Even at day 14 (21 days after surgery) there were samples where the ingrowth had not penetrated to the center. The samples that had received the application of PAA did not consistently show any more rapid ingrowth than did the control samples. By day 56, the samples all showed thick spicules of bone ingrowth filling the interstices of the implant at the level of the cortex. In the medullary level of the implant, there were scattered spicules of bone.

During the early stages of bone ingrowth, there was an activation of the endosteum wherever the implant came in contact with the endosteum, or came very close to the endosteum. At day 1 and day 3, there was a considerable amount of new bone spicules emerging from the endosteum and almost appearing to reach for the implant. Spicules of bone were seen lining the sides of the implant as late as day 10. But at day 56, the spicules of medullary bone were all gone except for a few scattered spicules inside the implant.

During this period, the soft tissue that filled the interstices of the implant gradually changed from a loose areolar connective tissue that contained mostly stellate

cells, long, flat spindle-shaped cells and some round cells to either bone or normal hematopoietic tissue.

The changes observed on the periosteal surface of the bone during this time period were essentially the same as that seen in the empty defect series. Calluses that were composed of cancellous new bone, cartilage, and fibrous connective tissue at the early time periods were gradually converted to compacted bone.

Implant Series, Midsegments

The H and E stained slides from the midsegments were transverse sections taken through a point near the center of the midsegments. Although the midsegments did not contain any defects or implants, they did display callus formation, activation of the periosteum, and some endosteal new bone growth.

The time sequence of tissues from the midsegments observed in the implant series was very similar to that seen in the empty defect series. The calluses were observed to go through three overlapping stages of transformation. In the first stage, extensive cartilage calluses were seen in the day 1 through day 5 samples. In the second stage, these were largely replaced by cancellous bone in the day 5 through day 14 samples. In the third stage, the spaces between the spicules of cancellous bone were filled to form compacted cancellous bone. As early as day 10, some of the

smaller callus formations were completely compacted cancellous bone. At day 56, all of the remaining calluses had been transformed into compacted cancellous bone. These stages overlapped. Cancellous bone was seen as early as day 1 in both the control and activated samples, but more frequently in the activated samples. Residues of cartilage in its final stages of mineralization were seen as late as day 10 in both a control and an activated sample.

Most of the samples from the midsegments of the implant series did not show any endosteal new bone. This was expected, since there was no hole drilled in the midsegment and the microscope slides from the midsegments were taken at a point midway between the implants. However, a few spicules of active endosteal new bone growth were observed in a control day 3 sample, an experimental day 5 sample, and both control day 5 samples. More extensive areas of endosteal new bone growth were observed in one experimental day 7 sample and one experimental day 14 sample.

Endosteal Activation Series

Transverse cross sections were made through the center of the proximal, mid, and distal segments and stained with hematoxylin and eosin.

Initial Rabbit The decision to proceed with this series was prompted by the results from one rabbit that survived an endosteal injection of 300 mg of PAA per kg of

body weight. This injection was made without first aspirating any medullary material. The rabbit was killed 7 days after the application of PAA. Transverse cross sections were made from the proximal, mid, and distal segments from the femurs of this rabbit. Sections from the proximal and midsegments were stained with H & E, and the sections from the distal segments were stained with Lillie's silver impregnation technique. The control sections from this animal, Figure 26, all showed a normal appearing femur. There was no new bone formation in either the periosteum nor the endosteum. All the microscopic sections from the experimental femur showed areas of both periosteal and endosteal new bone formation (Figures 23 and 25). In the medullary canal, anastomosing spicules of bone were seen emerging from the endosteum. These spicules of bone were covered with darkly stained osteoblastic cells. Cancellous bone was seen partially ringing the periosteal surface of the cortex. This cancellous bone did not resemble a fracture callus. It contained no cartilage, and it was spread in an even, thin strip around the cortex. There was no single large lump of tissue as was seen in the cortical calluses of the other two series.

Rest of Series In the rest of the endosteal activation series, greater survivability was achieved by (1) reducing the amount of PAA injected from 300 to 100 mg per

kg of body weight and by (2) aspirating an amount of medullary tissue and fluid equal to the volume being applied. In the rest of the series, both the radiation (Table 12) and the microscopic results were not as conclusive. Little endosteal new bone was seen in any of the day 1 samples examined or in any of the day 5 samples. One day 3 sample from an activated femur showed a single large spicule of endosteal new bone. The other sample was from a control femur, and it showed two broad fingers of bone covered with osteoblastic cells emerging from the endosteum (Figure 31). They appeared to encircle an area of the cortex that may have been pierced by one of the sharp surgical instruments used in this procedure. Spicules of endosteal bone covered with osteoblastic cells were often seen in both control and experimental samples at days 7 and 10 (Figures 32, 33, and 34).

In a rabbit at day 7 that gave a total femur activation ratio from the strontium tracer of 1.038, endosteal new bone was seen in all segments of both the control and the experimental femur. The endosteal new bone was fairly extensive in the proximal and distal segments from the experimental femur. Extensive areas of endosteal new bone were seen in all samples taken from the 10 day period. This was observed in both experimental and control samples. In one experimental section from the midsegment, about three

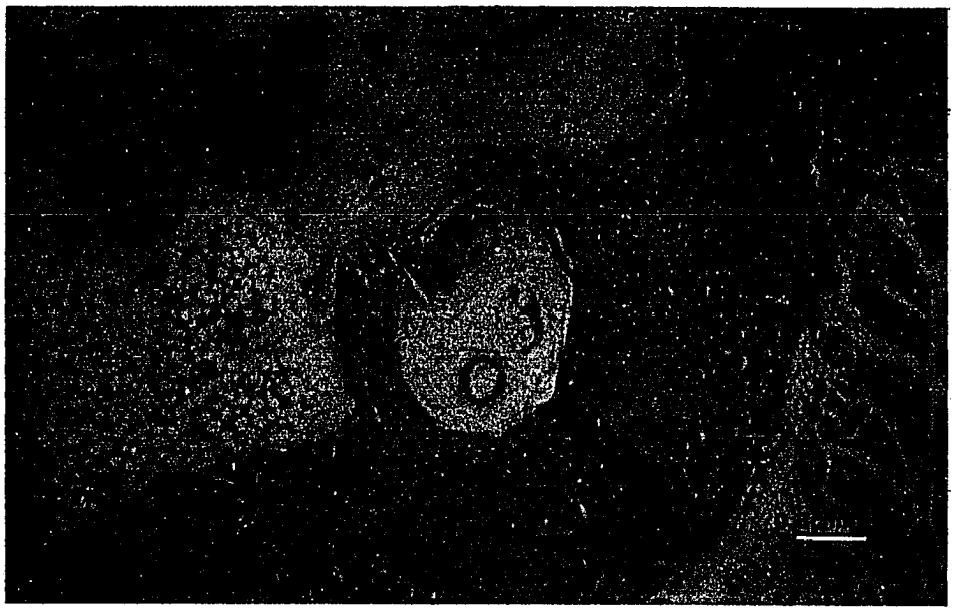

FIGURE 31. Sample from a control femur from the EA series at day 3 (H and E)

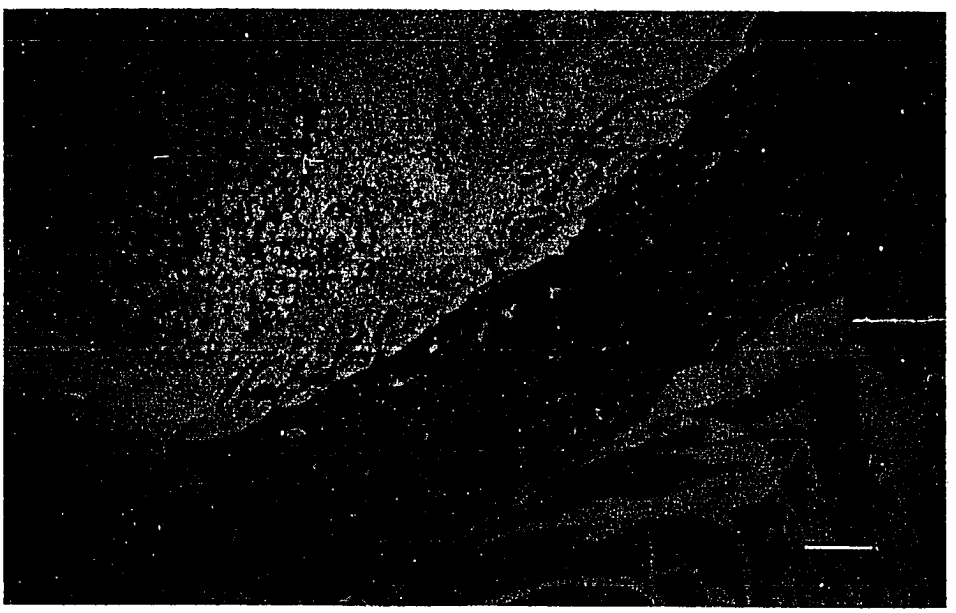

FIGURE 32. Sample from a control femur from the EA series at day 7 (H and E)

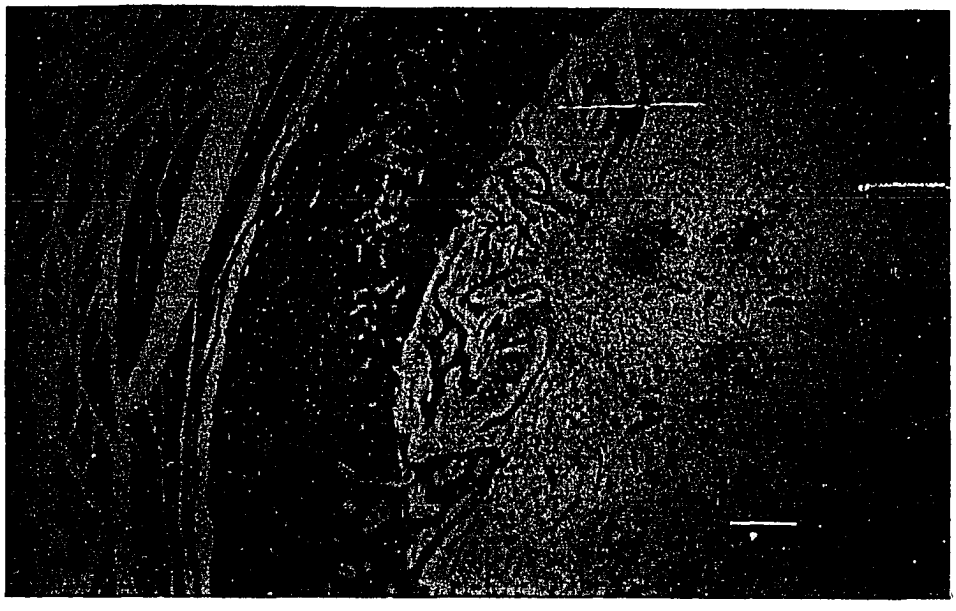

FIGURE 33. Sample from an experimental femur from the EA series at day 10 (H and E)

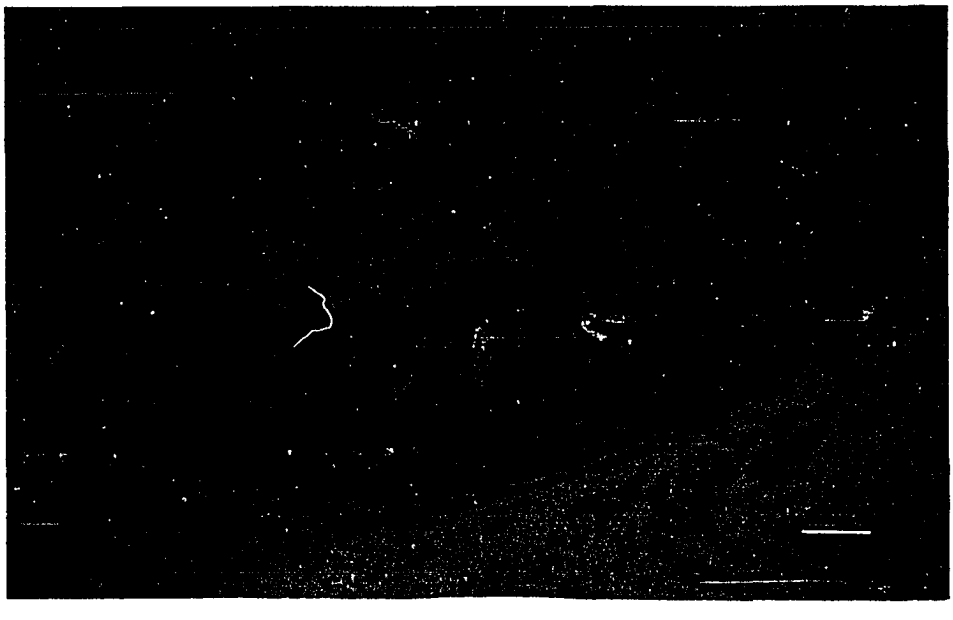

FIGURE 34. Sample from the contraleral control femur of the sample in the Figure 33 (H and E)

quarters of the endosteum were covered with spicules of new bone lined with palisades of osteoblasts.

The medullary canal in these samples showed signs of the damage done when a small hole was drilled through the trochanter fosse and when about 2 ml of medullary tissue and fluid was aspirated from each femur. Chips of necrotic bone were observed in samples as late as day 7. A clot of red blood cells was present in the medullary canal in all the day 1 and day 3 samples and one of the day 5 samples. The medullary canal in one experimental day 5 sample displayed a circular tissue-free area or hole about 1 mm in diameter. At day 3, polymorphonuclear leukocytes or white blood cells were observed in the medullary canal. By comparison, at day 7 and day 10, a single large red blood cell clot was not observed in the medullary canal. In its place was an area of fairly acellular loose areolar connective tissue occupying one-third to one-half of the medullary canal and often containing scattered clumps of red blood cells. The rest of the medullary tissue was normal appearing hematopoietic tissue.

The periosteum in these samples usually displayed some areas of new bone growth. In most of the samples, this appeared to be the normal new bone growth occurring by apposition of a layer of new primary osteons onto the outer rim of the cortex. A thickening of the cambium layer of the

periosteum with darkly stained polygonal-shaped cells lining the surface of the underlying bone was usually seen. The new bone would take the form of small lumps or ruffles on the surface of the old cortex. Trabeculae of cancellous new bone, as was observed in the calluses of the other series, was generally not present on the periosteum.

Due to their wide variability, the results from the endosteal activation series, Table 12, were not as conclusive as we would have liked. The techniques that we used to apply the PAA or the control pyrogen-free saline, evidently stimulated endosteal new bone growth by itself. Prior to the PAA injection or the sham injection, a probe was first inserted down the medullary canal to make sure that the medullary canal had been located. Then a volume of medullary tissue and fluid equal to the volume of fluid to be injected (usually about 2 ml) was aspirated from the medullary canal. This aspiration of medullary tissue and fluid was performed upon advice that this could prevent embolism. Such embolism was considered to be a possible cause of the early failure of many of the first endosteal applications. However, microscopic examination showed that this technique injured the medullary canal. The large amount of endosteal new bone growth that was seen in both the control and experimental femurs 7 and 10 days after this assault on the medullary canal (Figures 32, 33, and 34) was

probably due to an injury response or due to the physical stimulus to the endosteum from the instruments used.

A graphic summary of the microscopic examination is presented in Figure 35. In this figure, the occurrence of certain features is noted. A solid line means the feature was seen in all, or almost all, samples examined in the time range given. A broken line indicates that the feature was seen in some of the samples examined in the given time range. The markings begin at the time when observations began.

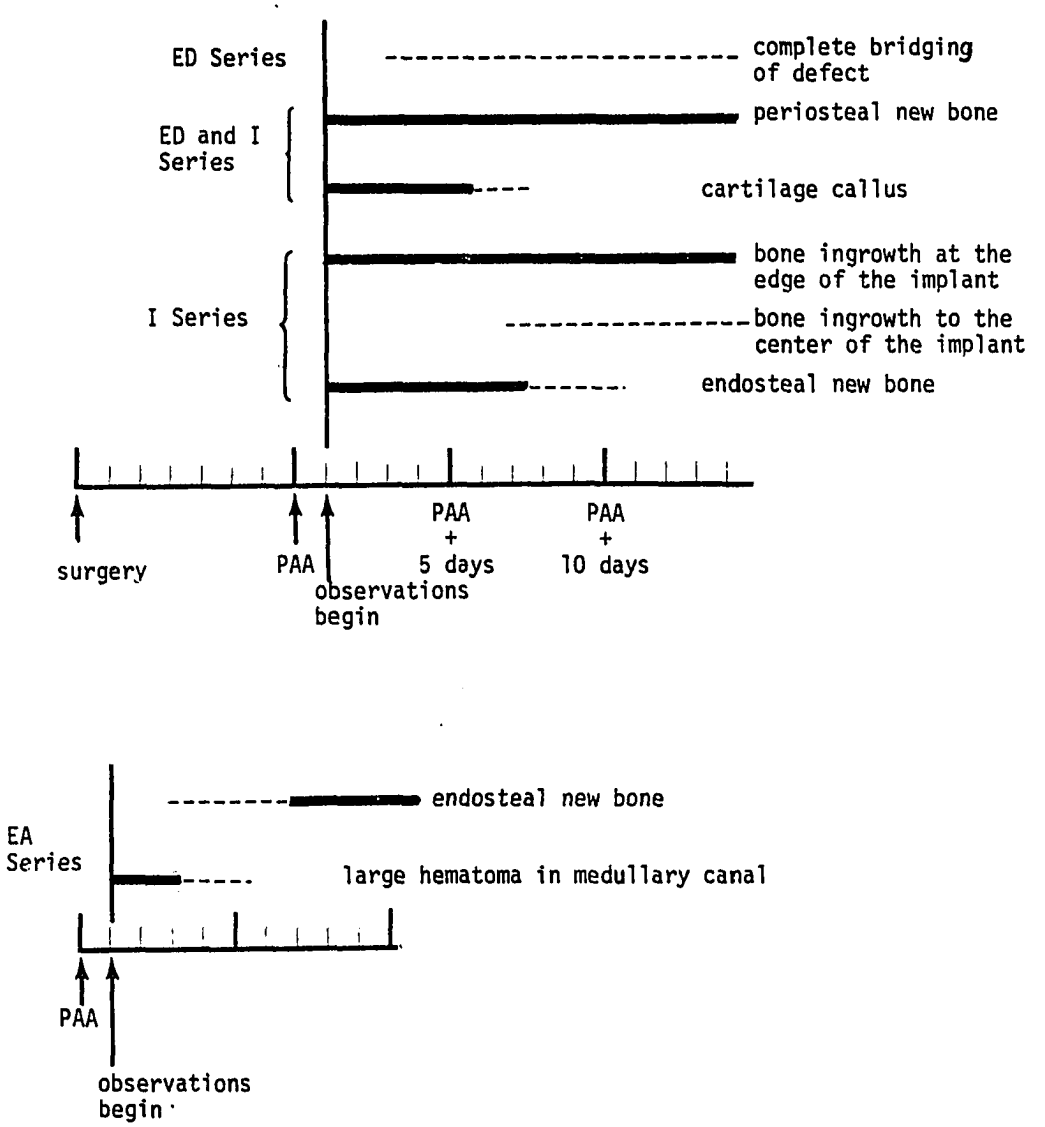

FIGURE 35. Summary of microscopic examination showing certain tissues and events observed in the ED, I, and EA series

CONCLUSIONS

This study was not able to show that PAA encouraged bone growth into a porous implant or accelerated healing of a defect. What it did show, was that PAA significantly enhanced the amount of periosteal callus formation associated with an injury to the bone. This enhancement of periosteal callus formation began as early as one day after the application of PAA ($p<.05$), and continued for 14 days after its application. With the exception of endosteal new bone observed in some rabbits, the bone growth effects of this compound seemed to be confined exclusively to the periosteum.

The mechanism of PAA remains unresolved. As described in the Literature Review, its effects may be due to a glycoprotein or biological interaction of a negatively charged chemical species, or to some type of morphogen that activates specific cells. To the best of our knowledge, no research has been undertaken in recent years to characterize either its chemical structure or its mechanism of action.

The aspects of differentiation are described in the results section and discussed later in this section. Possible future applications based on our findings are discussed under Recommendations and Considerations for Future Research.

The potency values obtained from the preliminary trials on rats, rabbits, and puppies (Tables 2, 3, 4, 5, and 6) showed that by following the procedure of patent 3,458,397 (Myers et al. 1966) we were able to successfully extract a periosteal activation agent from cancellous bone. The last four batches of the extract prepared by us all seemed to have roughly the same potency; however, they were all much less potent than the agent used by Tornberg and Bassett (1977). The phenomenon we observed in rats in response to the application of this extract did not seem to be any different from what they observed in rats.

In larger animals, such as the rabbits and the puppy, PAA did not elicit a response as spectacular as it did in the rat. In the rat, potency values as high as 393 (Table 2) were observed in response to 120 mg of PAA per kg of body weight. In the rabbit, 600 mg of PAA per kg of body weight had to be applied to produce a potency value of 235 (Table 5). Such species differences may be due to the difference in surface area to volume in different bones (Table 7).

The periosteal activation agent used in this study apparently worked by promoting and enhancing normal endochondral ossification that occurs in the periosteum in response to an injury. Both the strontium-85 uptake data and the image analysis confirm that in the empty defect series, the samples that had received an application of PAA

experienced more new bone growth than the control samples. All 18 of the activated femurs in this series showed a greater total uptake of strontium than their respective contralateral controls. The odds against this happening by chance are 262,144 to 1.

Some points about the strontium-85 data from the empty defect series are that they showed an enhancement of bone growth in the experimental femur that continued for at least 14 days, and that they showed peaks at day 5 ($p<.05$) and day 14. The continued enhanced bone growth at day 10 ($p<0.05$) and day 14 is interesting because the previous data published on PAA stated that new bone formation was completed in about 7 days in the rat (Tornberg and Bassett, 1977). This longer term enhancement of bone growth is more consistent with studies done using demineralized bone powder to accelerate healing of defects in the rat mandible where the periosteum had been removed (Kaban and Glowacki, 1981). In that study, the uptake of calcium-45 reached its peak in 14 days. Another study compared the osteogenic response of four different graft materials in the calvaria of 35 guinea pigs. It showed that the uptake of strontium-85 peaked at 28 or 35 days for all four of the substances (Mellonig, et al. 1981). The four substances tested were freeze-dried allograft, decalcified freeze-dried allograft, autogenous bone blend, and autogenous osseous coagulum. However,

autogenous bone blend and autogenous osseous coagulum showed an initial peak at day 14. There was no strontium-85 uptake peak in that study at day 5, and the researchers did not observe any particular phase change at day 14.

The strontium uptake peak at day 5, does, however, fit in with the previously published data on PAA. Tornberg and Bassett (1977) reported that the mineralization phase of the periosteal activation response occurred from 60 hours to day 7, with numerous areas of crystal formation being observed by 72 hours (3 days). It should be remembered that the strontium-85 uptake data is a measure of bone growth activity from the time the strontium was injected to the time the animal was killed, 24 hours later.

Even as early as 1 day after the application of PAA, both the implant series and the empty defect series indicated an enhanced uptake of strontium in the experimental femur ($p<.05$ for both series). This is surprising since in the earlier work on PAA, mineralization was not observed until 60 hours after the application of PAA (Tornberg and Bassett, 1977). These differences (enhanced mineralization as early as day 1 and continuing at least through day 14) may be due to the different model used in this experiment. In the model used by Tornberg and Bassett (1977), the periosteal activation agent was applied to the resting periosteum of the midshaft region of 250 g mature

Sprague-Dawley rats. The bones in these rats were intact and were not undergoing fracture or defect repair. In the model used in this experiment, PAA was applied to the periosteum of rabbit femurs that were in the process of bone repair. The periosteum of these rabbits had already been activated by the defect surgery that occurred 7 days earlier. Microscopic examination of the 1 day samples did show large cartilage repair calluses which obviously had not formed "overnight". The application of PAA at this stage of repair served to further activate the periosteum to cause an almost immediate increase in the amount of mineralization.

Placing an implant in the defect, as was done in the implant series, added complicating influences to the model. About one-third of the strontium uptake data from the implant series gave negative results where the control samples were more radioactive than the experimental samples. There are a few factors that may account for this. One possibility is that the implants applied and transmitted stresses to the bone that encouraged bone formation and bone resorption. It has been shown that living bone will respond to the stresses applied to it by forming new bone in areas of dynamic compression and by allowing old bone to be resorbed in areas of dynamic tension (Wolff, 1892; Bassett, 1971). Another possible factor was revealed in the microscopic examination of the implant series. New bone

growth from the endosteum seemed to be elicited whenever the base of the implant came in contact with or came close to the endosteum. The physical contact of the implant with the endosteum may have elicited an activation of the endosteum. Slight differences in the precise location of the defect, in the angle that the defect hole was drilled, in the tightness of fit between the implant and the defect hole, in the size of the femur, and in how well the base of the implant abutted against the endosteum on the opposite side of the cortex would all influence the distribution and amount of new bone growth. Attempts were made to keep all these factors uniform. The location of the defect holes were carefully measured. The defect hole was always drilled in about the same location on the same side of the bone. An effort was made to hold the drill at the same angle when boring the hole. The implant was always cut to fit the hole drilled, so that the base of the implant abutted against the opposing endosteum and the top of the implant was flush, or almost flush, with the periosteal surface of the bone. The rabbits used were all of the same breed, New Zealand white, and they all came from the same breeder. The femurs from the smaller rabbits were generally a little smaller than the femurs from the larger rabbits, but there were no noticeable differences in size between the left and right femur of the same rabbit. In all of these steps, there were slight

differences that could not be avoided. The sum of all these differences may be responsible for the greater scatter of data in the implant series compared with the data from the empty defect series.

The pore sizes of the implants were adequate for bone ingrowth. Previous workers have shown that an interconnecting pore size of 100 μm in diameter is sufficient in a biocompatible materials to permit bone ingrowth (Hulbert et al. 1970). The Biopore implants used in this study had an average pore size of 127 μm diameter, and 89.5% of the pores were greater than or equal to 117 μm in diameter. The material the implants were constructed of was a high purity, medical grade, high density polyethylene. This material is currently used in orthopedic applications. It has been used successfully in a porous form as a matrix for bone ingrowth many times (Spector et al. 1976, Klawitter et al. 1976, Spector et al. 1979). Microscopic examination of these porous plugs after they had been implanted, showed the surface openings of pores were not damaged by the implantation procedure. Short penetrations of bone ingrowth (approximately 0.1 to 0.2 mm) was observed at the edges of the implant as early as eight days after surgery.

The amount of new bone seen on the samples stained with H & E correlated with the strontium uptake data moderately well for the empty defect series (r=0.47, 95% C. I.=-.04 to

+.85 for proximal segments; r=0.66, 95% C. I.=-.17 to +.92 for mid segments) and very well for the implant series (r=0.825, 99% C. I.=.30 to .98 for the proximal segments; r=0.852, 95% C. I.=.25 to .94 for the mid segments). Close examination of the components of these data showed that these correlations were due almost entirely to the large masses of periosteal new bone formed on the outer circumference of the femurs (which was enhanced by PAA). There was not convincing evidence that the application of PAA enhanced bone growth inside the defects or inside the medullary canal. The data from the Quantimet® image analysis computer, that was capable of measuring the area of bone ingrowth in a given cross section with a high degree of accuracy, also did not indicate that the amount of bone ingrowth had been influenced by periosteal application of PAA. These results indicate that the agent as applied in these experiments is almost exclusively a periosteal activation agent. It did very little or nothing to stimulate or accelerate bone growth outside of the periosteum or bone ingrowth into a porous high density polyethylene implant. This work thus establishes some possible limitations on the application of PAA. It also establishes that even when the periosteum has already been activated by an injury, PAA will enhance the amount of new bone formation during a time period of 1 to 10 or 14 days

after its application.

In the proximal segments from the implant series (Table 17), the fraction of the new bone that arose from the endosteum varied considerably, from a low of 0% in some of the day 56 samples and 0.7% in one day 14 sample to as high as 56.2% in day 1 sample. Generally, both the absolute amount of endosteal new bone measured in mm^2 and the percent of the total new bone that came from the endosteum was larger in the shorter term samples from days 1, 3, and 5 than in the longer term samples from days 7, 10, 14, and 56. This may indicate that the endosteal new bone, whether it is due to PAA or to surgical trauma, is formed earlier and is resorbed sooner.

In the initial rabbit that survived the endosteal application of 300 mg of PAA per kg of body weight (treatment without first aspirating medullary material), there was no activation of the endosteum seen in any of the control cross sections. The experimental cross sections all showed activated areas of the endosteum (Figure 23) at 7 days. Not only was the endosteum activated in the experimental femur from this rabbit, but the periosteum also showed new bone growth. No periosteal new bone was seen in the control samples. In this one rabbit, it seems that a large endosteal application of PAA may have stimulated new bone growth at both the endosteum and periosteum. Perhaps

the force of injecting the PAA into the medullary canal was strong enough to force it into the blood supply where it was carried to the outside of the bone. Or perhaps, from this large amount of PAA injected, enough was able to ooze out of openings in the bone to stimulate the periosteum.

The injury response is probably largely responsible for the wide scatter of the strontium data from the other rabbits of the endosteal activation series. It may also be responsible for the large amount of "negative" data from this series where the control samples were more radioactive (sometimes nearly twice as radioactive) than the experimental samples. Most of this negative data occurred at the early time periods (day 1 and day 3). The later time periods (days 5, 7, and 10) gave largely positive strontium uptake data for the total femur. Due to the high variability in the data, it is difficult to tell if this indicates a trend, or if it is just a random fluctuation.

The observations of the 5 special stains (Gamori's reticulin, Alcian blue at pH 1.0 and 2.5, PAS, and Masson's trichrome) did not reveal anything unusual about the periosteal and endosteal new bone observed in the samples examined. The samples examined with these stains were only ones that showed periosteal and endosteal new bone that may have been elicited by their treatment. Due to the expense involved, no extensive study was made of defect repair or

bone ingrowth using these stains.

One question that will have to go unanswered is: in the absence of any other injury or endosteal stimulus, does PAA activate the cells of the endosteum to produce new bone? On the basis of data from just one rabbit, it appears that the answer to this question may be yes. For a definite answer to this, additional experiments need to be performed as follows: apply PAA to the endosteum of a series of animals with a minimum of assault to the endosteum and medullary canal and compare with controls from the contralateral limbs.

It has been over four year since Tornberg and Bassett (1977) published their original paper on the effects of this substance which I have chosen to call periosteal activation agent. It has been well over a decade since Squibb Laboratory originally developed and patented this substance. In that time no one, to my knowledge, has established what the activation agent or agents are. There are a number of reasons that may explain why so little research has been done on PAA. Probably, the main reason why little research has been done on PAA is because of the expense that would be involved in getting government approval for its use in human medicine. It would have to be shown fairly conclusively that it does not cause unwanted bone growth or cancer. Another obvious reason is because there does not exist a

good commercial source of PAA. Squibb Laboratories stopped manufactoring PAA over a decade ago (R. C. Millonig, The Squibb Institute for Medical Research, Princeton, N. J. 08540, personal communication) and all of their old supplies are gone. This researcher had to go through considerable effort to extract the agent from the ground ribs of calves. The agent used in this study is not as potent as the agent that was extracted at Squibb laboratory. Tornberg and Bassett (1977) used a batch of PAA that had been prepared at Squibb Laboratories some years earlier. They were able to elicit what they called an "explosive" subperiosteal osteogenesis by using 2.4 mg of agent per kg of body weight in the rat. To produce the same phenomenon, we had to use about 250 mg of PAA per kg of body weight in the rat. Another reason why so little research has been done on PAA may be because those interested in bone stimulation have chosen to pursue other paths of achieving it. Urist et al. (1979a) has been trying to characterize bone morphogenetic glycoprotein (BMP). A number of researchers have done animal experiments and clinical work using demineralized bone matrix to elicit osteogenesis (Mellonig et al. 1981; Mulliken and Glowacki, 1980; Kaban and Glowacki, 1981; Glowacki et al. 1981).

There are a number of reasons why the batch of agent used in this study was not as potent as the agent prepared

at Squibb. For one thing, the potency of the agent extracted will vary with the individual animal it is extracted from. In other words, the ribs of one calf may provide a more potent batch than the ribs from some other calf. The extract from one of our trial batches seemed to be more potent than the extract used for the main part of this study (Tables 2 and 3). A second possible reason may be that we were not able to adequately duplicate the precise techniques and equipment used at Squibb Laboratories. The workers at Squibb Laboratories, where the agent was first developed, may have perfected a certain expertise in handling the substance, and they may have used equipment more suitable for working with it. In the case of the current investigation, the meat grinder from the Iowa State Meat Laboratory that was used to grind the bone, may have overheated the bone. The third possible reason may be because of the broad specifications of the patent procedure. In many places the patented procedure was not specific, it offered widely varying ranges in the time period certain steps should be done. For instance, it specified that the ground bone should be digested in the acid pepsin bath for 4 hours to 48 hours. It did not specify an optimal time within that range. So, we selected a time period closer to the longer limit to give the enzyme more time to release the activation agent.

RECOMMENDATIONS AND CONSIDERATIONS FOR FURTHER RESEARCH

It is unfortunate that previous workers discontinued research on this periosteal activation agent in the 1960s. It seems that a substance that has such an intense and immediate effect on the periosteum would be worthy of research to determine what it is, how it works, and what its potential applications may be. At the time they stopped research on the substance, they were pursuing the possibility that the active agent is a glycoprotein. Because of a lack of further research on its chemical structure, to the best of our knowledge, not even its approximate molecular weight is known (R. C. Millonig, The Squibb Institute for Medical Research, Princeton, N. J. 08540, personal communcation).

Research should be conducted to establish the chemical composition of the active agent or agents in this extract, and to prepare samples of the pure active agent or agents. The extract that we are now using is most likely a collection of many hundreds or perhaps thousands of different compounds. If only the active agent or agents could be separated from this extract, then we may have a substance that is hundreds or thousands of times more potent than the raw extract used in this study. By removing the unneccessary compounds from this extract, we may be removing some substances that may cause adverse side effects or

adverse long-term effects in some animals. Also by isolating the precise agents responsible for the activation response, we will be providing the research community with a well characterized substance that may be used for basic research on bone. The best way to determine if PAA will stimulate activation of the endosteum, may be by using just the pure activating agents. Such research on the pure activation agents may lead to efficacious applications in human or veterinary medicine. Once the pure agents have been identified, it may be possible to mass produce them by using recombinant DNA techniques.

The biochemical process of identifying the activation agent or agents may start by using molecular sieve techniques to identify the approximate molecular weights of the agents. Electrophoresis may then be used to isolate the specific substance or substances. Recently Hanamura et al. (1980) have been able to obtain values for the approximate molecular weights of BMP by molecular sieve techniques utilizing thin-channel diafiltration and gel filtration and gel electrophoresis. Similar techniques can be applied to PAA. However, if the action of PAA is due to the influence of two or more chemical species, isolating those particular species may be difficult. A preliminary molecular sieve study that we conducted gave an indication that the molecular weight of the active agent or agents in PAA is

greater than 1000 Daltons.

In order to use PAA or its agents in humans, some basic conditions will have to be satisfied first. First, it must be shown that it is relatively safe to use. Something that stimulates such a rapid growth of bone may be suspected of being carcinogenic or causing ectopic bone formation. Though no cancer or ectopic bone formation was observed in any of the animals that we used in this study for time period up to 56 days, or in any of the rats that Tornberg and Bassett (1977) used (they observed them for up to 42 days after application), that still does not prove that PAA will not cause cancer or ectopic bone formation. It may cause cancer after a longer delay. Some carcinogens take about 20 years to cause cancers in humans. It may cause cancer in other species of animals that have not been examined, or it may cause cancers at a frequency so low that it has not been detected yet. Second, it will need to be shown that it does work in humans. To the best of my knowledge, no human research has ever been done with this particular extract.

The ability of PAA to activate the resting periosteum as demonstrated by Tornberg and Bassett (1977) and its ability to enhance periosteal callus formation as is demonstrated in this study may have a number of orthopedic applications. It may be used to stimulate bone growth from

the periosteum to encourage reattachment of broken tendons or ligaments or attachment of synthetic ligaments. It may be used to encourage periosteal attachment of artificial joints. Such applications would be based on new periosteal growth into the pores of a fabric or into the ridges or pores of an orthopedic prosthesis that attaches to the outside of the bone rather than inside the medullary canal. Before these ideas can be applied, it will be necessary to examine the response of such periosteal new bone to specific biocompatible porous materials.

Periosteal activation may be useful anywhere it is needed to stimulate growth in the periosteum. An endoprosthesis has been developed as an artificial hip implant that is designed with a sleeve that fits over the outside of the femoral shaft. On the inside of the sleeve there is an array of ridges. The endoprosthesis is attached to the bone by periosteal bone growth into the indentations of the grooves. This implant design has been shown to be effective in human applications (Plenk et al. 1978), thus showing that in some cases, periosteal new bone can provide a permanent bond to a grooved material. A periosteal activation agent may be extremely useful in accelerating bone ingrowth and interlocking into such a prosthesis.

One scenario for efficacious application of PAA involves using the skeleton as a scaffold to attach

prostheses and monitoring devices. It may be possible to do this by affixing a biocompatible porous material to the outside of the implantable device. The pores should be of suitable size (over 100 μm in diameter) to permit bone ingrowth and may be impregnated with a purified PAA. The periosteum of the bone where this device is to be attached could be stimulated with PAA, and the porous interface of the device would be attached to it. In a matter of weeks, the clamping instrument used could be removed and the device would stay attached to the skeleton by the mechanical interlocking of the bone ingrowth.

Even if it is not feasible to use PAA in human applications, it may be useful in veterinary applications. It may be used to help attach, via porous interfaces, artificial joints in companion animals and in certain valuable breeding animals. Certain breeds of large bulls often become lame when their crucial ligaments fail under the forces of their weight. A periosteal activation agent may be used to attach synthetic replacement ligaments to the periosteum of their long bones. At the site of attachment with the bone, these materials would present a woven network with spaces large enough to permit bone ingrowth. It may be specific enough to encourage bone ingrowth at the site of periosteal attachment without mineralizing the rest of the ligament.

Further research should be done to investigate the effects that PAA may have on the endosteum. The isolated rabbit results from this study suggest that PAA may stimulate the cells of the endosteum. A way should be found to apply PAA to the endosteum with a minimum of assault to the endosteum.

Further research should also be conducted on more efficient ways to apply PAA. Since it seems to act only on the cells of the cambium layer of the periosteum (or possibly on the cells of the endosteum), ways should be found to target PAA precisely to the sites of the periosteum where new bone growth is desired. It would have been desirable in this study to use an X-ray viewer to observe more precisely where the PAA was being applied. Also, experiments could be performed with PAA embedded within the pores of a material. For example, if it is desired to encourage periosteal bone ingrowth into a loose nylon mesh, the PAA would be incorporated into a resorbable gelatin held within the pores of the mesh. Then as the bone grew into the pores of the mesh, it would be constantly exposed to more PAA.

PAA, or its purified activation agents, may have research applications. It may be used to attach implanted instruments via porous or grooved interfaces to the periosteum in various animal models. It may be used in

basic research on the biology and biochemistry of bone growth and bone repair. The findings from such research may lead to applications that can not be foreseen today.

LITERATURE CITED

Alberts, L. R. 1978. The effects of galvanic currents on bone growth into porous polyethylene implants. M.S. Thesis. Iowa State University, Ames, Iowa.

Barth, A. 1893. Ueber histologishe Befunde nach Knochenimplatatichen. Arch. f. Klin. Chir. 46:409-417.

Bassett, C. A. L. 1962. Current concepts of bone formation. J. Bone Jt. Surg. 44-A:1217-1244.

Bassett, C. A. L. 1971. Effects of force on skeletal tissue. Pages 283-317 in J. A. Downey and R. C. Darling, eds. Physiological basis of rehabilitation medicine. W. B. Saunders Co., Philadelphia.

Bassett, C. A. L. and T. P. Ruedi. 1966. Transformation of fibrous tissue to bone in vivo. Nature 299:988-989.

Bassett, C. A. L., A. A. Pilla and R. J. Pawliuk. 1977. A nonsurgical salvage of surgically-resistant pseudarthroses and non-unions by pulsing electromagnetic fields. Clin. Orthop. Relat. Res. 124:128-143.

Becker, R. O., J. A. Spadaro and A. A. Marino. 1977. Clinical experiences with low intensity direct current stimulation of bone growth. Clin. Orthop. Relat. Res. 124:75-83.

Berking, S. 1977. Bud formation in Hydra: inhibition by an endogenous morphogen. Wilhelm Roux's Archives 181:215-225.

Borgens, R. B., J. W. Vanable, Jr. and L. Jaffe. 1979. Bioelectricity and regeneration. Bioscience 29(8):468-474.

Boutin, P. 1977. L'arthroplastic totale de la hanche par prothèse en alumine résultats de 150 cas d'ancrage direct de la pièce acétabulaire. International Orthopaedics (SICOT) 1:87-94.

Bridges, J. B. and J. Pritchard. 1958. Bone and cartilage induction in the rabbit. J. Anat. 92:28-38.

Carter, D. R. and D. M. Spengle. 1978. Mechanical properties and composition of cortical bone. Clin. Orthop. Rel. Res. 135:192-210.

David, F. N. 1938. Tables of the ordinates and probability integral of the distribution of the correlation coefficient in small samples. Cambridge University Press for the Biometrika trustees.

de Groot, K. 1973. Some considerations about bone-induction. Calcif. Tissue Res. 13:335-337.

Douglas, B. S. 1972. Conservative management of guillotine amputation of the finger in children. Australian Paediatric Journal 8:86-89.

Elves, M. W. 1974. An evaluation of the use of strontium 85 for the assessment of experimental bone grafts. Acta Orthop. Scand. 45:641-651.

Englestad, R. B. 1934. Ueber die Wirkungen der Roentgensstrahlen auf die Lungen. Acta Radiol. (Suppl.) 19:1-93.

Fell, H. B. 1928. Experiments on the differentiation in vitro of cartilage and bone. Part 1. Arch. f. Exper. Zellforsch. 7:390-412.

Fell, H. B. 1932a. The osteogenic capacity in vitro of periosteum and endosteum isolated from the limb skeleton of fowl embryos and young chicks. J. Anat. 66:157-180.

Fell, H. B. 1932b. Chondrogenesis in cultures of endosteum. Proc. Roy. Soc. London Ser. B 112:417-427.

Ferguson, T. H. 1976. Bone ingrowth and related tensile properties of a porous implant. M.S. Thesis. Iowa State University, Ames, Iowa.

Friedman, B., K. Heiple, J. C. Vessely and H. Hanaoka. 1968. Ultrastructural investigation of bone induction by an osteosarcoma, using diffusion chambers. Clin. Orthop. Relat. Res. 59:39-57.

Fukada, E., T. Takamatsu and I. Yasuda. 1975. Callus formation by electret. Jpn. J. Appl. Physiol. 14:2079.

Glowacki, J., L. B. Kaban, J. E. Murray, J. Folkman and J. B. Mulliken. 1981. Application of the biological principle of induced osteogenesis for craniofacial defects. The Lancet 8227:959-963.

Gomori, G. 1937. Silver impregnation of reticulin in paraffin sections. Am. J. Pathol. 13:993-1002.

Hanamura, H., Y. Higuchi, M. Nakagawa, H. Iwata, M. R. Urist. 1980. Solubilization and purification of bone morphogenetic protein (BMP) from Dunn osteosarcoma. Clin. Orthop. Relat. Res. 153:232-240.

Hartshorne, E. 1841. The causes and treatment of pseudarthrosis. Am. J. Med. Sci. New Series 1:143-156.

Holm, N. J. 1980. The formation of stress by acrylic bone cements during fixation of the acetabular prosthesis. Acta Orthop. Scand. 51:719-726.

Hulbert, S. I., F. A. Young, R. S. Mathews, J. J. Klawitter, C. D. Talbert, F. H. Sterling. 1970. Potential of ceramic materials as permanently implantable skeletal prostheses. J. Biomed. Mater. Res. 4(1):433-456.

Illingworth, C. M. 1974. Trapped fingers and amputated finger tips in children. J. Pediatr. Surg. 9(6):853-858.

Illingworth, C. M. and A. T. Barker. 1980. Measurement of electrical currents emerging during the regeneration of amputated finger tips in children. Clin. Phys. Physiol. Meas. 1:87-89.

Judet, R., M. Siguiere, B. Brumpt and T. Judet. 1978. A noncemented total hip prosthesis. Clin. Orthop. Relat. Res. 137:76-84.

Kaban, L. B. and J. Glowacki. 1981. Induced osteogenesis in the repair of experimental mandibular defects in rats. J. Dent. Res. 60(7):1356-1365.

Klawitter, J. J., J. G. Bagwell, A. M. Weinstein, B. W. Sauer and J. R. Pruitt. 1976. An evaluation of bone growth into porous high density polyethylene. J. Biomed. Mater. Res. 10:311-323.

Lev, R. and S. S. Spicer. 1964. Specific staining of sulfated groups with alcian blue at low pH. J. Histochem. Cytochem. 12:309.

Lillie, R. D. 1928. Kalkfaerbung mit nachfolgender Entkalkung, eine neue Methode. Z. Wiss. Mikrosk. 45:380.

Lillie, R. D. and H. M. Fullmer. 1976. Histopathologic technic and practical histochemistry. McGraw-Hill, New York.

Lord, G. A., J. R. Hardy and F. J. Kummer. 1979. An uncemented total hip replacement. Clin. Orthop. Relat. Res. 141:2-16.

Luna, L. G. (ed.). 1968. Manual of histological staining methods of the armed forces institute of pathology. Third edition. McGraw-Hill, New York.

Masson, P. J. 1929. Some histological methods trichromestainings and their preliminary technique. J. Tech. Methods 12:75-90.

McManus, J. F. A. 1948. Histological and histochemical uses of periodic acid. Stain Technol. 23:99-108.

Mellonig, J. T., G. M. Bowers and R. C. Bailey. 1981. Comparison of bone graft materials part 1. New bone formation with autografts and allografts determinded by strontium-85. J. Periodontol.-Periodontics 52:291-302.

Mulliken, J. B. and J. Glowacki. 1980. Induced osteogenesis for repair and construction in the craniofacial region. Plast Reconstr. Surg. 65:553-559.

Myers, D. V., G. T. Barry, A. Borman, R. C. Millonig, W. L. Westcott and M. B. Young. 1966. Process of producing osteogenic material. U.S. Patent 3,458,397.

Novak, B. and F. W. Bentrop. 1972. An electrophysiological study of regneration in Acetabularia mediterranea. Planta 108:227-244.

Nuccitelli, R. and L. F. Jaffe. 1974. Spontaneous current pulses through developing focoid eggs. Proc. Natl. Acad. Sci. U.S.A. 71:4855-4859.

Ostrawski, K. and K. Wlodarski. 1971. Induction of heterotopic bone formation. Volume 3, pages 299-366 in G. H. Bourne, ed. The biochemistry and physiology of bone. Academic Press, New York.

Plenk, H., M. Salzer, H. Locke, N. Stark, G. Punzet and K. Zweymuller. 1978. Extracortical attachment of bioceramic endoprostheses to long bones without bone cement. Clin. Orthop. Relat. Res. 132:252-265.

Ruedi, T. P. and C. A. L. Bassett. 1967. Repair and remodelling in millipore-isolated defects in cortical bone. Acta Anat. 68:509-531.

Schaller, H. and A. Gierer. 1973. Distribution of the head-activating substance in Hydra and its localisation in membranous particles in nerve cells. J. Embryol. Exp. Morphol. 29:39-52.

Smith, D. M., M. R. A. Khairi, J. Norton and C. C. Johnston, Jr. 1976. Age and activity effects on rate of bone mineral loss. J. Clin. Invest. 58:716-721.

Smith, S. D. 1967. Induction of partial limb regeneration in Rana pipiens by galvanic stimulation. Anat. Rec. 158:89-98.

Spector, M., S. L. Harman and A. Kreutner. 1979. Characteristics of tissue growth into proplast and porous polyethylene implants in bone. J. Biomed. Mater. Res. 13:677-692.

Spector, M., W. R. Flemmming, A. Kreutner and B. W. Sauer. 1976. Bone growth into porous high density polyethylene. J. Biomed. Mater. Res. (Symp. no. 7) 10:595-603.

Tornberg, D. W. and C. A. L. Bassett. 1977. Activation of the resting periosteum. Clin. Orthop. Relat. Res. 129:305-312.

Urist, M. R. 1965. Bone formation by autoinduction. Science 150:893-899.

Urist, M. R. and F. C. McLean. 1952. Osteogenic potency and new-bone formation by induction in transplants to the anterior chamber of the eye. J. Bone Jt. Surg. 34-A:443-476.

Urist, M. R. and A. J. Mikulski. 1979. A soluble bone morphogenetic protein extracted from bone matrix with a mixed aqueous and nonaqueous solvent (40616). Proc. Soc. Exp. Biol. Med. 162:48-53.

Urist, M. R., T. A. Dowel, P. H. Hay and B. S. Strates. 1968. Inductive substances for bone formation. Clin. Orthop. Relat. Res. 59:54-96.

Urist, M. R., P. H. Hay, F. Dubuc and K. Buring. 1969. Osteogenic competence. Clin. Orthop. Relat. Res. 64:194-220.

Urist, M. R., A. J. Mikulski and A. Lietze. 1979a. Solubilized and insolubilized bone morphogenetic protein. Proc. Natl. Acad. Sci. U.S.A. 76(4):1828-1832.

Urist, M. R., T. T. Grant, T. S. Lindholm, J. M. Mirra, H. Hirano and G. A. M. Finerman. 1979b. Induction of new-bone formation in the hostbed by human bone-tumor transplants in arthymic nude mice. J. Bone Jt. Surg. 61:1207-1216.

Weinstein, A. H., J. J. Klawitter, T. W. Cleveland and D. C. Amos. 1976. Electrical stimulation of bone growth into porous Al2O3. J. Biomed. Mater. Res. 10:231-247.

Weisenseel, M. H., H. R. Nuccitelli and L. F. Jaffe. 1975. Large electrical currents traverse growing pollen tubes. J. Cell. Biol. 66:556-567.

Weisenseel, M. H., A. Dorn and L. F. Jaffe. 1979. Natural H+ currents traverse growing root hairs and roots of barley (Hordeum vulgure L.). Plant Physiol. 64:512-518.

Wheeler, E. J. and D. Lewis. 1977. An X-ray study of the paracrystaline nature of bone apatite. Calcif. Tissue Res. 24:243-248.

Wolff, J. 1892. Das Gesetz der Transformation der Knochen. A. Hirschwald, Berlin.

Woodruff, R. I. and W. H. Telfer. 1980. Electrophoresis of proteins in intercellular bridges. Nature 286:84-86.

APPENDIX A

Statistics of Radiation Counting

Any radiation rate meter will show fluctuations in the readings from any source known to be constant. The only way to find the true rate of disintegration for a radiation source is to count all disintegrations until the source has decayed, and then average the number of counts at that time. Since this is usually impractical, an estimate of the true radiation rate can be made measuring the rate for a sample period of time.

In a truly random process, the probability that exactly N events will occur in time t is given by:

$$Pn = (Rt)Ne^{-Rt}/N!$$

where R = true mean rate of occurrence

N! = N factorial = 1 X 2 X 3 ... N

The above equation is an expression of the Poisson distribution, a statistical measure of the uncertainty in N is the standard deviation, $\sigma = \sqrt{N}$. In any reasonable counting situation, we may assume that t is known precisely, so that fluctuations in R = N/t are due entirely to fluctuations in N. Then;

$$S = \sqrt{N}/t$$

A measure of N and t determines a value of R, which is only an estimate of the true value R. Thus, S is only an

estimate, but usually a sufficiently good one of ρ.

It is sometimes convenient to express standard deviation as a fraction of the quantity being measured. The coefficient of variation, V, is:

$$Vn = \sqrt{N}/N = 1/\sqrt{N}$$

The coefficient of variation of the rate will have the same value:

$$Vr = S/R = (\sqrt{N}/t)/(N/t) = 1/\sqrt{N}$$

When taking radiation measurements it is almost always necessary to take into account background counts. The count rate due to the sample will be:

$$Rs = Rt - Rb$$

where the small letters refer to sample, sample plus background, and background, respectively.

The standard deviation of a sum or difference is given by:

$$Ss = \sqrt{St^2 + Sb^2}$$

thus,
$$Ss = \sqrt{(Nt/tt^2) + (Nb/tb^2)}$$
$$= \sqrt{(Rt/tt) + (Rb/Tb)}$$ where tt and tb are the counting times with and without the sample. The corresponding coefficient of variation is:

$$Vs = Ss/Rs = Ss/(Rt-Rb)$$

Example

For the segments of the femurs from rabbit V of the empty defect series, day 7, three five minute counts were taken of each segment. For the proximal segments, the counts were:

active segment :	4275	control segment : 3870
	4155	3920
	4198	3770
total	12,628	11,560
average = Rt	4,209.3	3,853.3

The background radiation was 899 counts for each 5 minute count. Subtracting background from each of the 5 minute counts we have:

active segment :	3376	control segment : 2971
	3256	3021
	3299	2871
total	9,931	8,863
average = Rt	3,310	2,954

The activation ratios for the proximal segment is then,

$$9,931/8,863 = 1.12$$

The standard deviation of each segment for 5 minute counts is then (5 minutes is being treated as one unit of time, so, tt = tb = 1):

For active segments	For control segments

$St = \sqrt{4,209.3}$ $\qquad$ $St = \sqrt{3,853.3}$

$Sb = \sqrt{899}$ $\qquad$ $Sb = \sqrt{899}$

$Ss = \sqrt{St^2 + Sb^2}$ $\qquad$ $Ss = \sqrt{St^2 + Sb^2}$

$= \sqrt{4,209.3 + 899}$ $\qquad$ $= \sqrt{3,853.3 + 899}$

$= 71.47$ $\qquad$ $= 68.94$

The coefficient of variation for 5 minute counts are

For the active segment	For the control segment
$Vs = Ss/Rs = 71.47/3310$	$Vs = 68.94/2954$
$= 0.02159$	$= 0.02334$
$= 2.16\%$	$= 2.33\%$

The standard deviation of the mean, $S\bar{s}$ is:

$$S\bar{s} = Ss/\sqrt{n}$$

where n is the number of samples measured

For the active segment	For the control segment
$S\bar{s} = 71.47/\sqrt{3}$	$S\bar{s} = 68.94/\sqrt{3}$
$= 41.26$	$= 39.80$

We have developed two standard deviations, the standard deviation of the 5 minute count time Ss, and the standard deviation of the means of the 5 minute count times $S\bar{s}$. There is a probability of 0.683 that any single measurement of the rate will be within $\pm\sigma$ of the true value (where σ is the true standard deviation). Similarly, there is a probability of 0.683 that any mean value calculated will be within $\pm\sigma$ of the true mean value. The standard deviations

we measure, Ss and $S_{\bar{s}}$, are estimates of the true standard deviations, σ_s and $\sigma_{\bar{s}}$. The coefficient of variation, V, expresses the standard deviation as a function of the quantity being measured. For most of the samples counted, the coefficient of variation for the total count time was less than 5% for individual segments and less than 2.5% for the total femoral counts where the counts from each of the segments from the same femur were summed.

APPENDIX B

Absorption of Gamma Radiation by the Sample

The radioactive samples were counted inside a deep well counter. This is a type of counter where the crystal detector is a cylinder with a cylindrical hole in the center. The sample to be counted is placed in the hole in the detector. For the Picker® counter used, the crystal size was 7.62 cm (3 inches) in diameter and 7.62 cm high. The well in the center of the crystal was 2.8575 cm (1.125 inches) in diameter and 5.08 cm (2 inches) high. The samples were placed in test tubes containing 2 ml of neutral buffered formalin. The test tubes with the samples were mechanically lowered into the deep well counter.

If we take a look at the geometry of the counting situation, the outer surface of the bone is closer to a detector surface then the endosteal or inner surface of the bone. A gamma ray emitted from the inside surface of the femur may travel through the bone before it can be detected. What is the probability that such a gamma emission will be absorbed by the bone? The geometry of the counting situation is illustrated in Figure 36.

The standard formula for absorption of gamma radiation is:

$$I = Io \times e^{-plu}$$

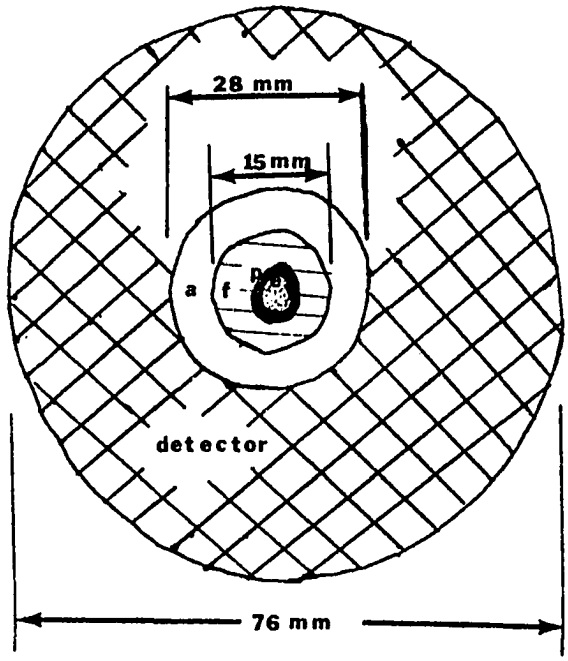

a = air and glass
e = endosteal surface
f = neutral buffered formalin
p = periosteal surface

FIGURE 36. Counting geometry for sample in Picker® deep well counter

where I = intensity of gamma radiation at a given distance

Io = intensity of gamma radiation at surface o

p = density of the material the gamma rays pass through

l = length of the distance the gamma rays pass through

u = mass absorption coefficient (cm^2/g)

A gamma ray that originates in the endosteal surface of the bone and heads directly to the closest detector surface, will have to travel through a given length of bone, l, before it reaches the periosteal surface, Figure 37.

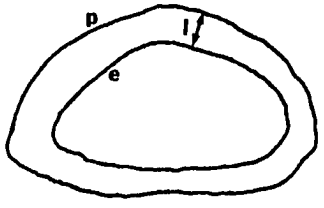

e = endosteal surface
p = periosteal surface
l = width of cortex of femur, usually 0.8 mm to 1.2 mm

FIGURE 37. Transverse cross section of a femur being counted in a deep well detector

The cortical thickness of the rabbit femurs, l, varied from 0.8 to 1.5 mm with an average of about 1.2 mm. The density of cortical bone is about 1.8 gm/cm^3 (Carter and Spengle, 1978). At the energy of strontium-85 decay, 0.510 MeV, the mass absorption coefficient varies from 0.9 cm^2/g to 1.1 cm^2/g for a wide range of materials (water, carbon, copper, iron, and air). If the mass absorption coefficient is assumed to be 1.0 cm^2/g, and the density is 1.8 g/cm^3, and the length is 0.12 cm, then,

$$I = Io \times e^{-(1.0)(1.8)(0.12)}$$

$$I = 0.806Io$$

If the gamma ray travels through 0.2 cm of bone, then,

$$I = 0.700 I_o.$$

Although this is not a rigorous analysis of the self-absorption problem, it does show that strontium-85 from endosteal new bone is less likely to be detected than the strontium in the periosteal new bone. Thus, about 80% of the gamma radiation from strontium-85 will pass through 1.2 mm of cortical bone without being absorbed, and about 70% of such gamma radiation will pass through 2 mm of cortical bone.

APPENDIX C

Correlation Statistics

Correlation is a measure of the linear relation that exists between two variables. The sample linear correlation coefficient, r, also called the simple correlation, the total correlation and the product-moment correlation, is used for descriptive purposes and is defined by:

$$r = \frac{\Sigma(X-\bar{x})(Y-\bar{y})/(n-1)}{\sqrt{\Sigma(X-\bar{x})^2/(n-1)}\sqrt{\Sigma(Y-\bar{y})^2/(n-1)}}$$

$$= \frac{\Sigma(X-\bar{x})(Y-\bar{y})}{\sqrt{\Sigma(X-\bar{x})^2\Sigma(Y-\bar{y})^2}}$$

Where X, and Y are variables

$\bar{x}$, and $\bar{y}$ are mean values of X and Y respectively and Σ signifies summation of all values of X and Y functions.

The correlation coefficient, r, is an estimate of the corresponding population correlation coefficient ρ. The correlation coefficient will always have a value between -1 and +1. Values near +1 or -1 indicate a high degree of correlation while values near zero indicate a low degree of correlation. Negative values indicate that the two variables tend to vary in opposite directions. In other words, as X increases, Y tends to decrease.

The coefficient of determination is r^2, the square of the correlation coefficient. In regression analysis, r^2 is the proportion of a total sum of squares that is attributable to another source of variation, the independent variable. In other words, r^2 gives the variation in a dependent variable that is explained by the independent variable.

Confidence limits on ρ can be found by using the charts prepared by David (1938).

Example

To correlate the image analysis data from the midsegment of the empty defect series with the strontium tracer data from the same segments, set up the table as shown in Table 23.

Then calculate

$$\sum X = 11.067$$

$$\sum X^2 = 21.777$$

$$\sum Y = 9.585$$

$$\sum Y^2 = 14.808$$

$$\sum XY = 16.925$$

Use the functional formula for r,

$$r = \frac{\sum XY - \frac{\sum X \sum Y}{n}}{\sqrt{\left[\sum X^2 - \frac{(\sum X)^2}{n}\right]\left[\sum Y^2 - \frac{(\sum Y)^2}{n}\right]}}$$

TABLE 23. X are the ratios from the image analysis data and Y are the activation ratios from the strontium tracer

Rabbit	X	Y
ED1I	0.478	0.895
ED3III	1.284	1.142
ED5III	2.609	1.708
ED71	0.656	0.793
ED7V	1.558	1.375
ED10IV	2.55	1.324
ED14I	1.932	2.348

$$r = 1.771419 / (4.280)(1.683)$$

$$r = 0.660$$

$$r^2 = 0.4355$$

From the chart of Confidence Belts for the Correlation Coefficient, ρ, where P = .95 and P = .99 (David, 1938), we find that with n = 7 and r = 0.660, that the 95% confidence interval is from -0.17 to +0.92, which means that there is at least a 95% probability that the actual correlation is between -0.17 and +0.92. The probability correlation coeficient is a non-dimensional value.